GSBS Dissertations and Theses   Graduate School of Biomedical Sciences

2019-04-02

Neural Bursting Activity Mediates Subtype-Specific Neural Regeneration by an L-type Calcium Channel

Kendra Takle Ruppell
University of Massachusetts Medical School

Let us know how access to this document benefits you.

Repository Citation

NEURAL BURSTING ACTIVITY MEDIATES SUBTYPE-SPECIFIC NEURAL

REGENERATION BY AN L-TYPE CALCIUM CHANNEL

A Dissertation Presented

By

Kendra Takle Ruppell

Submitted to the Faculty of the

University of Massachusetts Graduate School of Biomedical Sciences, Worcester

in partial fulfillment of the requirements for the degree of

DOCTOR OF PHILOSOPHY

APRIL 2ND, 2019

NEUROSCIENCE

NEURAL BURSTING ACTIVITY MEDIATES SUBTYPE-SPECIFIC NEURAL

REGENERATION BY AN L-TYPE CALCIUM CHANNEL

A Dissertation Presented
By

Kendra Takle Ruppell

This work was undertaken in the Graduate School of Biomedical Sciences

Neuroscience Program

Under the mentorship of

_____
Yang Xiang, Ph.D., Thesis Advisor

_____
Mark Alkema, Ph.D., Member of Committee

_____
Alexandra Byrne Ph.D., Member of Committee

_____
Dori Schafer Ph.D., Member of Committee

_____
Zhigang He Ph.D., External Member of Committee

_____
Eric Baehrecke Ph.D., Chair of Committee

_____
Mary Ellen Lane, Ph.D.,
Dean of the Graduate School of Biomedical Sciences

April 2nd, 2019

Dedication

I dedicate this work to my dogs, Pippin and Ofelia. Thanks for loving me unconditionally, making me laugh every day, and reminding me to live in the moment.

Acknowledgements

I like to thank my whole lab for teaching me techniques, helping with troubleshooting, and giving me suggestions. In particular, Fei Wang is the co-first author on the work detailed in Chapters II and III and contributed significantly to the experimental design, execution, analysis and manuscript preparation. Fei went out of his way to help me with my experiments and often works very hard late into the evening on our project. Fei is always patient and takes time to explain things to me, I really appreciate everything you do, Fei!

Thanks to Pengyu for always listening when I need to talk and giving me good advice about science and life. I am also grateful to Jiaxin for always making me think about my data in a new way and giving me critical suggestions. Thanks to Ye for helping with all the antibody staining in this Thesis and for always having an infectious positive attitude.

I am grateful to my mentor Yang for taking the time to teach me difficult techniques like electrophysiology and demonstrating rigorous experimental design and analysis. Thanks for giving me the freedom to follow where the science leads us, usually in new and interesting directions.

I would also like to thank everyone in the Neurobiology Department for making our department a pleasurable work environment. I am especially grateful to my Committee members, present and past, especially my chair Eric Baehrecke for going above and beyond with instrumental guidance through these final stages of my Thesis work. Committee members Dori Schafer and Mark Alkema have stuck with me from the beginning and helped guide my project as well as my professional development, I am eternally grateful for all that you do! Thanks to my additional Dissertation Exam Committee members Alex Byrne and external examiner Zhigang He.

Thanks to my parents and sister for always loving and supporting me in every way you do. Thanks to my loving husband Evan for being my best friend, confidant, and cheerleader. Thanks to my in-laws for all your encouragement and positivity. Thanks to my friends for being awesome!

Abstract

Axons are injured after stroke, spinal cord injury, or neurodegenerative disease such as ALS. Most axons do not regenerate. A recent report suggests that not all neurons are poor regenerators, but rather a small subset can regenerate robustly. What intrinsic property of these regenerating neurons allows them to regenerate, but not their neighbors, remains a mystery. This subtype-specific regeneration has also been observed in *Drosophila* larvae sensory neurons. We exploited this powerful genetic system to unravel the intrinsic mechanism of subtype-specific neuron regeneration. We found that neuron bursting activity after axotomy correlates with regeneration ability. Furthermore, neuron bursting activity is necessary for regeneration of a regenerative neuron subtype, and sufficient for regeneration of a non-regenerative neuron subtype. This optogenetically-induced regeneration is dependent on a bursting pattern, not simply overall activity increase. We conclude that neuron bursting activity is an intrinsic mechanism of subtype-specific regeneration. We then discovered through a reverse genetic screen that an L-type voltage gated calcium channel (VGCC) promotes neuron bursting and subsequent regeneration. This VGCC has high expression in the regenerative neuron and weak expression in the non-regenerative neuron. This suggests that VGCC expression level is the molecular mechanism of subtype-specific neuron regeneration. Together, our findings identify a cellular and molecular intrinsic mechanism of subtype-specific regeneration, which is why some neurons are able to regenerate while the

majority of neurons do not. Perhaps VGCC activation or neuron activity pattern

modulation could be used therapeutically for patients with nerve injury.

TABLE OF CONTENTS

List of Figures

List of Copyrighted Material Produced by the Author

Appendix II represents work previously published and is presented in accordance

with copyright law.

Reprinted with permission from "Wu X*, Zhang Y*, Takle K*, Bisel O, Li Z, Lee H,

Lois C, Xiang Y, Han G. Dye-Sensitized Core/Active Shell Upconversion

Nanoparticles for Optogenetics and Bioimaging Applications. (2015) *ACS nano*.

Copyrighted 2016 American Chemical Society.

Preface

The work presented in **Chapter II** represents unpublished work being prepared for submission.

The work presented in **Chapter III** represents unpublished work being prepared for submission.

The work presented in **Appendix I** represents unpublished work.

The work presented in **Appendix II** represents published work that is reprinted with permission from "Wu X*, Zhang Y*, Takle K*, Bisel O, Li Z, Lee H, Lois C, Xiang Y, Han G. Dye-Sensitized Core/Active Shell Upconversion Nanoparticles for Optogenetics and Bioimaging Applications. (2015) *ACS nano.* Copyrighted 2016 American Chemical Society.

Chapter I

GENERAL INTRODUCTION

1.1 Neural regeneration

Complex behaviors, thoughts, and perceptions result from the proper development and elaborate networks of the 100 billion neurons inside the human brain. Each neuron, or brain cell, contains three components: the dendrite, the soma, and the axon. The dendrite receives information from other neurons or from the environment, while the axon transmits neuronal signals to effector neurons in order to execute commands. Axons often span great distances to reach their target, for example the longest axon in the human body sends sensory information from your toe to your spinal cord. Their remarkable length subjects axons to damage. In fact, axons are often severed as a result of trauma, metabolic disease, or neurodegeneration. Some axons can regrow back to their original target. This process, known as axon regeneration, is essential to regain function of disconnected neurons. Unfortunately, very few axons have the ability to regenerate rendering spinal cord injury, painful neuropathies, stroke, and neurodegenerative diseases devastating and irreversible. Identifying the mechanisms to promote regeneration is crucial for developing novel therapeutic strategies for nerve regeneration for patients. Why only a small number of axons can regenerate and how we can encourage other severed axons to regenerate are currently important questions for neuroscientists and clinicians. While our knowledge about neuron regeneration has expanded greatly in recent years, many basic biological questions remain unanswered.

Axon regeneration begins with an actin-rich growth cone, which elongates, finds its correct target, remyelinates, and ultimately forms a terminal with its synaptic partner (Tedeschi and Bradke, 2017). Regeneration can fail at any of these steps, but most often fails to even form a growth cone (reviewed in Liu *et al.*, 2011). Astonishingly, some studies have found that after overcoming this initial barrier to regeneration, some axons can navigate through the complex brain milieu to find their proper targets (Steinmetz *et al.*, 2005; Bei *et al.*, 2016). Unfortunately, manipulations to overcome this initial barrier only allow regeneration in a very small subset of axons and have not resulted in therapy for patients with nerve injury. Finding new ways to overcome this critical initial barrier to regeneration and more importantly, determining why only a small subset of axons are able to regenerate after a given manipulation has the potential to result in functional therapeutic regeneration for patients.

Whether this lack of regeneration is due to extrinsic factors, such as an inflammatory growth environment, or reduced intrinsic regeneration ability of neurons is hotly debated. Interestingly, while regeneration in the central nervous system (CNS) is almost non-existent, regeneration in the peripheral nervous system (PNS) is slightly more robust (Ramon y Cajal, 1928). The observation that dorsal root ganglion (DRG) neurons, which span from PNS to CNS, can regenerate the axon in the PNS but not the axon in the CNS led to much speculation that extrinsic inhibitory factors in the CNS prevent regeneration (review in (Liu *et al.*, 2011)). In addition, after transplantation studies

demonstrated axotomized (severed) CNS neurons could regenerate on growth

permissive PNS 'bridges,' researchers searched for the inhibitory extrinsic factors

that must be preventing regeneration in the CNS environment (David and

Aguayo, 1981). Many extrinsic factors hostile to regeneration were identified

such as glia scarring (Ramon y Cajal, 1928; Windle and Chambers, 1950;

Pasterkamp *et al.*, 1999; Bundesen *et al.*, 2003), which was later found to be pro-

regenerative (Anderson *et al.*, 2016), myelin associated inhibitors (Schnell and

Schwab, 1990; McKerracher *et al.*, 1994; Huang *et al.*, 1999; Wang *et al.*, 2002),

and lack of neurotrophic factors (Lindsay, 1988; Lewin *et al.*, 1997; Sterne *et al.*,

1997). Unfortunately, removal of these inhibitory factors thus far does not result

in dramatic or consistent regeneration (Liu *et al.*, 2011). Now the focus has

shifted towards finding intrinsic factors that might enhance neuron regeneration

ability. It is likely that a balance between removing extrinsic inhibitory factors and

promoting intrinsic factors will be necessary for robust functional regeneration in

many diverse types of neurons.

1.2 Intrinsic mechanisms of regeneration

There are many animal models for studying regeneration, and these

models have given us many important insights into the mechanisms of

regeneration. In mammals, the widely used models include optic nerve injury,

which is used to study CNS regeneration (McConnell and Berry, 1982; So and

Yip, 1998; Park *et al.*, 2008; Duan *et al.*, 2015; Lim *et al.*, 2016; S. Li *et al.*,

2016), and dorsal root ganglia (DRG) injury (Lindsay, 1988; Cai *et al.*, 1999; X.-J. Song *et al.*, 1999; Neumann *et al.*, 2002; Udina *et al.*, 2008), which contains axons extending in both the PNS and the CNS. Mammalian models have demonstrated that CNS regeneration can be enhanced by 'priming,' making a prior lesion in the PNS (Mcquarrie and Grafstein, 1973; Richardson and Issa, 1984; Neumann and Woolf, 1999). The results from priming studies are further evidence that a neuron's intrinsic state is a key determinant for regeneration (Neumann and Woolf, 1999). Mammalian models also first identified the importance of intrinsic growth signaling pathways such as SOCS3 (suppressor of cytokine signaling 3, (Smith *et al.*, 2009)) and PTEN/mTOR (mammalian target of rapamyacin, (Park *et al.*, 2008)) in regeneration. Deleting PTEN releases its inhibition of mTOR signaling, which is a pro-regenerative intrinsic signal. The development-associated transcription factors of the KLF (Krüppel-like factor) family have also been shown to regulate intrinsic axon regeneration ability (Moore *et al.*, 2009) in mammals. This is just a small fraction of the many genes associated with regeneration discovered in mammals.

There are also invertebrate models for regeneration that have contributed significantly to the field. *C. elegans* neurons exhibit regeneration and forward genetic screens have led to the identification of over 100 genes that influence axon regeneration, most notably *dlk-1* kinase (Hammarlund *et al.*, 2009; Yan *et al.*, 2009; He and Jin, 2016). *Drosophila* sensory neurons C4da (the nociceptor) and C1da (a proprioceptor (Hughes and Thomas, 2007)) are used to study axon

regeneration and have implicated the Akt pathway, including the mTOR inhibitor PTEN and microRNA bantam, the splicing pathway, and microtubules in axon regeneration (Stone *et al.*, 2010; Song *et al.*, 2012, 2015). These studies have also highlighted remarkable parallels between mammalian and *Drosophila* neural regeneration (He and Jin, 2016). For example, like mammalian DRG neurons, Drosophila C4da neurons have axon extending in both the PNS and the CNS. The PNS C4da axon can robustly regenerate while the CNS C4da axon cannot (Song *et al.*, 2012). Also, a prior 'priming' PNS lesion can enhance regeneration in the CNS, as is the case in mammals (Song *et al.*, 2012).

Recently, neural activity has been identified as an intrinsic mechanism to promote axon regeneration (Lim *et al.*, 2016). Neural activity plays essential roles in axon growth and guidance during development of the nervous system (Reviewed in Spitzer, 2006). Axons do not extend by default, they must fire action potential at physiological levels in order to respond to growth factors (Goldberg, Espinosa, *et al.*, 2002). Also patterned electrical stimulation promotes axon growth preferentially in axons that are exposed to growth factors (Ming *et al.*, 2001; Singh and Miller, 2005). Neural activity has also been shown to promote axon regeneration after injury. After sciatic nerve lesion, electrical stimulation promoted axon outgrowth in mouse (Udina *et al.*, 2008). In a recent study, Lim and colleagues (2016) found that increasing neural activity in severed retinal ganglion cells (RGCs), either by visual stimulation or chemogenetics, promoted limited regeneration *in vivo* (Lim *et al.*, 2016). Other studies have found

that modulating neural activity through G protein-coupled receptor (GPCR) signaling can enhance axon regeneration capacity by elevating mammalian target of rapamycin (mTOR) signaling (S. Li *et al.*, 2016). To our knowledge, no studies have compared *in vivo* neuronal activity in regenerative and non-regenerative neurons to determine if neuron activity is the intrinsic mediator of subtype-specific neuron regeneration.

Decades of research have identified many ways to promote regeneration intrinsically: priming, increasing growth signaling/transcription by mTOR, PSOC3, and KLF, *dlk-1* activation, and neural activity (Park *et al.*, 2008; Udina *et al.*, 2008; Hammarlund *et al.*, 2009; Moore *et al.*, 2009; Smith *et al.*, 2009; Yan *et al.*, 2009; Lim *et al.*, 2016; S. Li *et al.*, 2016). Unfortunately, therapeutic functional regeneration remains largely unsuccessful (Liu *et al.*, 2011).

Stem cell therapies for spinal cord injury is one promising therapeutic strategy, although the formation of teratomas can be problematic and human trials are therefore limited (reviewed in Ronaghi *et al.*, 2010). PNS nerve transplant after spinal cord injury results in some axon regeneration, with no functional regeneration detected in non-human primates (Levi *et al.*, 2002). One clinical trial in human found PNS transplant to result in some functional regeneration, but this study had only one participant (Cheng, Liao and Liao, 2004). Human trials delivering neurotrophic growth factors to the site of axon injury has resulted in serious side effects such as severe pain, fever, numbness, and depression (Apfel, 2002). The minimal regeneration we observe after pro-

regenerative treatments led Duan et al (2016) to ask whether all neurons are equal in regeneration, and launched the field of subtype-specific neuron regeneration.

1.3 Subtype-specific neuron regeneration

Most axons cannot regenerate after injury, even in a growth permissive environment (Ramon Y Cajal, 1928; Canty *et al.*, 2013). This argues that regeneration is an intrinsic ability of only some neurons (Canty *et al.*, 2013), reviewed in (He and Jin, 2016). Recently, it was discovered that neurons are not uniformly poor regenerators, but rather a small subset of neurons can regenerate robustly, this is known as subtype-specific regeneration (Duan *et al.*, 2015).

Understanding why some neurons can regenerate after manipulation, while others cannot is critical for providing therapeutic strategies that promote regeneration in the majority of neurons. We can't treat all neurons alike because they have intrinsic differences that dictate regeneration ability. To emphasize these differences, a recent RNA-seq analysis of DRG neurons observed tremendous heterogeneity in response to axotomy among the different subtypes of neurons (Hu *et al.*, 2016). We have some hints about subtype-specific regeneration: Duan and colleagues (2015) observed that, after artificial mTOR activation, only a small subset of RGCs, the alpha-RGCs regenerate robustly while most other types of RGCs do not regenerate. They noted that alpha-RGCs are also unique in having high mTOR activity, a known regulator of regeneration,

and osteopontin (OPN), which activates mTOR (Duan *et al.*, 2015). Alpha-RGCs have higher intrinsic levels of activity than other subtypes of RGCs (Krieger *et al.*, 2017). Interestingly, neural activity is known to promote mTOR activity (Knight *et al.*, 2012; S. Li *et al.*, 2016). It is possible that this high activity level in alpha-RGCs is what allows for selective regeneration of this subtype of neuron. Unfortunately, alpha-RGCs only represent about 6% of all RGCs; new strategies to promote regeneration in other types of RGCs are essential (Norsworthy *et al.*, 2017).

Drosophila also show subtype-specific neural regeneration. C3da and C4da are primary sensory neurons whose dendrites (receives information) tile the body wall of *Drosophila* larvae (Grueber *et al.*, 2003). Their somas (cell bodies) are adjacent to one another and they share the same axon bundle (sends information to brain) and dendritic fields (**Fig. 2.1C**). C4da is a nociceptor that detects harmful stimuli such as heat, noxious chemicals, and harmful light (Tracey *et al.*, 2003; Xiang *et al.*, 2010). C3da is a sensory neuron that detects gentle touch (Yan *et al.*, 2013). Song et al. (2012) discovered that upon axon cutting (axotomy), C4da regenerates robustly, while C3da does not. The intrinsic trait governing this subtype-specific regeneration is unknown, this system provides an ideal tool to uncover that trait.

1.4 What remains unknown

The identification of a novel treatment to promote regeneration would be extremely beneficial. Equally important is to understand subtype-specific regeneration so clinicians know that not every neuron can be regenerated in the same manner. Regenerating entire severed axon bundles may require multiple simultaneous treatments to ensure the majority of axons regenerate. Already combinatorial regeneration treatments have shown enhanced regeneration effects compared with single treatments in mouse models (Kadoya *et al.*, 2009; Kurimoto *et al.*, 2010; Sun *et al.*, 2011; O'Donovan, 2016). Current human therapies for spinal cord injury can only try to save remaining axons from degenerating, pro-axon regeneration treatment is limited to physical therapy and occasionally experimental stem cell transplants (Case and Tessier-lavigne, 2005; Tsintou, Dalamagkas and Seifalian, 2015). The axon regeneration success rate is usually low in these treatments and therefore any novel whole axon bundle approach to regeneration would greatly benefit patients.

To this end, this Thesis aims to answer these important questions: What causes subtype-specific regeneration? Is neural activity an intrinsic mediator of subtype-specific axon regeneration? If so, what mechanism is regulating neural activity during regeneration? If we can answer these questions, we are closer to understanding why and how different types of neurons regenerate differently. Perhaps we could predict how a neuron will respond to a given treatment based on its neural activity. If we know a neuron will have a low regenerative response

to a given treatment, perhaps we can manipulate its neural activity to achieve better results.

We are in a unique position to answer these questions with our single-cell 2-photon mediated axotomy model for subtype-specific regeneration. We can monitor and compare neuron activity in the regenerating C4da neuron and in the non-regenerating C3da neuron. We can manipulate neuron activity to promote or block regeneration. We can also perform genetic screens searching for the molecular mechanisms of subtype-specific regeneration.

The answers to these questions will provide researchers with a novel activity-dependent pathway to promote regeneration in certain cell types, as well as identifying the cellular and molecular intrinsic mediator of subtype-specific regeneration. Future studies should look for conservation of this phenomenon across different cell types. If the discoveries herein are conserved across species, they will provide novel therapeutic targets for patients suffering from nerve injury.

1.5 *Drosophila* as a model for subtype-specific regeneration

Drosophila neuron regeneration is remarkably similar to mammalian regeneration (Song *et al.*, 2012; He and Jin, 2016), and has the benefit of over 100 years of genetic tool building. This is a powerful system to investigate the cellular and molecular mechanisms that determine neuronal intrinsic regenerative ability. There are many reasons why *Drosophila* is an excellent model system to

study neuron activity and subtype-specific regeneration. Most salient is the powerful genetic toolkit generated for *Drosophila* over the past century. Precise spatial and temporal control of gene expression means we can reliably label and manipulate C3da and C4da neurons. The transparent cuticle allows for *in vivo* imaging, axotomy, and optogenetics. C3da and C4da are easily accessible for electrophysiology recording (Xiang *et al.*, 2010). We also anticipate that findings we make may be conserved in mammals because of anatomical similarities, like the mammalian DRG, C4da regenerates in the PNS, not the CNS, except with a priming cut (Song *et al.*, 2012). There are also molecular similarities, PTEN reduction increases mTOR signaling, which promotes regeneration, while overexpressing PTEN decreases mTOR signaling, which blocks regeneration (Song *et al.*, 2012), as has been observed in mammals (Park *et al.*, 2008). Another benefit of using *Drosophila* to study subtype-specific regeneration is the remarkable precision with which we can cut single axons using 2-photon microscopy ((Song *et al.*, 2012), described in Chapter II). This high resolution, manipulable, and quantifiable system is optimized for identifying the intrinsic mechanism of subtype-specific neuron regeneration.

Identifying the intrinsic mechanism that determines neuronal regenerative ability is crucial for developing novel therapeutic strategies for nerve regeneration for patients with spinal cord injury, peripheral neuropathies, nerve damage from surgery, and even neurodegenerative diseases such as multiple sclerosis and Alzheimer's disease (reviewed by He and Jin, 2016).

1.6 Thesis overview

In this Thesis I will demonstrate in Chapter II that subtype-specific neuron regeneration is mediated by neural bursting activities. After axotomy, the regenerative C4da neuron shows bursting activities and spontaneous calcium spikes while the non-regenerative C3da neuron does not show bursting activities or spontaneous calcium spikes. This is the first report that neuron activity is different in neurons of differing regenerative capacity. Blocking neural bursting activity in the regenerative C4da neuron blocks regeneration. Conversely, promoting neural bursting activity in the non-bursting, non-regenerative C3da neuron is sufficient to promote *de novo* regeneration. We also show for the first time that the pattern of bursting is important for optimal regeneration: high frequency consolidated bursts promote regeneration better than tonic firing. In Chapter III we identify through a reverse-genetic screen the L-type voltage-gated calcium channel (VGCC) Ca-α1D as a promoter of neuron bursting after axotomy. Knocking down the Ca-α1D channel reduces neuron bursting in C4da, this also results in significantly reduced neuron regeneration. Endogenous knock-in lines reveal Ca-α1D expression is higher in C4da than in C3da. This may explain why C4da is able to burst and regenerate upon injury while C3da cannot. Together our data identify a cellular and molecular intrinsic mechanism for subtype-specific neuron regeneration: neural bursting by Ca-α1D.

Chapter II

Subtype-specific neural regeneration is mediated by neural bursting activity

ABSTRACT

Some subtypes of neurons regenerate robustly, while other subtypes of neurons do not. We hypothesized that differences in intrinsic neural activity determine the regenerative ability of neurons, and furthermore, that manipulation of neural activity can either inhibit or promote regeneration. To test our hypothesis, we generated a 2-photon mediated axotomy model for single-cell analysis of the physiology of regenerating and non-regenerating neurons, C4da and C3da, respectively. We found that after undergoing Wallerian degeneration, regenerative C4da neurons alter their firing pattern to strong bursting, while the non-regenerative C3da neurons do not alter their firing pattern. This correlation between neuron bursting and regeneration is the first evidence of intrinsic activity differences between neurons of differing regenerative ability. We next determined that neuron bursting is necessary for the regeneration of the regenerative C4da neurons. We also found that using optogenetics to force the non-bursting, non-regenerating C3da neuron to burst was sufficient for *de novo* regeneration. Astonishingly, the pattern of activity we delivered was critical for robust regeneration. Strong bursting, but not tonic firing was sufficient to promote regeneration. Together, the data suggests that neural bursting activity is a cell intrinsic mediator of subtype-specific regeneration.

INTRODUCTION

The recent discovery that certain neuron subtypes can regenerate robustly while the majority cannot begs the question of what drives this subtype-specific neuron regeneration (Duan *et al.*, 2015). Neuron activity is known to be important for axon growth in early development and regeneration (Ming *et al.*, 2001; Goldberg, Espinosa, *et al.*, 2002; Singh and Miller, 2005; Udina *et al.*, 2008; Lim *et al.*, 2016; S. Li *et al.*, 2016), but to our knowledge, no studies have compared the intrinsic activity level of regenerative and non-regenerative neuron subtypes. This led to our hypothesis that neuron activity is the intrinsic mediator of subtype-specific neuron regeneration. To test this hypothesis, we needed a system that allowed for precision axotomy of a homogenous cell population for reliable neuron activity manipulation and quantification.

We turned to a model developed by Song and colleagues (2012), the peripheral sensory neurons of *Drosophila* larvae, in particular, C4da, a nociceptor, and C3da, a gentle touch sensor (Tracey *et al.*, 2003; Xiang *et al.*, 2010; Yan *et al.*, 2013). These neurons tile the body wall of *Drosophila* larvae, their dendritic fields overlap, they share the same axon bundle, and even project to adjacent interneurons that ultimately act on the same CNS target (Grueber *et al.*, 2003; Ohyama *et al.*, 2015). Interestingly, after axotomy and subsequent axon degeneration, the C4da neuron regenerates robustly while the C3da neuron does not regenerate (Song *et al.*, 2012). Their nearly identical extrinsic environment suggests that an intrinsic cue is mediating this subtype-specific

regeneration. To determine if neural activity is this intrinsic cue driving subtype-specific regeneration, we can benefit from *Drosophila's* many advantages. Firstly, *Drosophila* larvae are transparent so we can cut axons, quantify regeneration, and monitor calcium activity *in vivo*. These neurons are also accessible for electrophysiology recordings (Xiang *et al.*, 2010). The most salient advantage of *Drosophila* is the extensive genetic toolkit developed over the past century. This allows us precise spatial and temporal control of gene expression, including $K_{ir}2.1$, and inward rectifying potassium channel that blocks neuron activity, and channelrhodopsin (ChR2), a light activated ion channel that results in neuron activity upon light illumination (optogenetics). Using these tools, we can measure and manipulate neuron activity and monitor subsequent regeneration.

Clinically, promoting CNS regeneration is more important than PNS regeneration. In general, while some PNS axons can regenerate, almost no CNS axons can regenerate (Ramon y Cajal, 1928). This could be due to suboptimal extrinsic factors: lack of proper growth factors (Lindsay, 1988; Lewin *et al.*, 1997; Sterne *et al.*, 1997), glia scarring (Ramon y Cajal, 1928; Windle and Chambers, 1950; Pasterkamp *et al.*, 1999; Bundesen *et al.*, 2003)), and myelin associated inhibitors (Schnell and Schwab, 1990; McKerracher *et al.*, 1994; Huang *et al.*, 1999; Wang *et al.*, 2002). Unfortunately, optimizing the extrinsic environment does not result in significant regeneration for the majority of neurons. The results from 'priming' studies, where a pre-cut to the PNS to allow regeneration in the CNS, suggests that intrinsic promoters of regeneration can overcome these

extrinsic barriers (Mcquarrie and Grafstein, 1973; Richardson and Issa, 1984; Neumann and Woolf, 1999). Like mammalian DRG neurons, the C4da neuron has axon extending in the PNS and the CNS. The PNS regenerates while the CNS does not (Song *et al.*, 2012). If our hypothesis that neural activity mediates regeneration is supported, then can manipulating neuron activity promote CNS regeneration?

If intrinsic neural activity determines the regenerative ability of a neuron, this helps explain why certain subtypes of neurons can regenerate better than other subtypes. If neuron activity manipulation can promote regeneration in non-regenerative neurons, we might be able to manipulate the intrinsic activity level of a neuron to promote regeneration therapeutically. This manipulation could prove vital for neurons not normally amendable to other regenerative therapies.

RESULTS

Generation and characterization of 2-photon model for single cell axotomy

In order to study the intrinsic effects of severing a single axon, it was critical that we established a method for single-axon cutting without damaging any of the surrounding axons, wrapping glia, epidermis, etc (**Fig. 2.1C**). For this we turned to a method developed by Song and colleagues (2012) that employs a 2-photon laser to cut a single axon (Song *et al.*, 2012). The advantage of using a 2-photon laser in this context is clear when we compare the light path of regular confocal microscopy, which illuminates the entire sample but only a single z-

plane of light is collected, to the light of a 2-photon laser, which illuminates only a single z-plane of light and collects all the light. Axotomy with a confocal laser would result in a large, dual cone shape of damage to surrounding tissue, while axotomy with a 2-photon laser is constrained to a single point (**Fig. 2.1C**). Using the 2-photon laser, we were able to fine-tune the parameters detailed in Song et. al 2012 to achieve single-cell axotomy with no detectable damage to surrounding glia, epidermis, or axons (**Fig. 2.1D, 2.5A**), see Materials and Methods for parameters).
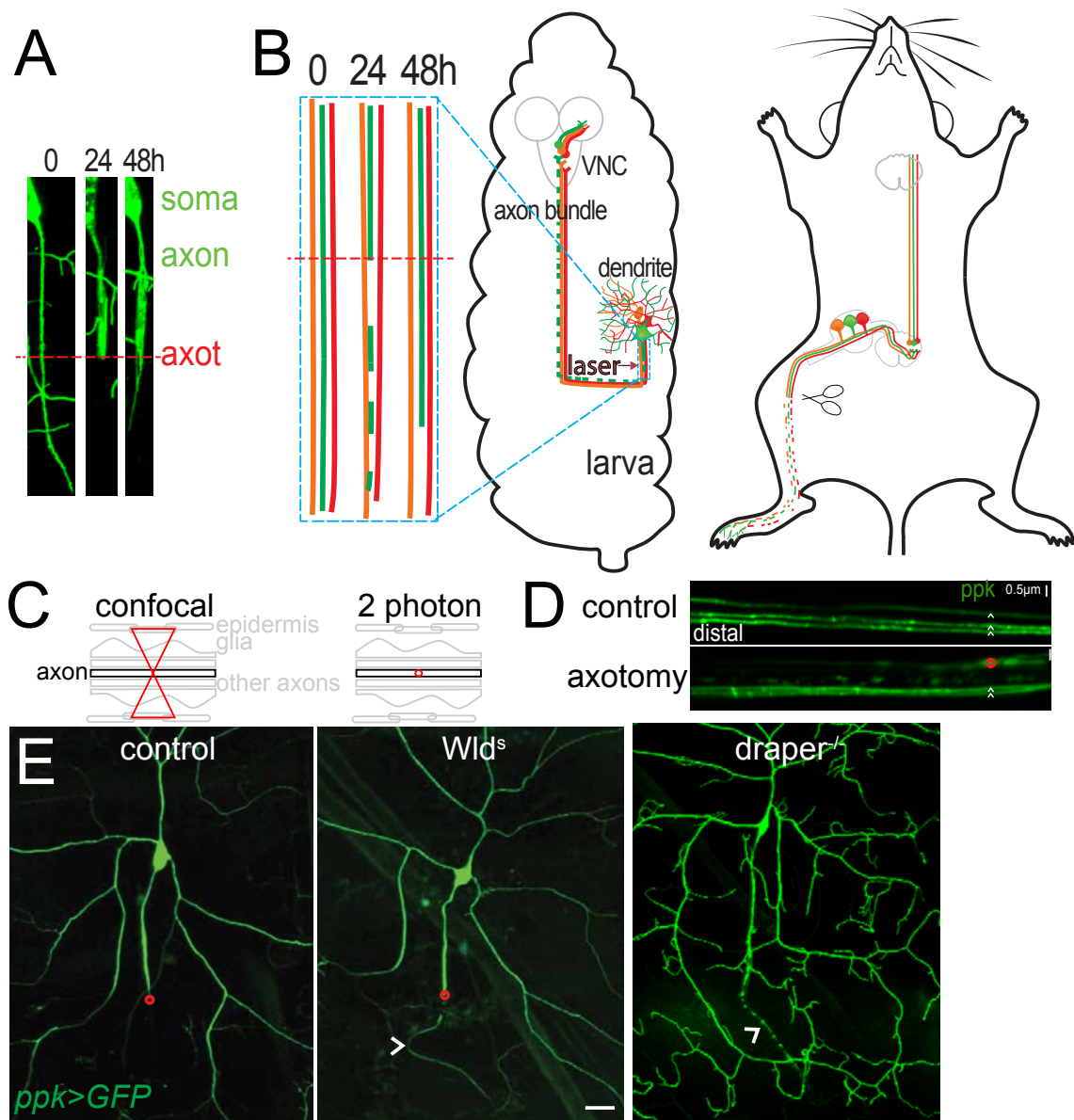
Figure 2.1 Characterization of 2-photon mediated single-cell axotomy. A, Schematic of single-cell axotomy of C4da neurons. A single cut axon distally degenerates by 24 hours post axotomy (hpa) leaving the proximal stump intact. By 48 hpa the proximal axon stump begins to regenerate. **B**, Schematic of single-cell axotomy in C4da in *Drosophila* larva compared to mouse Sciatic Nerve Lesion, note different axon polarity. **C**, Light illumination of confocal versus 2-photon microscope. **D**, Three C4da axons are labeled with GFP>Ppk (left), top panel shows uncut control, bottom panel shows single axon cutting specificity at 24hpa, the top axon is cut while the bottom two remain intact. **E**, wt control, Wallerian degeneration Slow (Wld^S) overexpressing, and draper mutant C4da neurons 24hpa. Axon is not degenerated in Wld^S or draper mutant larva, white arrowhead. Scale bar 20μm.

We axotomized a single C4da neuron and observed that the distal portion of the axon degenerates while proximal axon, soma, and dendrites remain intact (**Fig. 2.1A, B, E**). We noted similarities to a mouse model of axotomy called sciatic nerve lesion (SNL, (Kim and Chung, 1992)), this model is widely used to study axotomy and it's effect on the neuron in mouse (**Fig. 2.1B**, right). The distal degeneration we observed appeared to be Wallerian degeneration, an active process of degeneration (Waller, 1850), but to confirm we expressed inhibitors of Wallerian degeneration in C4da to determine if we could block this degeneration. We used the binary expression system of *Drosophila,* which allows us precise spatiotemporal control of gene expression. This system is composed of two elements: GAL4 is a transcription factor that binds to and activates its target, UAS. We can drive expression of GAL4 in specific cell types, for example sensory neurons, by using a tissue specific enhancer that is expressed only in sensory neurons. UAS is expressed in all cells, but it is only activated in cells that express GAL4, in this example, sensory neurons. By fusing UAS with any gene, for example green fluorescent protein (GFP), we can use this system to express GFP exclusively in sensory neurons.

We used the GAL4-UAS system to express WldS, a mutant protein that prevents Wallerian degeneration (Lunn *et al.,* 1989), in exclusively C4da neurons using the specific driver pickpocket. This prevented degeneration, suggesting that this process is Wallerian degeneration (**Fig. 2.1E**). We also confirmed our result by knocking out Draper, a gene necessary for the clearance stage of

Wallerian degeneration (MacDonald *et al.*, 2006). Degeneration was again

incomplete, this result was consistent with our previous finding that C4da

undergoes Wallerian degeneration upon axotomy (**Fig. 2.1E**).

Subtype-specific neuronal activity correlates with regeneration

C4da can regenerate, while it's neighbor, C3da, cannot (**Fig. 2.2A-D**,

C4da regeneration index 0.47, C3da index 0.03, and (Song *et al.*, 2012)). The

regeneration index is calculated by normalizing new axon growth to a fixed point

in the growing larva (see methods). To understand the intrinsic difference

between these two neurons that allows only one to regenerate, we performed

electrophysiology on regenerating neurons (24 hours post axotomy, hpa).

We recorded from C4da neurons and noted that the baseline firing pattern

changed to strong bursting upon axotomy (**Fig. 2.2E, F**). We also observed this

bursting phenomenon by calcium imaging (**Fig. 2.3A, B**). Simultaneous recording

and calcium imaging demonstrated a close correlation between neuron bursting

and calcium spikes (**Fig. 2.4C**). We defined an electrophysiology burst as five or

more action potentials (APs) with an interspike interval of less than 100ms, the

definition that best distinguishes control from axotomized neurons (**Fig. 2.4A**),

then we quantified the number of bursts per minute (**Fig. 2.2F**, axotomized 4.20

bursts/minute, control 0 bursts/minute) and the percent of APs found in bursts

(**Fig. 2.4B**, axotomized 34.96%, control 0%). Overall baseline firing was also

slightly increased after axotomy (**Fig. 2.2G**, axotomized 1.14Hz, control 0.57Hz).

We used calcium imaging to determine that exclusively axon cutting resulted in this bursting pattern, not dendrite cutting or damaging inflammation via UVC light (Babcock, Landry and Galko, 2009) (**Fig. 2.3E**). Calcium bursts are herein referred to as spikes for clarity. Neuron bursting activities can refer to either AP bursts or calcium spikes. Calcium spikes were detected using the FindPeaks function in Matlab (**Fig. 2.4D**). The output from this analysis provides values for spike prominence, or the intensity (amplitude) of a spike (**Fig. 2.4E**). This allows us to separate high frequency from low frequency spikes (**Fig. 2.4F**). This analysis confirms that while controls like uncut C4da occasionally show spikes, these spikes are of a low frequency nature (**Fig. 2.4F**). Bursting began as early as 6 hpa and continued through 24 hpa (**Fig. 2.3G**). When one single C4da axon was cut from within the bundle (**Fig. 2.1D**), specifically that axon showed the spiking activity, other intact axons did not show calcium spiking (**Fig. 2.3H, I**). This suggests that our single-cell axotomy model is not only morphologically specific, but functionally specific as well.

We also recorded from C3da neurons 24 hpa. Their typical firing pattern is similar to C4da, but interestingly, C3da neurons do not display burst firing after axotomy (**Fig. 2.2E, F**). We confirmed this with calcium imaging (**Fig. 2.3C-F**). Bursting ability mirrors the regeneration ability of these two neurons; namely, the non-bursting C3da neuron is unable to regenerate while the bursting C4da neuron regenerates robustly ((Song *et al.*, 2012), **Fig. 2.2A-D**). The factors that dictate this subtype-specific intrinsic regeneration ability remain unknown.
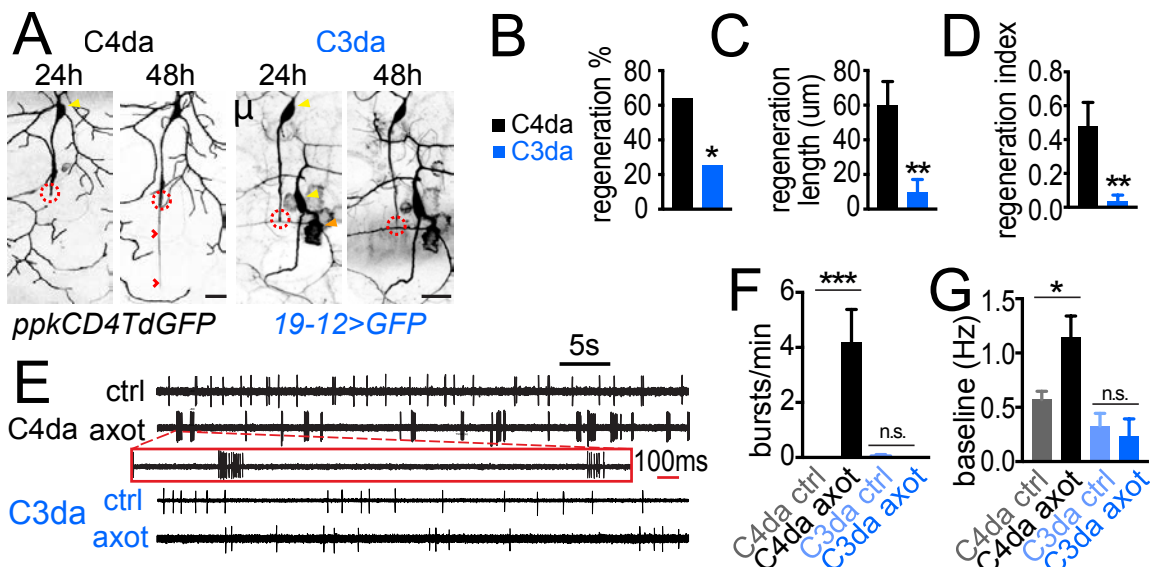
Subtype-specific neural regeneration correlates with neural activity. A, Example image of C4da neurons at 24 and 48 hpa with regeneration. Example C3da image at 24 and 48 hpa with no notable regeneration. Red circle indicates cut site, red arrowheads indicate regrowth, yellow arrowhead marks soma(s), orange arrowhead marks hemocyte debris. Scale bar 20µm. **B-D**, Regeneration quantification including percentage of larvae regenerated (**B**), regeneration length (**C**), and regeneration length normalized to growing larvae, termed the regeneration index (**D**) n=25, 12 for B-D. **E**, Example recordings showing baseline firing from C4da and C3da control and axotomized neurons scale bar 5s, red box is zoomed in on first two C4da axotomy bursts, red scale bar 100ms. **F-G**, E-phys quantification of neuron bursting (**F**) and baseline firing (**G**) n=17, 19, 10, 7. Fishers Exact Test (B), Student's t-test (C, D), one-way ANOVA with multiple comparisons and Bonferroni Correction (F, G). *$p<.05$, **$p<.01$, ***$p<.001$. Error bars represent SEM.
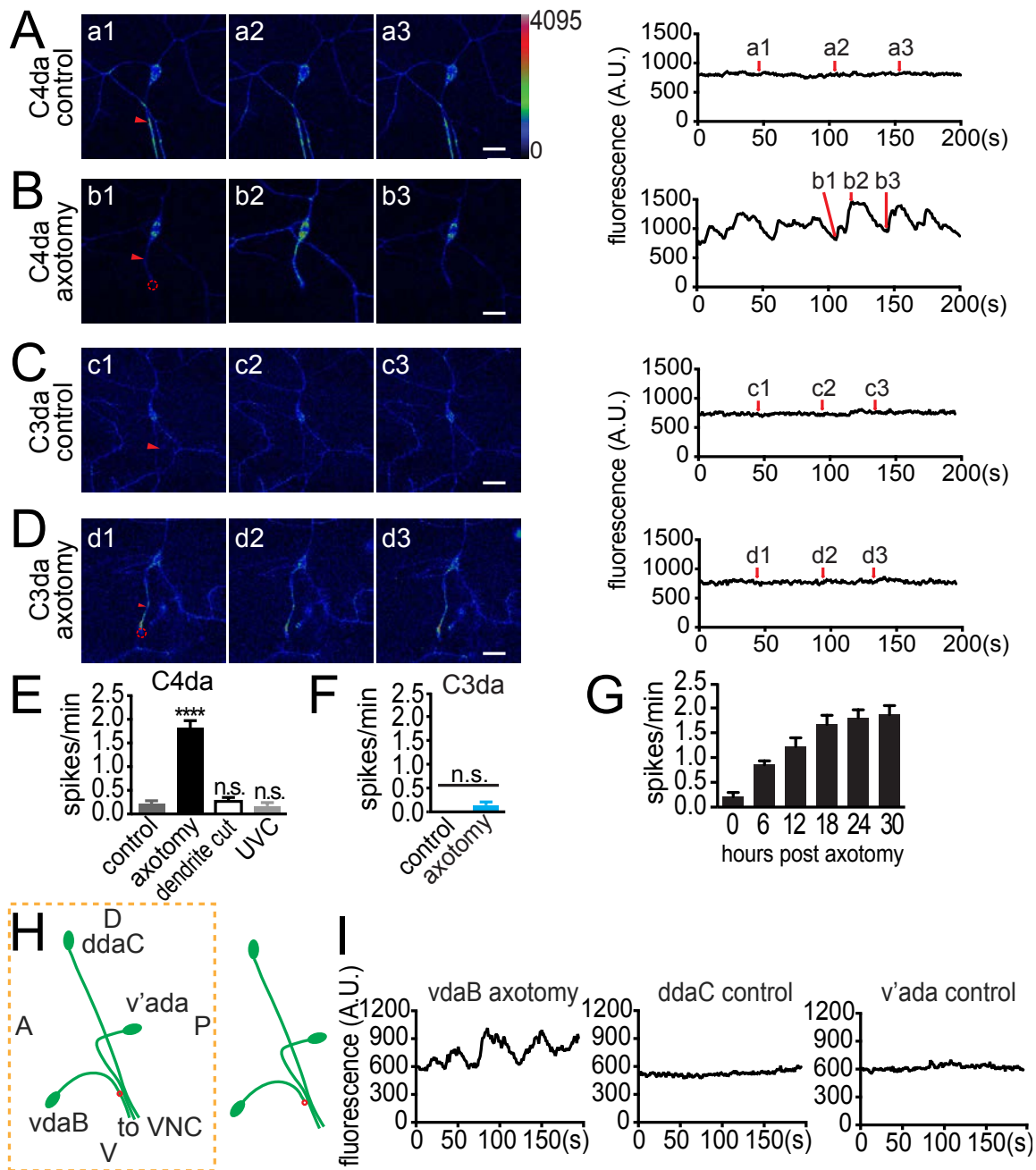
Figure 2.3 Subtype-specific neural regeneration correlates with neuronal calcium spikes. A-D, Example calcium imaging traces of C4da control (**A**) and axotomized (**B**) neurons and C3da control (**C**) and axotomized (**D**) neurons. Images are still frames at time point indicated by red arrow. Red arrowhead indicates axon of C4da or C3da. Red circle indicates cut site. Scale bar, 20μm. **E-F,** Summary of calcium imaging data measuring number of calcium spikes per minute, For C4da neuron, spikes were measured after axotomy, dendrite cut, and inflammation-inducing UVC treatment. C4da n=11, 26, 10, 10. C3da n=7, 7. **G**, Time course of C4da spontaneous calcium spikes, n=11, 9, 15, 22, 27, 12. **H**, Schematic of specific axotomy on ventral C4da axon (from axons in **Fig2.1D**). Left panel: Each hemi-segment possesses three C4da: ddaC (dorsal C4da) , v'ada (lateral C4da) and vdaB (ventral C4da). Dashed box represents body segment outline. Oval ball represents soma and curve line represents projecting axon. Three axons merge together to VNC. Red circle represents cut site on ventral C4da axon. D, dorsal. V, ventral. A, anterior. P, posterior. Right panel: 24h after ventral C4da axotomy, distal axon is degenerated while lateral and dorsal C4da axons are intact. **I**, Example GCaMP calcium imaging traces from three C4da in the same hemi-segment at 120h AEL. Among three C4da, only vdaB is axotomized at 96h AEL as **H** illustrates and only vdaB shows spontaneous calcium spikes.
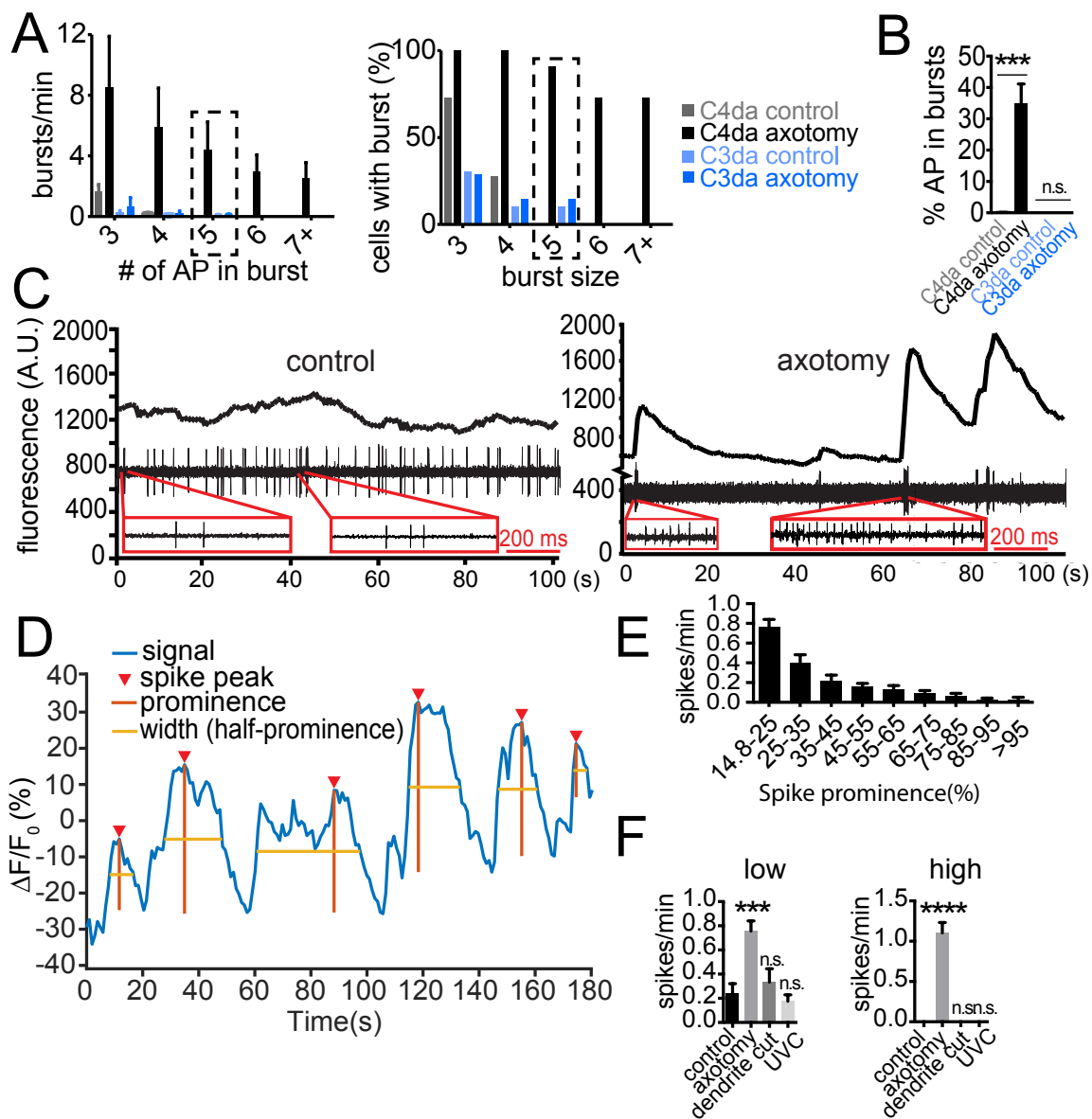
Figure 2.4 Defining a burst and spike. A, The average number of bursts per minute of a given burst size (# of APs), left. Right, the percent of C3da and C4da axotomized and control cells that show bursts (<100ms ISI) of a given AP number. 5 spike bursts was chosen as the minimum number to define a burst. n=17, 19, 10, 7. **B,** Percent of AP that are within bursts. One-way ANOVA with multiple comparisons and Bonferroni correction. ***p*<.01, n=17, 19, 10, 7. **C,** Simultaneous GCaMP imaging and recording show strong correlation between AP bursts and calcium spikes. **D**, Example GCaMP6 calcium imaging trace from **Fig**. **2.3B** after findpeaks function with matlab. Blue curve is normalized GCaMP6 signal. Red triangle marks the spike peak position. Vertical straight line indicates spike prominence (amplitude) based on program calculation. See methods for details. **E**. Distribution of spike prominences of spontaneous calcium spikes 24h after C4da axotomy at 96h AEL. n=11. **F**. C4da spontaneous spikes from **Fig. 2.3E**. are divided to into low and high prominence with an artificial cutoff of 25%. Only the axotomy group shows spikes with high prominence of more than 25%. n=11, 26, 10, 10. One-way ANOVA with Bonferroni Correction (**B, F**), ****p*<.001, *****p*<.0001. Error bars indicate SEM. One way ANOVA with Bonferroni Correction.

The order of events after C4da axotomy: degeneration, bursting, regeneration, hints that neuron bursting might be important for regeneration. It is unclear if bursting continues after the axon has regenerated, as third instar larvae usually pupate by this time point. One simple way of blocking regeneration in C4da is to sever the entire axon bundle including glia wrapping, as opposed to severing a single axon (Song *et al.*, 2012). We performed bundle cutting and recorded from C4da neurons (**Fig. 2.5A**). C4da neurons with complete bundle cutting no longer show bursting by electrophysiology, further supporting a correlation between neuron bursting after axotomy and regeneration (**Fig. 2.3B**).
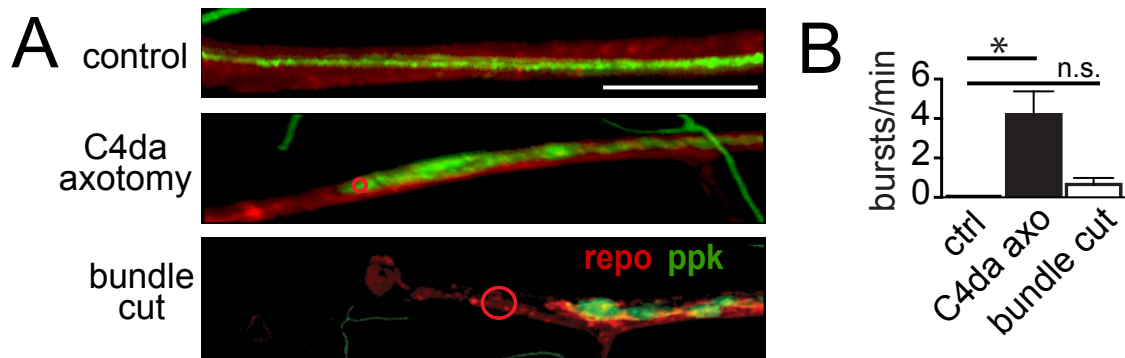
Figure 2.5. Integrity of glia sheath is necessary for C4da spontaneous bursting. A, Single C4da axon labeled with GFP>Ppk and glia wrapping labeled with TdTomato>Repo. Top, uncut control. Middle, single-cell C4da axotomy with glia intact. Bottom, large damage are with entire bundle severed including wrapping glia. Red circle represents area of laser illumination. Scale bar 20μm. **B**, Quantification of spontaneous bursting in control, C4da axotomy, and bundle cut neurons. One way ANOVA with Bonferroni Correction *p<.05.

Neuron activity is necessary and sufficient for regeneration

The correlation between bursting and regeneration begs the question of whether bursting is necessary for regeneration. We reduced neuron bursting by overexpressing the inward rectifying potassium channel ($K_{ir}2.1$) in C4da neurons (**Fig. 2.7D**). Preventing neuron bursting reduces regeneration (**Fig. 2.7A-C**, control index 0.18, $K_{ir}2.1$ index -0.04). Neuron bursting is necessary for regeneration.

We next tested whether neuron bursting is sufficient for regeneration. The average burst characteristics of C4da were determined (~4 bursts per minute, 7 APs per burst, ISI=41 ms, **Fig. 2.6A**). By expressing the light activated ion channel, channelrhodopsin (ChR2) in non-bursting, non-regenerative C3da neurons, we were able to use blue light pulses to mimic C4da bursting (**Fig. 2.6B, C,** (Zhang *et al.*, 2007)). We found that C3da neurons forced to burst fire regenerated nearly as well as the intrinsically regenerative C4da neurons (**Fig. 2.7H-J** C3da>ChR2 index 0.28, C4da index 0.47 from **Fig. 2.2**). Control neurons lacking any part of the optogenetic system (ChR2, retinol, light) did not regenerate (**Fig. 2.7I, J**, index: 0.06, 0.06, 0.05).

Neuron activity has been shown to promote regeneration (Udina *et al.*, 2008; Lim *et al.*, 2016; S. Li *et al.*, 2016). Because promoting bursting in C3da increases overall activity of the neuron, we asked if neuron bursting or just overall activity increase was responsible for promoting regeneration. To distinguish these possibilities, we used a series of ChR2 induced firing patterns

in C3da: the original burst firing protocol, a semi-tonic protocol, and a tonic

protocol (**Fig. 2.7G**). The semi-tonic firing pattern resulted in the same overall

number of APs per minute (~25 APs/min, **Fig. 2.7G**) but the pattern was spread

out resulting in smaller bursts than the original burst protocol (~2.5 vs ~6.5

APs/burst, **Fig. 2.7F**). For the tonic light protocol, AP was spread out even

further, resulting in 1.4 APs/burst every 2 seconds (**Fig. 2.7F**). This led to

significantly higher number of AP/minute compared to burst and semi-tonic light

protocols (42 vs 25 APs/min, **Fig. 2.7G**). If only overall activity increase was

promoting regeneration, we would expect the tonic firing protocol to have even

more robust regeneration than the burst firing protocol. This is not what we

observed, instead we found that tonic firing does not result in significant

regeneration, only burst firing had a significant regenerative effect for both the

regeneration index and percentage (**Fig 2.7I, J**). There is a trend towards higher

regeneration, so we cannot exclude the possibility that general activity increase

slightly promotes regeneration, but the effect is clearly not as robust as the burst

firing. The semi-tonic light pattern resulted in significant regeneration based on

the regeneration index, but not the regeneration percentage (**Fig. 2.7I, J**). Again

we do see a trend towards even higher regeneration with the semi-tonic light

protocol. We delivered the tonic, semi-tonic, and burst light pattern while

recording the neuron's calcium response and found that the burst light pattern

triggered a strong calcium spike, the tonic and semi-tonic light pattern did not

result in as significant a change in calcium levels (**Fig. 2.6D-F**). These results

together suggest that neuron bursting is sufficient to promote neuron

regeneration.

A C4da axotomy

B C3da ChR2 burst

C

D tonic, 5ms blue

E semi-tonic, 30ms blue

F burst, 300ms blue

G GCaMP influx after ChR2 stimuation
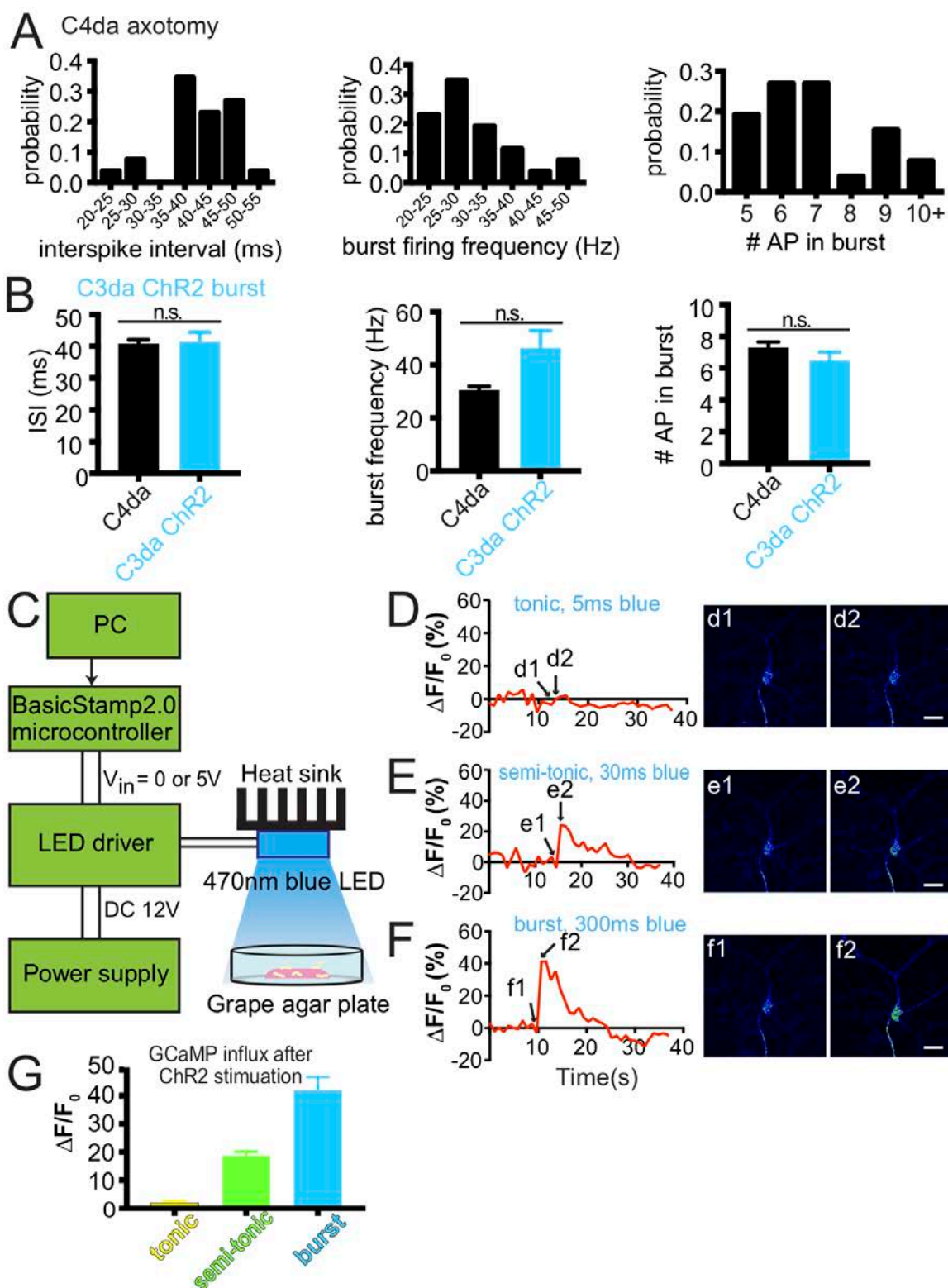
Figure 2.6. Optogenetics methods for inducing burst, semi-tonic, and tonic firing. A, C4da detailed burst analysis to identify average interspike interval (ISI), frequency of firing within a burst and the number of AP in a burst, n=26. **B,** A blue light intensity/duration that activates C3da>ChR2 to match the ISI, frequency, and AP number in C4da, n=26, 6. **C,** Schematic of ChR2 light delivery set up, briefly, we use a computer to set up the BasicStamp 2.0 microcontroller to deliver specific light pulses from a 470nm LED onto our larvae in a grape agar plate. **D-F**, GCaMP influx while delivering tonic (**D**), semi-tonic (**E**), and burst light patterns (**F**) n=8, 8, 8. Quantified in **G**. Student's t-test (B).
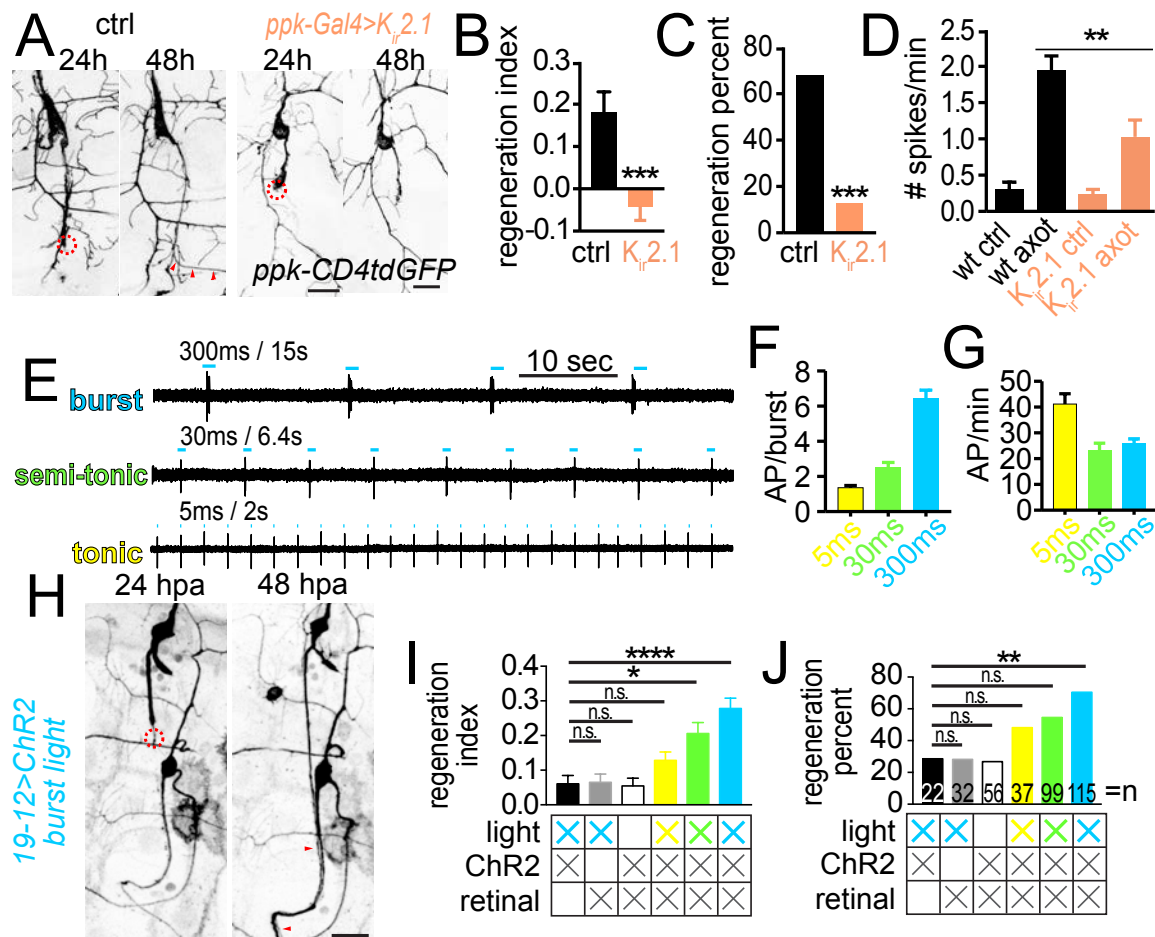
Figure 2.7. Neural burst activity pattern is necessary and sufficient for regeneration. A, Sample C4da regeneration images for wt control and $K_{ir}2.1$ larvae with quantification (**B**, **C**). Red circle indicates cut site, red arrowhead shows axon regeneration. n=25, 16. **D**, Calcium imaging spikes per minute quantification for wt larvae and larvae overexpressing $K_{ir}2.1$ under control and axotomy condition. n=10, 11, 10, 10. **E**, Representative electrophysiological recordings for burst, semi-tonic, and tonic light pattern. Blue lines represent light delivery, lines not to scale. **F**, number of AP triggered by each light pulse (burst). **G**, Total number of AP per minute for each of the three light patterns n=11, 7, 7. **H,** Sample regeneration images for C3da neurons bearing ChR2 with burst light stimulation, scale bar 20μm. **I-J,** regeneration quantification for ChR2 experiments including 3 controls (no retinal n=22, no ChR2 n=14, no light n=56) and 3 light patterns (tonic n=37, semi-tonic n=99, burst n=115). Fishers Exact Test (C), Student's t-test (B), one-way ANOVA with multiple comparisons and

Bonferroni Correction (D, I). Chi-squared test with post hoc pairwise comparison via Fisher's Exact test (J). $*p<.05$, $**p<.01$, $***p<.001$. Error bars indicate SEM.

Neuron activity has been shown to promote regeneration (Udina *et al.*, 2008; Lim *et al.*, 2016; S. Li *et al.*, 2016). This is the first study to show intrinsic differences in neuronal activity between regenerative and non-regenerative neuron subtypes and to furthermore show that neuronal activity is both necessary and sufficient for regeneration. This is also the first report that not just overall neuronal activity, but activity pattern is critical for regeneration. Neuronal activity pattern mediates subtype-specific neuron regeneration.

Neural activity and regeneration in the CNS

New treatments for regeneration in the CNS are just as therapeutically important as treatments for regeneration in the PNS. For this reason, we looked closer at the distal portion of the C4da axon that lies in the CNS. Excitingly, while C4da axon regenerates in the PNS, C4da does not regenerate in the CNS (Song *et al.*, 2012). This *Drosophila* model mimics what is observed in mammalian DRG neurons. We cut C4da axon in the CNS (**Fig. 2.8A**) and recorded from the somas 24 hpa. We did not observe bursting by electrophysiology (**Fig. 2.8B, C**). The correlation between neuron bursting and regeneration led to our hypothesis that perhaps optogenetics-induced busting would result in CNS regeneration, as it led to C3da regeneration.

We cut axons within the CNS as previously published (Song *et al.*, 2012). We expressed ChR2 in C4da neurons and identified a light pattern that resulted in bursting comparable to C4da PNS axotomy conditions (**Fig. 2.8B, D**). Upon

CNS axotomy, we delivered this light pattern to the larvae for 48 hours but did

not observe significant regeneration (**Fig. 2.8E**). This result does not support our

hypothesis that neuron bursting can promote regeneration in the CNS.
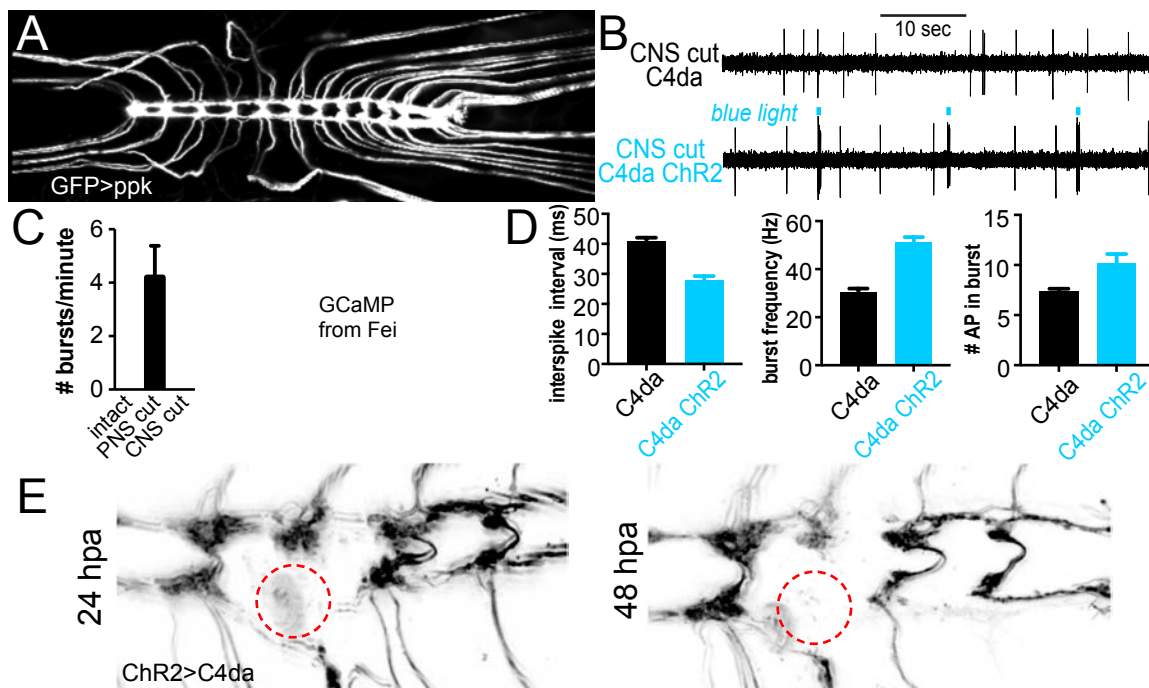
Figure 2.8 Neuron bursting is not sufficient to promote CNS regeneration in C4da. A, C4da neurons labeled with GFP>ppk at their nerve terminals in the CNS. **B**, Ephys recording shows no bursting after CNS axotomy, top. Bottom, recording of axotomized C4da neurons expressing ChR2 forced to burst by blue light pulses (blue line). **C**, Quantification of C4da bursting in intact, PNS axotomy, and CNS axotomy conditions. **D**, Detailed burst analysis of C4da with PNS axotomy (black) and CNS axotomy with ChR2 (blue) showing interspike interval, burst frequency, and the number of AP per burst. **E**, CNS axotomy (red circle=damage area) does not show regeneration by 48 hpa.

DISCUSSION

We have identified neural bursting activities as an intrinsic mediator of subtype-specific neural regeneration. We cannot conclude whether it is AP bursting or calcium spikes driving this regeneration. The two are difficult to untangle. It could be that AP bursting alone is sufficient to promote regeneration, or it could be that AP bursting is just a means of inducing calcium spikes and if we could drive calcium spikes alone, this might be sufficient for regeneration. To determine which is true, one could use a sodium channel blocker that blocks AP but not calcium spikes. Alternatively, a calcium sponge such as parvalbumin might block calcium spikes but not AP bursting (Weavers *et al.*, 2016).

C4da burst firing not only occurs after axotomy, but also in response to noxious high temperatures. At 44°C C4da neurons display strong burst firing (Terada *et al.*, 2016). Since burst firing is both a normal physiological response of the C4da neuron and is also necessary for regeneration of the C4da neuron, it is possible that the firing pattern of C3da during a normal physiological response might promote C3da axon regeneration more robustly than mimicking the C4da bursting. C3da detects gentle touch and displays a strong "on" response and weak "off" response upon prolonged mechanical stimulation by dendrite displacement (Yan *et al.*, 2013). Using ChR2 to mimic this endogenous C3da firing pattern in axotomized C3da neurons might result in more robust axon regeneration. This would suggest that physiological levels of neuron activity are

optimal for maximizing axon regeneration, more so than neural bursting, which is a pattern intrinsic to C4da.

It is interesting that only axon cutting, but not dendrite cutting results in neuron bursting. This could be explained by the observation that axon cutting, but not dendrite cutting, dramatically upregulates the number of growing microtubules (Stone *et al.*, 2010). Axons and dendrites also have subtly different expression profiles (Kunimoto, 1995; Sheehan *et al.*, 1996; Wilson *et al.*, 2000). This result shows that the neuron bursting phenotype we observe in C4da is very specific to axotomy conditions, and not to general injury conditions as observed by the lack of bursting after dendrite cutting or UVC-induced inflammation. The time delay between axotomy and initial bursting (~6-12 hpa) suggests a transcriptional mechanism may play a role in bursting.

The dramatic effect of entire bundle cut, including glia wrapping, which prevents both neural bursting activity and regeneration in C4da, begs the question of whether we could induce bursting after bundle cutting to promote regeneration. This experiment would tell us if neuron bursting activity can overcome even structural challenges, such as lack of glia tract as guide and trophic support, to navigate a new terrain and promote regeneration. The answer may provide clues about what we can expect to observe in mice and humans, where it is unlikely that one single axon only is cut. In fact, it is usually an entire bundle of axons and glia that are injured in mouse models and human disease.

There are many potential reasons why we couldn't see regeneration in the CNS after inducing bursting. Primarily, that bursting activity is not sufficient to drive regeneration in the CNS of C4da. It is also possible, however, that our method for inducing bursting was not strong enough to drive regeneration. Action potential propagation may be weakened after traveling from the soma all though to the distal part of the axon in the CNS. Especially given the axon was damaged, transport and glia buffering might not be functioning at normal levels. To determine if weak AP propagation is the reason for no regeneration, future experiments should determine if there is calcium burst activity in the CNS during ChR2 stimulation using GCaMP imaging. It is possible that the bursts need to be stronger (higher intensity light delivery) to reach the CNS or that we should use a drug, 4-AP (voltage gated potassium channel blocker, 4-aminopyridine), shown to promote faithful action potential propagation in a regenerating neuron with damaged glia (Bei *et al.*, 2016). Alternatively, if there were no problem with AP propagation, it would be interesting to combine neuron activity promotion with a genetic approach to 'sensitize' the neuron to regeneration. Perhaps combining PTEN deletion or priming cut, which have been shown to promote CNS regeneration in *Drosophila*, with ChR2-induced bursting would drive stronger regeneration than either treatment alone (Song *et al.*, 2012).

In addition to the above CNS regeneration experiments, future studies should look for conservation of this phenomenon in other types of neurons. As neural activity has already been implicated in regeneration in mammals (Udina *et*

al., 2008; Lim *et al.*, 2016; S. Li *et al.*, 2016), it is possible that more examples of intrinsic neural activity regulating neuron regeneration ability will be discovered. It would be especially intriguing to measure the bursting activity of α-RGCs compared to other non-regenerative RGC types in the study performed by Duan et al 2015. A study has shown that α-RGCs in fact have higher basal activity levels as compared with other types of RGCs (Krieger *et al.*, 2017). This difference in activity level also explains the high mTOR levels observed in α-RGCs, as neural activity promotes mTOR activity (S. Li *et al.*, 2016). Assuming conservation of this correlation between neural activity and regeneration, efforts should be targeted towards manipulating neural activity with optogenetics to test the effect of different light patterns on regeneration in non-regenerative neurons.

Even assuming our hypothesis is true and conserved in other neuron subtypes, there are still several not so trivial obstacles to overcome for functional regeneration. Neural activity promotes axon extension after axotomy, but that is just the first step in the complex process of regeneration (Tedeschi and Bradke, 2017). The elongating axon must find its synaptic partner(s), likely receiving directional cues from neurotrophins, as in early axon development (O'Donovan, 2016). Once the axon has reached its target, the motile growth cone must differentiate into a presynaptic terminal capable of releasing neurotransmitters onto its target for neuron communication to occur (Tedeschi and Bradke, 2017). Finally, for fast transmission, the newly formed axon must remyelinate, this does not always occur naturally after regeneration, as was observed by Bei et al 2016.

Regenerated RGC axons were not functional until they used a drug 4-AP to artificially promote conduction in the place of myelin (Bei *et al.*, 2016). In our model, we are only concerned with overcoming this first barrier to regeneration, promoting axon elongation, but whether these other steps will naturally follow or require human intervention remains to be seen.

MATERIALS AND METHODS

Axotomy

Axotomy was performed 80-85h AEL (after egg laying) unless otherwise stated. We followed the protocol in *Song et. al 2012* with several modifications. Briefly, a larva was anesthetized with Sevofluorane for 3 minutes and mounted dorsal side up (for PNS) or ventral side up (for CNS). The bleaching function of a Zeiss 2-photon laser damaged a small circle on the axon with an ROI of ~1.5μm. We found 910nm worked well for this. PNS axons were cut three quarters of the way to the bipolar dendrite, while CNS axons were cut as in *Song et al 2012*. Following axotomy, larva recovered on a damp Kim Wipe and then were transferred to recovery vials containing regular brown food or white grape juice agar plates (for following optogenetic stimulation).

Optogenetics stimulation

Larvae were grown in regular brown food containing 400μM all trans retinal (ATR, sigma #R2500) at 25°C in constant dark condition. On 80h-85h AEL, early

3rd instar larvae were transferred from food, rinsed with water and anesthetized with sevoflurane vapor for axotomy injury. They recovered in regular brown ATR food for 6h in darkness. Next, we put them on a 35mm petri dish with 1mL white grape juice agar plates (made 1-2 days before) covered in dark condition for optogenetic stimulation thereafter. At 24 and 48 hours after axotomy, axon regeneration was measured by confocal microscopy.

470nm blue LED (LUXEON Rebel LED, mounted on a 10mm square coolbase and 50mm square and 25mm high alpha heat sink) was set over the grape-agar plate for ChR2 activation. Light pattern was programmed with BASIC Stamp 2.0 microcontroller and buckpuck DC driver (LUXEON, 700mA, externally dimmable).

Electrophysiology

Extracellular recording of C4da neuronal activity was performed as described previously (Xiang *et al.*, 2010). Axotomy was performed ~80h AEL. ~104 h AEL third instar larvae were dissected to make fillet preparations. Fillets were prepared in external saline solution composed of (in mM): NaCl 120, KCl 3, $MgCl_2$ 4, $CaCl_2$ 1.5, $NaHCO_3$ 10, trehalose 10, glucose 10, TES 5, sucrose 10, HEPES 10. The Osmolality was 305 mOsm kg^{-1} and the pH was 7.25. GFP-positive (C4da) neurons were located under a Zeiss D1 microscope with a 40X/1.0 NA water immersion objective lens. Gentle negative pressure was

applied to the C4da neuron to trap the soma in a recording pipette (5 µm tip

opening; 1.5–2.0 MΩ resistance) filled with external saline solution. Recordings

were performed with a 700A amplifier (Molecular Devices, Sunnyvale, CA), and

the data were acquired with Digidata 1440A (Molecular Devices) and Clampex

10.6 software (Molecular Devices). Extracellular recordings of action potentials

were obtained in voltage clamp mode with a holding potential of 0 mV, a 2 kHz

low-pass filter and a sampling frequency of 20 kHz.

Burst analysis

For the purposes of data analysis, a burst was defined as 5 or more APs each

having an interspike interval of less than 100ms. This definition clearly

differentiated axotomized from control neurons (Figure S1). The 'Burst Analysis'

function on Clampfit 10.6 was used to detect bursts.

Calcium Imaging

GCaMP calcium imaging of C4da neuronal activity was performed as described

previously (Xiang *et al.*, 2010). For *in vitro* calcium imaging, axotomy was

performed at 96h AEL and 120h AEL 3rd instar larvae were pinned ventral side up

on silicone elastomer plates and dissected in the same external saline solution

as electrophysiology. The internal organs were removed with fine forceps and the

body wall was stretched with insect pins after opening body wall. Time-lapse

imaging was performed under water objective lens (W Plan-Apochromat 20x/1.0

DIC CG=0.17 M27 75mm) by Zeiss LSM 700 confocal microscope. Frame rate is 0.97Hz. All soma ROIs were corrected for horizontal drifting with ImageJ slice alignment. Uncut C4da neurons from the same 3rd instar larvae were used as negative controls.

For UVC treated larvae, as an inflammatory nociception model (Babcock, Landry and Galko, 2009), larvae at 96h AEL were mounted dorsal side up with double-sided tape on microscope slides and placed in Spectrolinker XL-1000 ultraviolet crosslinker (Spectronics Corporation) with 20mJ/cm^2 254nm UV exposure. After treatment, larvae were recovered in regular food and imaged at 120h AEL.

Calcium imaging analysis

Each C4da or C3da neuron was imaged for 5 minutes as one sample unless otherwise stated. Original fluorescence signal (F) was firstly normalized to average intensity (F_0) of each sample by using following formula:

$F'=(F-F_0)/F_0$

After normalization, we utilized the findpeaks (to find local maxima) function in Matlab (MathsWorks incorporation) to extract and quantify calcium spike peaks from noisy background. Fluorescence signals in uncut C4da neurons also show some weak and irregular calcium spikes with minor prominence (small fluorescence amplitude). To rule out these weak spikes and render strong spikes to stand out (see simultaneous recording and calcium imaging figure), we first

calculate the standard deviation (σ) of time-lapse fluorescence signal in each uncut C4da neurons from 120h AEL larvae, then calculate the mean value of σ ($\overline{\sigma}$, n=11). We artificially set the three fold of $\overline{\sigma}$ ($3\overline{\sigma}$, here is 0.148) as minimum peak prominence (amplitude) parameter in findpeaks function.

After we get the position, quantity and prominence of each spike in one sample, we divide the quantity of spikes by recording duration (5 minutes, unless otherwise stated) as spike frequency and calculate the mean value of prominence from each spike as spike amplitude.

Regeneration analyses

We performed quantitative analysis in accordance with (Song *et al.*, 2012) with some modifications. Briefly, we took two images for each neuron at 24hpa (L_1) and 48 hpa (L_2). All axon growth that occurred in this time frame was counted as regeneration. We calculated Regeneration Length as L_2-L_1. The larvae are growing during this time period, so the Regeneration Index normalizes Regeneration Length to a fixed length in the larvae, namely, the length from the C3/4da soma to the bipolar dendrite (BD): L_1/BD_1 - L_2/BD_2. We also quantified the Regeneration Percentage as the percentage of larvae with a Regeneration Index ≥0.07.

Regeneration Imaging

We anesthetized larvae 24hpa using Sevoflurane and flattened larvae between a slide and coverglass with a thin bumper around the edge to maximize flatness without lethality. We always cut dorsal axon on the right side of the larva so we could easily identify the axotomized neuron. We took a z-stack image through the dendrites, soma, and axon of the axotomized neuron using a Zeiss D1 Confocal Microscope with a 20X water objective. We then recovered larvae on a wet kim wipe and transferred them to recovery vials/ grape agar plates depending on the experiment (see optogenetics Methods). At 48 hpa we again anesthetized the larvae and identified the same neuron by morphology of its dendrites and took a second image using the same parameters.

Fly Genotypes

note: X chromosome is w1118 unless otherwise noted. Chromosome IV has been omitted for simplicity.

Figure 2.1-2

PpkCD4TdGFP/+;UAS-Wld^S/+

PpkCD4TdGFP/+; +

Repo-Gal80/UAS-YFP; 19-12-Gal4/+

Figure 2.3

;;ppk-LexA,LexAop-myr:GCaMP6s/+   (C4da imaging)

;;NoMPC-LexA/LexAop-myr:GCaMP6s   (C3da imaging)

Figure 2.4

PpkCD4TdGFP/+; +

Repo-Gal80/UAS-YFP; 19-12-Gal4/+

;;ppk-LexA,LexAop-myr:GCaMP6s/+   (C4da imaging)

;;NoMPC-LexA/LexAop-myr:GCaMP6s   (C3da imaging)

Figure 2.5

PpkCD4TdGFP ; repo-Gal4, UAS-tdTomato

Figure 2.6-7

Kir regeneration

PpkCD4TdGFP/UAS-Kir2.1; Ppk-Gal4

PpkCD4TdGFP/UAS-Kir2.1; +

 (Kir2.1 overexpression)

ppk-Gal4/UAS-Kir2.1; ppk-LexA,LexAop-myr:GCaMP6s /+

ppk-Gal4/+; ppk-LexA,LexAop-myr:GCaMP6s /+

Optogenetic experiments

Repo-Gal80/UAS-ChR2-YFP; 19-12-Gal4/+

Repo-Gal80/UAS-YFP; 19-12-Gal4/+

Figure 2.8

PpkCD4TdGFP/+

ACKNOWLEDGEMENTS

Kendra Takle Ruppell[a, c], Fei Wang[a, c], Feng Li[b, c], Pavi Guttipatti[b], Ye Shang[a],

Yuanquan Song[b], Yang Xiang[a, d]

[a]Department of Neurobiology, University of Massachusetts Medical School, 364

Plantation Street-LRB725, Worcester, USA 01605

[b]Children's Hospital of Philadelphia, 3501 Civic Center Boulevard, Philadelphia,

PA, USA 19104

[c]These Authors contributed equally to this work

[d]Corresponding author, University of Massachusetts Medical School, 364 Plantation

Street-LRB725, Worcester, USA 01605. Yang.Xiang@umassmed.edu

Contributions Summary: K. T. R., F.W., Y.X. and Y.So. designed the

experiments.

K. T. R. performed preliminary experiments relating to Figure 2.3

K. T. R. performed experiments shown in Figure 2.1, Figure 2.2, Figure 2.4 A-C,

Figure 2.5, Figure 2.6 E-J, Figure 2.7 A-C, Figure 2.8

F. W. performed experiments shown in Figure 2.3, Figure 2.4 D-F, Figure 2.6 D,

Figure 2.7 C-G,

Y.So., F. L., P.G. performed experiments shown in Figure 2.6 A-C

K.T.R wrote the manuscript.

Chapter III

An L-type voltage gated calcium channel promotes neural bursting activities and subsequent regeneration of C4da

ABSTRACT

To determine the molecular mechanism promoting the neural bursting that leads to subtype-specific regeneration in Chapter II, we performed a candidate-based reverse genetic screen for ion channels that affect neuron bursting after axotomy. We discovered that an L-type voltage gated calcium channel (VGCC) promotes neuron bursting and subsequent regeneration. This VGCC, Ca-α1D, has high expression in the regenerative neuron and weak expression in the non-regenerative neuron. This may explain why the regenerative neuron can burst and regenerate, while the non-regenerative neuron cannot. Together, our findings suggest that Ca-α1D could be the molecular mechanism driving subtype-specific regeneration, that is, why certain subtypes neurons are able to regenerate while other neurons cannot.

INTRODUCTION

Our discovery that neural bursting activity mediates subtype-specific neuron regeneration (detailed in Chapter II, summarized below) aroused questions about the molecular origin of this neural burst activity after axotomy. Discerning how some subtypes of neurons are able to burst and subsequently regenerate, while other subtypes of neurons can neither burst nor regenerate would offer researchers and clinicians a molecular handle with which to predict, monitor, and manipulate regeneration.

In Chapter II we learned that after injury, not all neurons have the same intrinsic regenerative ability. Some neurons, for example Class IV dendritic arborization (C4da) neuron, regenerates robustly while other neurons, for example Class III dendritic arborization (C3da) neuron, does not regenerate (Song *et al.*, 2012). This general phenomenon is called subtype-specific neuron regeneration (Duan *et al.*, 2015; Norsworthy *et al.*, 2017; Nieuwenhuis *et al.*, 2018). Studies to elucidate the intrinsic mechanism mediating subtype-specific regeneration are ongoing (reviewed in Liu *et al.*, 2011). We show in Chapter II that upon axotomy, C4da shows strong neuron bursting activity by electrophysiology and calcium imaging. This bursting activity is necessary for axon regeneration. We also show that C3da does not alter its firing pattern upon axotomy, and it subsequently does not regenerate. Excitingly, use of optogenetics to induce neuron bursting in C3da is sufficient to promote *de* novo regeneration. Furthermore, the pattern of neural activity is critical for robust axon

regeneration: strong consolidated bursting regenerates better than a tonic increase in firing. We conclude that neural bursting activity is the intrinsic mediator of subtype-specific neuron regeneration. This novel report demonstrates why some neurons can regenerate while others cannot. It also provides an innovative therapeutic target for clinicians working to treat nerve injury from stroke, spinal cord injury, and neurodegenerative diseases. The work in this Chapter aims to go one step deeper into our understanding of subtype-specific neuron regeneration in C3da and C4da. We identified neural activity as the cellular mechanism of subtype-specific regeneration, but now we ask, what is the molecular mechanism? We know that differing levels of neuron activity dictate differing regeneration rates, but we do not have any hints as to why some neurons might have intrinsically higher levels of neural bursting activity. In this Chapter we ask the following: Why do some neurons have high neural bursting activity that allows them to regenerate while other neurons are unable to burst? What is the molecular mechanism driving this differential neural bursting response after axotomy? The answers to these questions will confer insight into the molecular mechanism of neural activity as a mediator of subtype-specific regeneration. It is also likely that any molecules we identify could be considered as therapeutic targets for nerve regeneration after injury. Manipulating neuron activity therapeutically could prove challenging in certain situations, but using an agonist to activate a specific molecule might be more feasible in those situations.

A burst is defined as a group of action potentials (APs) in rapid succession followed by a pause (Zeldenrust, Wadman and Englitz, 2018). Bursting in neurons is usually a sign that the cell is hyperexcitable (Skinner *et al.*, 1999). If neuronal activity is important for regeneration, it follows that ion channels play a salient role in mediating regeneration, as ion channels regulate neuronal excitability (Bernstein, 1902; Simms and Zamponi, 2014). Based on this fact, we performed a candidate-based reverse genetic screen to identify ion channels important for neural bursting in C4da. From this screen we identified two ion channels that regulate neural bursting in C4da: BK (big conductance potassium channel) and Ca-α1D (an L-type voltage gated calcium channel).

BK channels are expressed in nearly every cell where they play myriad roles in vascular tone regulation, bladder tone regulation, urinary K^+ excretion, and retinal circulation (reviewed in Vetri *et al.*, 2014). They are better known for their role in neurons, where they are involved in neuronal excitability and neurotransmitter release ((Wang *et al.*, 2001; Chen, Cai and Pan, 2009; Cao *et al.*, 2012). BK channels have also been implicated in brain ischemia (Liao *et al.*, 2010).

The mammalian homologue of Ca-α1D is Cav1.3 (cacna1d, 62% similarity 51% identity). $Ca_v1.3$ has low threshold activation, fast activation, and slow inactivation (Calin-Jageman and Lee, 2008). These features enable Cav1.3 to promote spontaneous and burst firing (Calin-Jageman and Lee, 2008). Cav1.3 promotes spontaneous firing (Cooper and White, 2000; C. Savio Chan *et al.*,

2007). Cav1.3 is also involved in fear conditioning, depressive-like behavior, Parkinson's disease, and sounds transduction in the inner ear (Platzer *et al.*, 2000; Sinnegger-Brauns *et al.*, 2004; Day *et al.*, 2006; Mckinney and Murphy, 2006). Cav1.3 is present in RGCs, although, whether it is expressed more strongly in αRGCs is unknown (Shi *et al.*, 2017). Ca-α1D in *Drosophila* is required for the high frequency bursting of C4da when exposed to a noxious temperature (Terada *et al.*, 2016).

VGCCs are important for regulating axon growth during development (Tang, Dent and Kalil, 2003). There are few studies looking at the role of L-type VGCCs in regeneration. Inhibition of L-type VGCC *egl-19* in *C.elegans* (Ca-α1D homologue) reduces axon regeneration (Ghosh-Roy *et al.*, 2010). Enes et al. (2010) found that knocking out Cav1.2 actually enhances axon regeneration, but this study had several caveats (see General Discussion). No studies to date have suggested that any VGCC might mediate subtype-specific neuron regeneration.

In this Chapter, we perform a screen to identify ion channels that regulate C4da neural bursting after axotomy. We identify BK and Ca-α1D as important for neural bursting. Ca-α1D, but not BK, is required for C4da axon regeneration. This suggests Ca-α1D promotes C4da regeneration by promoting neural bursting activities. Reporter lines for Ca-α1D reveal high Ca-α1D expression levels in C4da, but weak expression levels in C3da. This may explain why C4da can burst and regenerate while C3da cannot. This suggests Ca-α1D might be the

molecular mechanism behind the subtype-specific neuron regeneration we observe in C3da and C4da.

RESULTS

Reverse-genetic screen identifies ion channels that regulate C4da neural bursting

Ion channels regulate neuron excitability (Bernstein, 1902), so we performed a candidate-based reverse genetic screen looking for ion channels that regulate C4da bursting. For the screen, we used RNAi to knock down ion channel candidates specifically in C4da and looked for an effect on neural bursting. When a neuron fires a single action potential, there are three phases: depolarization (open Na^+ channels), repolarization (open K^+ channels), and hyperpolarization (K^+ channels remain open). Therefore, knocking down a Na^+ channel would reduce neuron excitability while knocking down a K^+ channel would increase neuron excitability. To ensure our screen captured both of these possibilities, we knocked down Na^+ channels and assayed for bursting via calcium imaging 24 hours after axotomy and we knocked down K^+ channels and assayed for bursting in uncut (non-axotomized) neurons. Knocking down a K^+ channel increases excitability of the neuron and could therefore lead to neural bursting, even in the absence of axotomy. We also knocked down Ca^+ channels and looked for reduced bursting after axotomy. We used at least 2 RNAi lines to verify the results of our screen. Using this approach, we identified two ion

channels that regulate C4da bursting: BK (big conductance potassium channel) and Ca-α1D (an L-type voltage gated calcium channel).

The BK channel weakly promotes bursting in uncut C4da neurons but does not enhance regeneration

The first hit from our genetic screen was the BK channel, called slo in *Drosophila*. Since the slo channel is a K$^+$ channel, we observed increased bursting in uncut control neurons when we reduced slo using RNAi (**Fig. 3.1A**). We confirmed the results of the RNAi with slo mutant (slo$^{-/-}$). We also observed a mild bursting phenotype in the uncut slo$^{-/-}$ neurons (**Fig. 3.1B, C**). This phenotype was not as strong as we observed in normal C4da axotomized neurons (~4 bursts/minute versus ~1 burst/minute, **Fig. 3.1C**). We manually isolated C4da neurons (**Fig. 3.1D**) and performed RT-PCR to demonstrate that slo is expressed in C4da neurons along with ppk, a positive control (**Fig. 3.1E**). To determine if slo is the molecular mechanism promoting bursting and subsequent regeneration in C4da, we looked at the regeneration phenotype of slo$^{-/-}$ larvae. We did not observe enhanced baseline regeneration in the PNS of C4da neurons in pilot studies. In Chapter II we showed that while C4da bursts and regenerated when cut in the peripheral nervous system (PNS), C4da neither bursts nor regenerates when cut in the central nervous system (CNS). We therefore looked at C4da CNS regeneration in slo$^{-/-}$ larvae. We expected that knocking out slo in C4da

would result in bursting and subsequent CNS regeneration. Inconsistent with our

hypothesis, pilot studies of slo$^{-/-}$ C4da neurons did not show CNS regeneration.
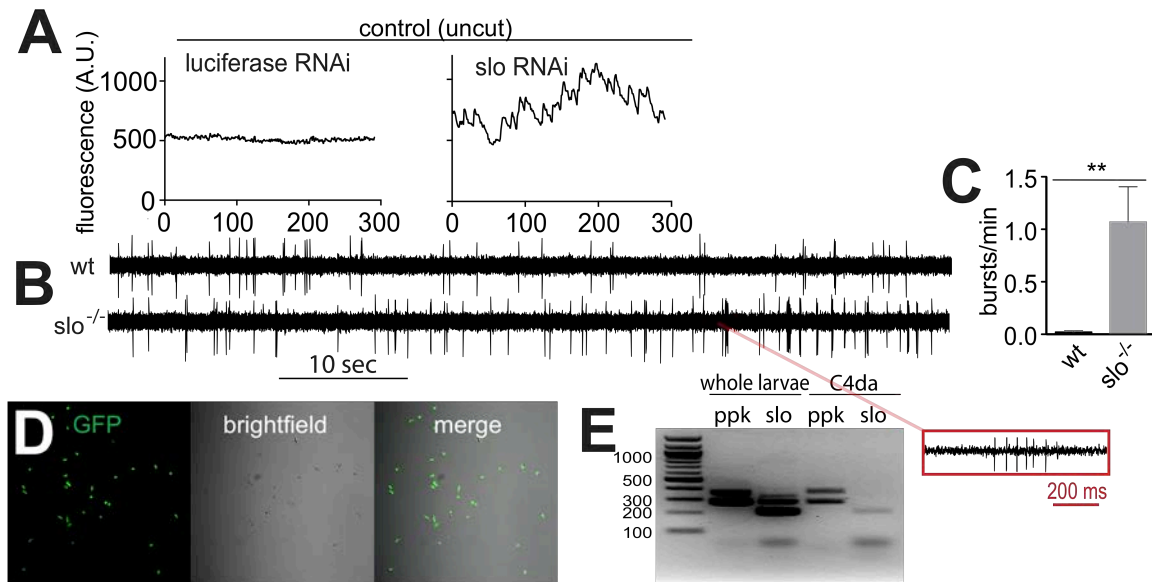
Figure 3.1. slo modulates neuron bursting. **A**, GCaMP6S fluorescence in intact (uncut) C4da neurons with slo and control (luciferase) RNAi. **B**, Recording of slo mutant C4da shows modest bursting compared to wt control, quantification in **C** *******p*<0.01 unpaired student's t-test with unequal variance. Red insert shows example burst with higher resolution. **D**, High purity of manually isolated C4da neurons labeled with GFP. **E**, RT-PCR of slo and ppk expression.

Calcium channels regulate neuronal excitability and regeneration

We identified through our screen an L-type voltage gated calcium channel

(VGCC) as an important mediator of neural hyperactivity after C4da neuron

axotomy. *Drosophila* L-type VGCC has three distinct subunits: α_1, β and $\alpha_2\delta$

(each encoded by *Ca-α1D*, *Ca-beta*, and *stj* respectively). α1 is the pore-forming

subunit while β and $\alpha_2\delta$ are auxiliary subunits. This L-type VGCC is broadly

expressed in central and peripheral nervous systems as well as muscles. It mediates inward calcium influx from extracellular space upon membrane depolarization and further modulates the depolarization phase of action potential firing. RNAi knockdown of either the α_1, β or $\alpha_2\delta$ subunit in C4da neurons specifically decreases the frequency and amplitude of spontaneous calcium spikes at 24hpa (**Fig. 3.3B, C**). Moreover, the pore-forming *Ca-α1D* hypomorphic mutant (AR66, (Eberl *et al.*, 1998)) also decreases the amplitude and frequency of spontaneous calcium spikes in C4da neurons at 24 hpa, corroborating the RNAi knockdown results (**Fig. 3.2A-D, Fig. 3.3A, B**). We did not observe differences in the kinetics of axon, soma, or dendrite calcium influx, due to our slow variant of GcaMP (GcaMP6S). In addition, nimodipine is a selective antagonist of L-type VGCCs and has been shown to reduce temperature-induced Ca-1D calcium transients in C4da neurons (Terada *et al.*, 2016). Acute application of 10 µM nimodipine in recording chamber blocks the spontaneous calcium spikes (**Fig. 3.2E**). Thus, both the genetic and pharmacological evidence indicates that L-type VGCC mediates neural bursting activity after C4da axotomy.

Next, we asked whether L-type VGCC also regulates regeneration. Excitingly, Ca-α1D mutants show reduced regeneration in C4da neurons (**Fig. 3.2F, G)**. In addition, RNAi knockdown of any of the α_1, β or $\alpha_2\delta$ subunits in C4da neurons also reduces C4da regeneration (**Fig. 3.3F, G**). In summary, L-type VGCC mediates both neuronal bursting activities and regeneration in C4da after

axotomy, which is consistent with our hypothesis that neuronal excitability

governs cell type-specific regeneration through the L-type VGCC Ca-1D.
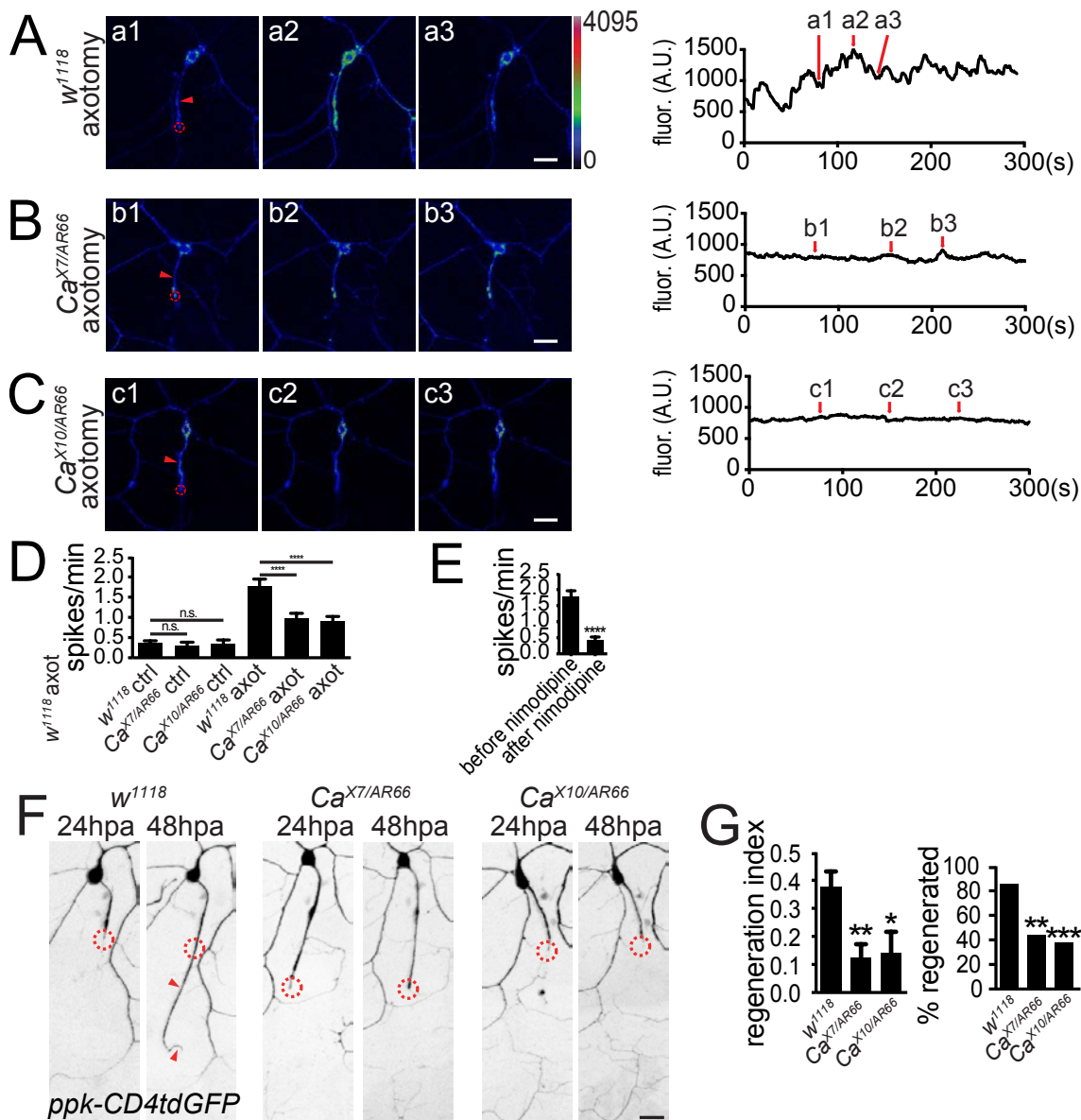
Figure 3.2. The L-type VGGC Ca-α1D regulates bursting and regeneration.
A-C, Example calcium imaging trace of control (**A**), *Ca-α1D^{X7}/Ca-α1D^{AR66}* (**B**)
and *Ca-α1D^{X10}/Ca-α1D^{AR66}*(**C**) mutant 24 hours post axotomy. Images are still
frames at time points indicated by red arrow. Red arrowhead indicates axon.
Red circle indicates cut site. Scale bar, 20μm. **D**, Quantification of calcium
spikes per minute in *w^{1118}*, *Ca-α1D^{X7}/Ca-α1D^{AR66}* and *Ca-α1D^{X10}/Ca-α1D^{AR66}*
mutants under control and axotomy conditions, n=12, 8, 8, 12, 9, 9. **E**, Calcium
spikes per minute before and after application of nimodipine (10μM, n=13, 13). **F-**
G, Sample regeneration images for control and *Ca-α1D^{X7}/Ca-α1D^{AR66}* mutant (**F**)
with quantification (**G**) n=34, 41, 32. Student's paired t-test (**E**), one-way ANOVA
with multiple comparisons and Bonferroni Correction (**C**, **D**, **G** left). Chi-squared
test with post hoc pairwise comparisons via Fisher's Exact Test (**G** right). *$p<.05$,
**$p<.01$, ***$p<.001$, ****$p<.0001$. Error bars indicate SEM.
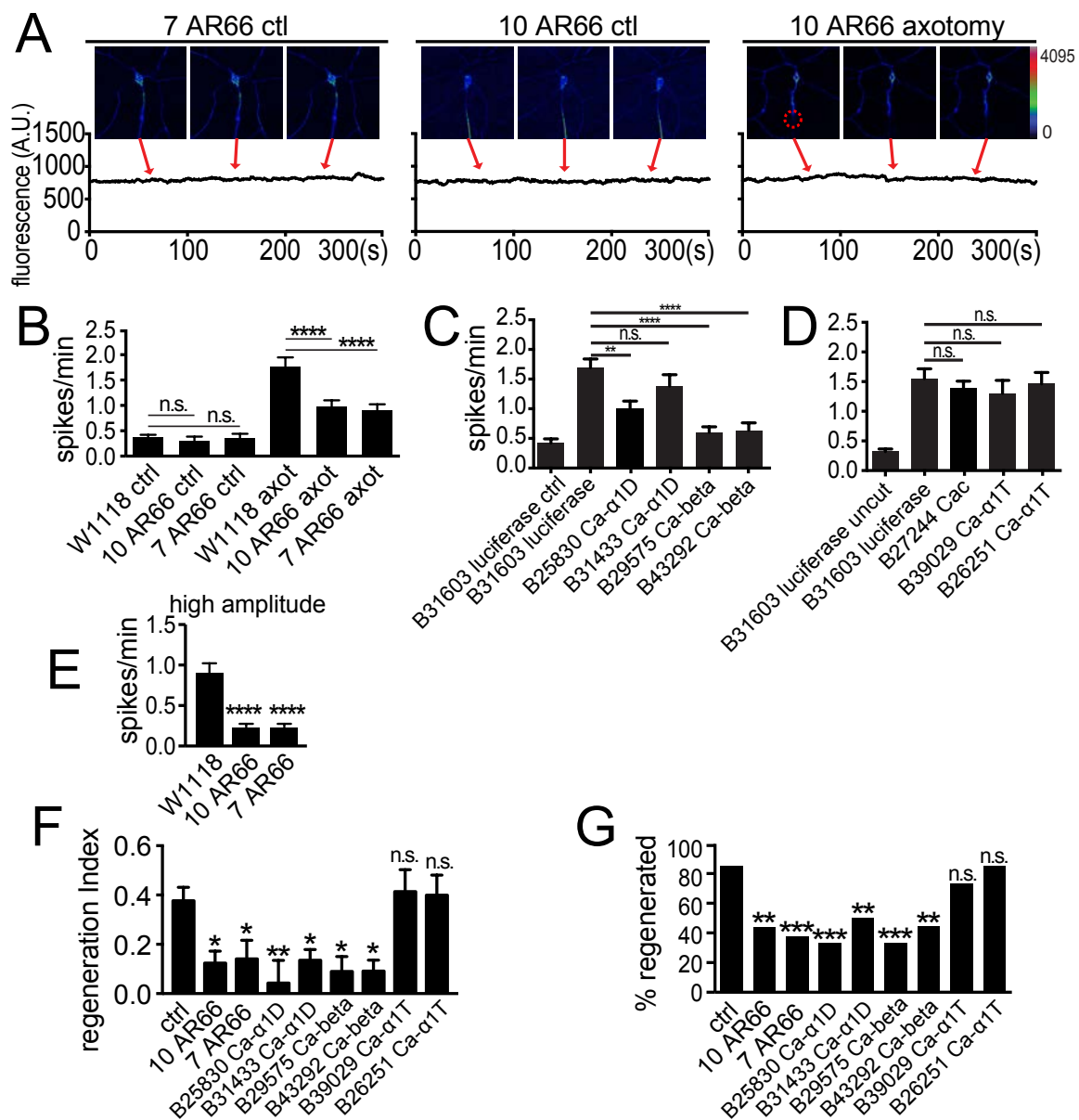
Figure 3.3. Ca-1D regulates bursting and regeneration, extended data sets.
A, Example calcium imaging traces of uncut $Ca\text{-}\alpha 1D^{X7}/Ca\text{-}\alpha 1D^{AR66}$ and $Ca\text{-}\alpha 1D^{X10}/Ca\text{-}\alpha 1D^{AR66}$ with axotomized $Ca\text{-}\alpha 1D^{X10}/Ca\alpha\text{-}1D^{AR66}$. Images are still frames from video at time indicated by red arrow, red circle shows laser cut site. **B**, Ca-1D mutant quantification of calcium spikes per minute for uncut control and axotomized neurons with genotype indicated, n=12, 8, 8, 12, 9, 9. **C**, Quantification of Ca-1D RNAi against alpha and beta subunits, and control (luciferase), n=11, 10, 10, 12, 11. **D**, Quantification of Ca-1D RNAi against [T and C], and control (luciferase), n=12, 10, 13, 12, 10. **E**, high amplitude spiking in control and mutants. **F-G**, Regeneration quantification for Ca-1D mutants, RNAi, and control neurons, showing Regeneration Index (**F**) and Regeneration Percent (**G**), n=34, 41, 32, 18, 38, 27, 25, 25, 26. One-Way ANOVA with multiple comparisons against control with Bonferroni Correction (B, C, D, E, F). Fisher's Exact Test (G). *$p<.05$, **$p<.01$, ***$p<.001$, ****$p<.0001$. Error bars indicate SEM.

C4da expresses Ca-α1D strongly while C3da has weaker expression

To characterize Ca-α1D expression in C4da and C3da neurons *in vivo*, we constructed two endogenous knock-in lines by CRISPR-Cas9: *Ca-α1D-T2A-Gal4* and *Ca-α1D-eGFP*. (**Fig. 3.4A**, see methods). T2A-Gal4 and eGFP tags are linked to the intracellular C-terminal of Ca-α1D membrane ion channel. T2A-Gal4 is co-expressed in the same peptide with Ca-α1D. Gal4 protein is released to cytoplasm upon self-cleavage of T2A sequence in recombinant proteins, then Gal4 protein can drive downstream UAS-reporter gene expression in target cells. Indeed, when using Ca-α1D-T2A-Gal4 to drive UAS-mCherry-NLS (showing nucleus, **Fig. 3.4B, C**) and UAS-CD4-TdTomato (showing plasma membrane, **Fig 3.4D**), C4da shows relatively strong Ca-α1D expression while C3da shows weaker Ca-α1D expression based on fluorescence intensity (**Fig. 3.4E**). Moreover, immunostaining of eGFP tag in homozygous Ca-α1D-eGFP line independently confirms that C4da expresses more Ca-α1D than C3da (**Fig. 3.4F-H**). We observed clear soma and axon expression of Ca-α1D in C4da while dendrite expression is relatively weak and barely detected.

Ca-α1D expression levels do not change upon axotomy in C3da or C4da

We hypothesized that upon axotomy of C4da, the expression of Ca-α1D would increase, leading to neuron bursting. Upon axotomy of C3da, we expected to see no change in the expression level of Ca-α1D. Contrary to our hypothesis,

pilot studies did not reveal a change in expression level of Ca-α1D in either C3da

or C4da upon axotomy.
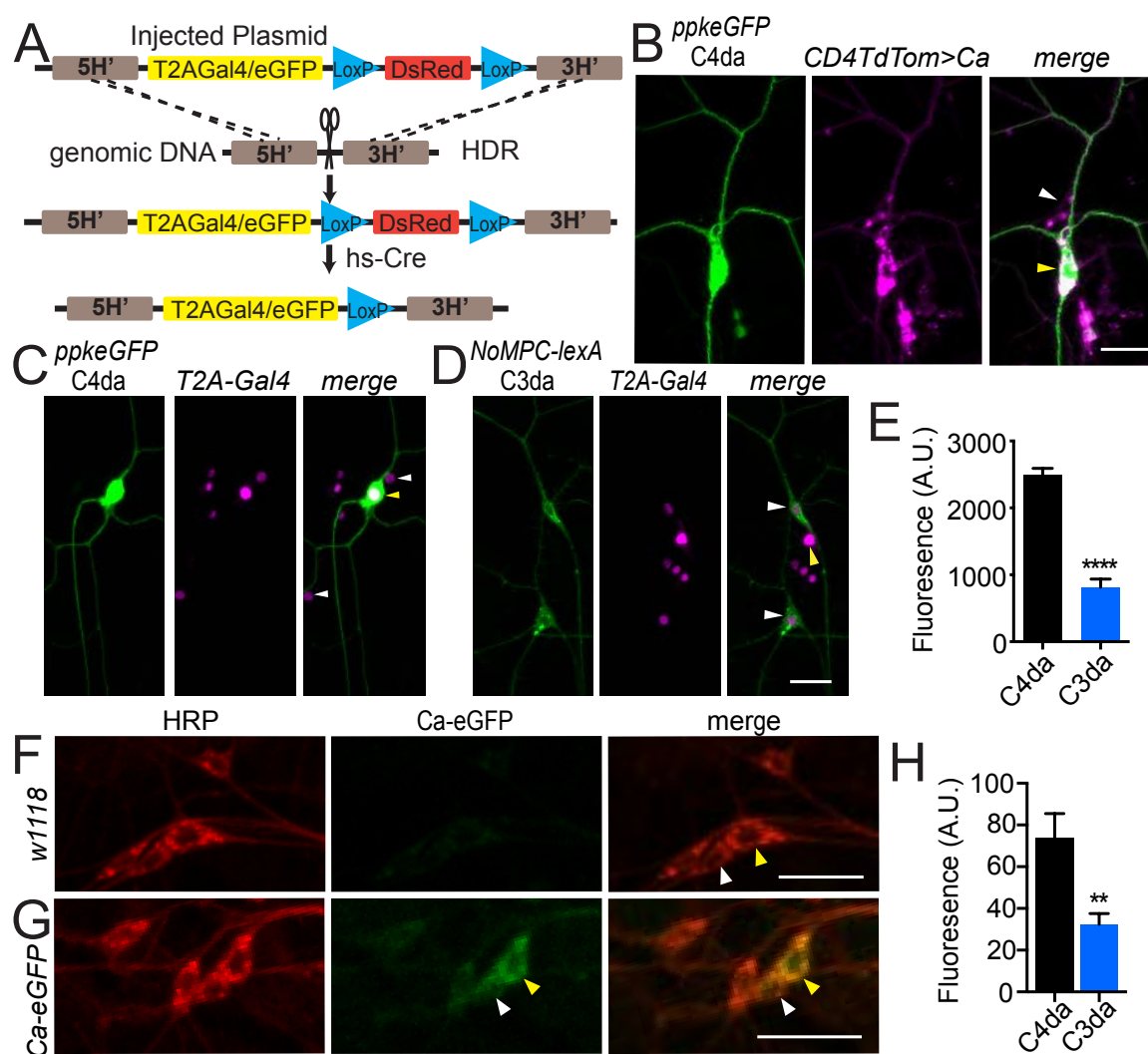
Figure 3.4. Ca-α1D is expressed strongly in C4da and weakly in C3da neurons. A, Genetic strategy for using CRISPR-Cas9 to produce T2A-Gal4- or eGFP-tagged Ca-α1D line, see Methods. **B**, ppkeGFP labels dorsal C4da (ddaC, indicated by yellow arrowhead). Ca-α1D-T2A-Gal4>UAS-CD4-TdTomato labels cells expressing Ca-α1D. The white arrowhead here indicates one of dorsal C3da neurons (ddaF). **C**, ppkeGFP labels dorsal C4da (ddaC, indicated by yellow arrowhead). Ca-α1D-T2A-Gal4>UAS-mCherry-NLS labels the nucleus of cells expressing Ca-α1D. Merge shows overlap. Other yet unidentified sensory neurons can be seen with this marker. **D**, NoMPC-LexA>LexAop2-myr-GCaMP6s labels two dorsal C3da neurons (top, ddaF; bottom, ddaA. Indicated by white arrowhead).Ca-α1D-T2A-Gal4>UAS-mCherry-NLS labels the nucleus of cells expressing Ca-α1D. Merge shows overlap. **E**, Summary of nuclear mCherry-NLS fluorescence from C4da and C3da soma regions of Ca-T2A-Gal4>mCherry-NLS larvae. n=17, 17. **F-G**, Red HRP signal labels all neuron cells, while green eGFP immunostaining signal labels C4da (ddaC, soma indicated by yellow arrowhead) and C3da (ddaF, soma indicated by white arrowhead). Merge shows overlap. **F**. Three panels are from w^{1118} negative control line. Scale bar, 20µm. **G**. Three panels are from homozygous Ca-α1D-eGFP line. Scale bar, 20µm. **H**, Summary of eGFP immunostaining fluorescence from C4da and C3da soma regions of Ca-α1D-eGFP larvae. n=8, 8. Student's t-test (**E** and **H**). *******p*<.01, *********p*<.0001. Error bars indicate SEM.

DISCUSSION

In this Chapter we show that Ca-α1D is the molecular mediator of neural bursting in C4da. Ca-α1D is required for neural bursting in C4da after axotomy and for subsequent regeneration. C4da has high Ca-α1D expression levels whereas C3da has relatively low Ca-α1D expression levels. We hypothesize that C4da is able to burst and then regenerate because it expresses high Ca-α1D while C3da cannot burst because it expresses low Ca-α1D, therefore C3da does not regenerate. This suggests that Ca-α1D is the molecular mediator of subtype-specific neuron regeneration. This demonstrates that L-type VGCCs could be used to promote regeneration therapeutically. Also, it suggests that perhaps neuron subtypes that are unable to regenerate have low expression of L-type VGCCs. In Chapter II we showed that neural activity is a cellular mechanism of subtype-specific regeneration, here we suggest that Ca-α1D is the molecular mechanism driving those changes in neural activity level that we observe in C3da and C4da.

VGCCs play a role in diseases including pain, epilepsy, migraine, ataxia, Huntington's disease and cancer (Simms and Zamponi, 2014; Chen *et al.*, 2018; Maklad, Sharma and Azimi, 2019). As a result, there are many therapies to manipulate VGCCs in human (reviewed in Belardetti and Zamponi, 2012). Cilnipidine is used to treat hypertension by blocking N-type VGCCs (Takahara, 2009). Verapamil and diltiazem have been used to treat hypertension, angina, and arrhythmia in humans for decades, these drugs work by blocking L-type

VGCCs (Ritz *et al.*, 2010). Recently, a study found that people taking these L-type VGCC blockers actually have a reduced incidence of Parkinson's disease (Ritz *et al.*, 2010). L-type VGCC blockers are also used to treat hyperinsulinemia (reviewed in Arnoux *et al.*, 2010). The abundance of safe and proven therapeutics to manipulate L-type VGCCs like Cav1.3 (Ca-α1D) means that increasing Cav1.3 to promote regeneration in mouse models and humans after nerve injury should be safe and relatively straightforward. Our extensive knowledge base about VGCCs function, localization, expression, isoforms, etc. will prove invaluable as we learn more about L-type VGCCs role in subtype-specific regeneration (reviewed in Simms and Zamponi, 2014).

We did not observe a change in Ca-α1D expression level after axotomy. This could indicate that a more subtle change, such as phosphorylation or protein translocation to/from the membrane might be taking place. This could increase the activity of Ca-α1D after axotomy in C4da, thereby leading to increased bursting compared to before the cut. It is also possible that no change in Ca-α1D activity is necessary for this bursting to occur. The burst activity could be regulated through a parallel pathway and only require high Ca-α1D expression to be present for robust bursting after axotomy.

Upon reduction of the BK channel, slo, we observed weak bursting in uncut C4da neurons but no effect on regeneration. We likely observed weak bursting because slo is not the molecular mechanism behind C4da bursting after axotomy. To strengthen this conclusion, future studies might look for expression

level changes or protein translocation of slo upon axotomy. If slo expression/availability is not reduced upon axotomy, this would support the hypothesis that slo is not the mechanism behind C4da bursting after axotomy. It is also possible that slo is playing a role together with Ca-α1D. Cav1.3 and BK channels cluster and are functionally coupled to promote BK channel activation at much lower voltages (Vivas *et al.*, 2017). It is conceivable that both slo and Ca- α1D manipulation will work synergistically to promote stronger bursting and potentially even regeneration.

We did not observe increased regeneration in slo^{−/−} C4da neurons in the PNS or the CNS. This is likely due to the fact that the bursting phenotype of slo^{−/−} is one quarter as strong as we observe in normal axotomized C4da neurons (1 burst/minute versus 4 bursts/minute). In *C. elegans*, SLO-1 reduction resulted in enhanced axon outgrowth (Chen *et al.*, 2011). However, in mammals it has been shown that BK reduction increases neural activity in intact neurons, but has no effect on axotomized neurons (Cao *et al.*, 2012). This effect could also explain why we did not observe a regeneration phenotype, because neuron activity was not increased after axotomy. Future studies should measure neural activity in axotomized slo^{−/−} neurons.

The bursting we observe in C4da after axotomy is reminiscent of burst pause firing in purkinje cells. AP can be generated in axon, but subsequent bursting AP are actually generated in dendrite (Davie, Clark and Häusser, 2008). Neurons with elaborate dendrites (like purkinje cells and C4da) can have bursting

originate from the dendrites leading to a qualitatively different mechanism of bursting (Krahe and Gabbiani, 2004). In addition to after axotomy, C4da also shows burst pause firing at high temperatures (Xiang *et al.*, 2010; Terada *et al.*, 2016). This thermally-induced burst firing requires TrpA1 and Ca-α1D (Terada *et al.*, 2016). TrpA1 is expressed in C4da dendrites (Xiang *et al.*, 2010). Interestingly, Cav1.3 has been shown in mammals to localize to dendrites (Simms and Zamponi, 2014), but our endogenous reporter lines only weakly detected Ca-α1D expression on the C4da dendrites. It is possible that, like purkinje cells, C4da bursting could originate from the dendrites. Burst firing is present in many neurons, but never before has it been linked to regeneration. Burst firing is particularly prevalent in sensory systems (reviewed in Krahe and Gabbiani, 2004).

MATERIALS AND METHODS

Axotomy

Axotomy was performed 80-85h AEL (after egg laying) unless otherwise stated. We followed the protocol in *Song et. al 2012* with several modifications. Briefly, a larva was anesthetized with Sevofluorane for 3 minutes and mounted dorsal side up (for PNS) or ventral side up (for CNS). The bleaching function of a Zeiss 2-photon laser damaged a small circle on the axon with an ROI of ~1.5µm. We found 910nm worked well for this. PNS axons were cut three quarters of the way to the bipolar dendrite, while CNS axons were cut as in *Song et al 2012*.

Following axotomy, larva recovered on a damp Kim Wipe and then were transferred to recovery vials containing regular brown food or white grape juice agar plates (for following optogenetic stimulation).

Electrophysiology

Extracellular recording of C4da neuronal activity was performed as described previously (Xiang *et al.*, 2010). Axotomy was performed ~80h AEL. ~104 h AEL third instar larvae were dissected to make fillet preparations. Fillets were prepared in external saline solution composed of (in mM): NaCl 120, KCl 3, $MgCl_2$ 4, $CaCl_2$ 1.5, $NaHCO_3$ 10, trehalose 10, glucose 10, TES 5, sucrose 10, HEPES 10. The Osmolality was 305 mOsm kg^{-1} and the pH was 7.25. GFP-positive (C4da) neurons were located under a Zeiss D1 microscope with a 40X/1.0 NA water immersion objective lens. Gentle negative pressure was applied to the C4da neuron to trap the soma in a recording pipette (5 μm tip opening; 1.5–2.0 MΩ resistance) filled with external saline solution. Recordings were performed with a 700A amplifier (Molecular Devices, Sunnyvale, CA), and the data were acquired with Digidata 1440A (Molecular Devices) and Clampex 10.6 software (Molecular Devices). Extracellular recordings of action potentials were obtained in voltage clamp mode with a holding potential of 0 mV, a 2 kHz low-pass filter and a sampling frequency of 20 kHz.

Burst analysis

For the purposes of data analysis, a burst was defined as 5 or more APs each

having an interspike interval of less than 100ms. This definition clearly

differentiated axotomized from control neurons (Figure S1). The 'Burst Analysis'

function on Clampfit 10.6 was used to detect bursts.

Calcium Imaging

GCaMP calcium imaging of C4da neuronal activity was performed as described

previously (Xiang *et al.*, 2010). For *in vitro* calcium imaging, axotomy was

performed at 96h AEL and 120h AEL 3rd instar larvae were pinned ventral side up

on silicone elastomer plates and dissected in the same external saline solution

as electrophysiology. The internal organs were removed with fine forceps and the

body wall was stretched with insect pins after opening body wall. Time-lapse

imaging was performed under water objective lens (W Plan-Apochromat 20x/1.0

DIC CG=0.17 M27 75mm) by Zeiss LSM 700 confocal microscope. Frame rate is

0.97Hz. All soma ROIs were corrected for horizontal drifting with ImageJ slice

alignment. Uncut C4da neurons from the same 3rd instar larvae were used as

negative controls.

 For UVC treated larvae, as an inflammatory nociception model (Babcock, Landry

and Galko, 2009), larvae at 96h AEL were mounted dorsal side up with double-

sided tape on microscope slides and placed in Spectrolinker XL-1000 ultraviolet

crosslinker (Spectronics Corporation) with $20mJ/cm^2$ 254nm UV exposure. After

treatment, larvae were recovered in regular food and imaged at 120h AEL.

Calcium imaging analysis

Each C4da or C3da neuron was imaged for 5 minutes as one sample unless otherwise stated. Original fluorescence signal (F) was firstly normalized to average intensity (F_0) of each sample by using following formula:

$F'=(F-F_0)/F_0$

After normalization, we utilized the findpeaks (to find local maxima) function in Matlab (MathsWorks incorporation) to extract and quantify calcium spike peaks from noisy background. Fluorescence signals in uncut C4da neurons also show some weak and irregular calcium spikes with minor prominence (small fluorescence amplitude). To rule out these weak spikes and render strong spikes to stand out (see simultaneous recording and calcium imaging figure), we first calculate the standard deviation (σ) of time-lapse fluorescence signal in each uncut C4da neurons from 120h AEL larvae, then calculate the mean value of σ ($\bar{\sigma}$, n=11). We artificially set the three fold of $\bar{\sigma}$ ($3\bar{\sigma}$, here is 0.148) as minimum peak prominence (amplitude) parameter in findpeaks function.

After we have the position, quantity and prominence of each spike in one sample, we divide the quantity of spikes by recording duration (5 minutes, unless otherwise stated) as spike frequency and calculate the mean value of prominence from each spike as spike amplitude.

Regeneration analyses

We performed quantitative analysis in accordance with (Song *et al.*, 2012) with some modifications. Briefly, we took two images for each neuron at 24hpa (L_1) and 48 hpa (L_2). All axon growth that occurred in this time frame was counted as regeneration. We calculated Regeneration Length as $\mathbf{L_2}$-$\mathbf{L_1}$. The larvae are growing during this time period, so the Regeneration Index normalizes Regeneration Length to a fixed length in the larvae, namely, the length from the C3/4da soma to the bipolar dendrite (BD): $\mathbf{L_1/BD_1 - L_2/BD_2}$. We also quantified the Regeneration Percentage as the percentage of larvae with a Regeneration Index ≥0.07.

Regeneration Imaging

We anesthetized larvae 24hpa using Sevoflurane and flattened larvae between a slide and coverglass with a thin bumper around the edge to maximize flatness without lethality. We always cut dorsal axon on the right side of the larva so we could easily identify the axotomized neuron. We took a z-stack image through the dendrites, soma, and axon of the axotomized neuron using a Zeiss D1 Confocal Microscope with a 20X water objective. We then recovered larvae on a wet kim wipe and transferred them to recovery vials/ grape agar plates depending on the experiment (see optogenetics Methods). At 48 hpa we again anesthetized the larvae and identified the same neuron by morphology of its dendrites and took a second image using the same parameters.

Crispr/Cas-9 endogenous knock in generation

Alternative splicing produces 10 different CDS (coding sequence) of Ca-α1D

annotated by Flybase (www.flybase.org). 8 of them (Ca-α1D-PE, PB, PA, PC, PJ,

PH, PF and PI) share same C-termini sequence, thus we chose to link T2A-Gal4

and eGFP tag after this C-termini, respectively. CRISPR target sequence, 5'-

ACAATCGCCGCTAAGAGGAC-3', is assumed to introduce double strand DNA

cut at around 20 bp upstream of Ca-α1D stop codon TAG. Rescue template

plasmid includes 2000 bp 5'homology and 2000 bp 3' homology sequence

flanking the stop codon TAG to assist homology-directed recombination (**Fig. 5A**).

Plasmid injection and fly transformant selection were performed by BestGene

Inc.. All genome-editing fly lines are confirmed by sequencing.

Immunostaining

We used TSA Plus Cyanine 5 (Cy5) detection kit (PerkinElmer, NEL745001KT)

to boost the immunostaining signals. 120h AEL 3rd larvae were dissected out in

the HL3 solution that was pre-cold on ice. HL3 solution formula: 70 mM NaCl, 5

mM KCl, 20 mM $MgCl_2$, 10 mM $NaHCO_3$, 5 mM trehalose, 115 mM sucrose, and

5 mM HEPES (final pH 7.2). We used fine glass microelectrode (pulled by P-97

microelectrode puller, Sutter Instrument Co.) to gently remove the muscle

segments covering the target C4da and C3da, since muscle cells show strong

Ca-α1D expression.

During each step of changing solutions, fillets are washed with washing buffer

(0.3% Triton X-100 in PBS) for 4 times of 15min. Larvae fillets were first fixed in 4%

paraformaldehyde for 30 min at RT and then incubated in 3% H_2O_2 solution to

quench endogenous peroxidase. Fillets were blocked in blocking buffer (0.3%

Triton X-100, 5% donkey serum (Sigma, D9663) and 0.1% bovine serum albumin

(Sigma) in PBS) for 1h at RT, incubated in anti-GFP first antibody (Thermo

Fisher, A-11122, 1:1500 in blocking buffer) for 40h at 4°C, and in anti-rabbit

HRP-conjugated second antibody (GE Healthcare, NA9340, 1:100 in blocking

buffer) for 2h at RT. Fillets were then incubated in TSA working solution

(PerkinElmer, NEL745001KT) for 3min at RT and in anti-HRP antibody (Jackson

immunoresearch, 123-545-021, 1:200 in blocking buffer) for 2h at RT. Fillets

were finally mounted with anti-fade mountant (Thermo Fisher, P36961) for 12h at

RT for following confocal imaging.

fly genotypes

$slo^{-/-}/slo^{-/-}$: ppkeGFP/+

$slo^{-/-}/slo^{-/-}$: ppk-LexA,LexAop-myr:GCaMP6s /+

Ca^{X10}/Ca^{AR66}; ppk-LexA,LexAop-myr:GCaMP6s /+

Ca^{X7}/Ca^{AR66}; ppk-LexA,LexAop-myr:GCaMP6s /+

B25830

  ;ppkGal4, UAS-Dicer 2.0/+; Caalpha-1D RNAi/ ppk-LexA,LexAop-

myr:GCaMP6s

B33413

;ppkGal4, UAS-Dicer 2.0/+; Caalpha-1D RNAi/ ppk-LexA,LexAop-myr:GCaMP6s

B29575

;ppkGal4, UAS-Dicer 2.0/+; Ca-beta RNAi/ ppk-LexA,LexAop-myr:GCaMP6s

B43292

;ppkGal4, UAS-Dicer 2.0/Caalpha-1D RNAi; ppk-LexA,LexAop-myr:GCaMP6s/+

B. Ca-T2A-Gal4/+;ppkeGFP/UAS-CD4-TdTomato

C. Ca-T2A-Gal4/+;ppkeGFP/UAS-mCherry-NLS

Ca-α1D-T2A-eGFP

W^{1118}

ACKNOWLEDGEMENTS

Kendra Takle Ruppell[a, c], Fei Wang[a, c], Feng Li[b, c], Pavi Guttipatti[b], Ye Shang[a],
Yuanquan Song[b], Yang Xiang[a, d]

[a]Department of Neurobiology, University of Massachusetts Medical School, 364
Plantation Street-LRB725, Worcester, USA 01605

[b]Children's Hospital of Philadelphia, 3501 Civic Center Boulevard, Philadelphia,
PA, USA 19104

[c]These Authors contributed equally to this work

[d]Corresponding author, University of Massachusetts Medical School, 364
Plantation Street-LRB725, Worcester, USA 01605. Yang.Xiang@umassmed.edu

Contributions Summary: F.W., K.T.R., Y.X. and Y.So. designed the experiments.

K. T. R. performed preliminary experiments relating to Figure 3.2.

F. W. performed genetic screen to identify BK, F. W. and F. L. performed genetic
screen to identify Ca-1D.

K.T.R. performed experiments shown in Figure 3.1 A-C

F.W. performed experiments shown in Figure 3.1 E, Figure 3.2 A-F, Figure 3.3 A-
E, and Figure 3.4 A-H.

F.L., P.G., and Y.So. performed experiments shown in Figure 3.2 G, Figure 3.3
F-G.

Y. Sh. performed experiments shown in Figure 3.4 F-H

K.T.R and F.W. wrote the manuscript.

Chapter IV

GENERAL DISCUSSION

Part I: Subtype-specific neural regeneration is mediated by neuron activity

Most neurons cannot regenerate (Ramon y Cajal, 1928). However, recent work has shown that not all neurons are uniformly poor regenerators, instead a small subset can regenerate robustly (Duan *et al.*, 2015). The mechanism underlying this subtype-specific regeneration remains unknown. Mounting evidence points to an intrinsic mechanism driving regeneration (Mcquarrie and Grafstein, 1973; Richardson and Issa, 1984; Neumann and Woolf, 1999; Liu *et al.*, 2011). We hypothesized that neural activity is the intrinsic mechanism driving subtype-specific regeneration.

Drosophila larvae also show subtype-specific neuron regeneration, C4da regenerates robustly while neighboring C3da does not regenerate. (Song *et al.*, 2012). This is a well-defined system to investigate the intrinsic mechanism underlying subtype-specific regeneration. These neurons are easy to cut, image, activate with optogenetics *in vivo*, and record, as they lie under a transparent cuticle. Genetic manipulation of C4da and C3da is powerful using the GAL4-UAS system with highly specific C4da and C3da drivers. It is also possible to cut a single axon from within the sensory neuron bundle using a 2-photon laser (Song *et al.*, 2012). In this Thesis we sought the factors that dictate subtype-specific neuron regeneration in *Drosophila*.

We have shown that the regenerative C4da neuron shows burst activities upon axotomy, while the non-regenerative C3da neuron does not alter its firing pattern upon axotomy. This is the first report of an intrinsic difference in neural

activity in regenerative and non-regenerative neuron subtypes. Since subtype-specific regeneration correlates with subtype-specific neuron burst activities, we hypothesized that neuron burst activity is the intrinsic mediator of subtype-specific neuron regeneration. Indeed, we found that reducing neuron bursting reduces C4da regeneration. Conversely, promoting bursting in non-bursting, non-regenerating C3da via optogenetics was sufficient to drive robust regeneration. Interestingly, a burst action potential pattern was more efficient at promoting regeneration than a tonic action potential pattern in C3da. This is the first report of neural activity pattern being critical for robust regeneration. Promoting neuron bursting after CNS axotomy was not sufficient to promote CNS regeneration.

Together, our data identify neural bursting activity as an intrinsic mediator of subtype-specific regeneration. Our work not only supports the role of neural activity as a pro-regenerative signal (Udina *et al.*, 2008; Lim *et al.*, 2016; S. Li *et al.*, 2016), but also shows that neural activity is necessary and sufficient for regeneration, and furthermore, that a specific physiological pattern of activity is important for robust regeneration. This gives researchers clues about why some neurons do not regenerate when exposed to non-physiological levels of activity (Enes *et al.*, 2010). It also demonstrates that the pro-regenerative effect of neural activity observed in many systems is not an artificial condition, but a deliberate mechanism of the regeneration system. It also suggests that neural activity could be manipulated to regenerate non-regenerative neurons. Armed with the knowledge that some neuron subtypes may have intrinsically high neural activity

leading to regeneration while other neuron subtypes have low activity and therefore can not regenerate, scientists and clinicians will have a tool to predict, monitor, and manipulate axon regeneration.

Neuron activity as an intrinsic mechanism of subtype-specific regeneration

Many mechanisms of regeneration have been identified, both inhibitory extrinsic mechanisms such as glia scarring (Ramon y Cajal, 1928; Windle and Chambers, 1950; Pasterkamp *et al.*, 1999; Bundesen *et al.*, 2003), myelin associated inhibitors (Schnell and Schwab, 1990; McKerracher *et al.*, 1994; Huang *et al.*, 1999; Wang *et al.*, 2002), and absence of growth factors (Lindsay, 1988; Lewin *et al.*, 1997; Sterne *et al.*, 1997), as well as pro-regenerative intrinsic mechanisms such as mTOR (Park *et al.*, 2008), *dlk-1* (Hammarlund *et al.*, 2009), and even neuron activity (Lim *et al.*, 2016; S. Li *et al.*, 2016) among others. Unfortunately, even armed with this knowledge, we still cannot achieve therapeutically significant regeneration (Liu *et al.*, 2011; Norsworthy *et al.*, 2017). This is the reason the concept of subtype-specific regeneration is so exciting, it suggests the possibility that not every neuron can be regenerated in the same way. In Duan et al.'s pivotal subtype-specific regeneration study, all neurons were exposed to pro-regenerative mTOR signaling, but only the α-RGCs were able to respond and regenerate (Duan *et al.*, 2015). α-RGCs have intrinsically high mTOR levels as well as high levels of growth factor receptor (IGF-1). These neurons also show increased neural activity relative to other RGCs (Krieger *et*

al., 2017). This makes sense, as neural activity promotes mTOR activity in mouse brain (S. Li *et al.*, 2016). I would predict that reducing α-RGC activity would block axon regeneration, as would reducing α-RGCs Cav1.3 expression. It is known that during neural development, neurons exposed to growth factor (NGF) respond to neural activity by extending their axons, neurons not exposed to growth factor inhibit axon extension upon neural activity stimulation (Singh and Miller, 2005). Perhaps the higher α-RGC activity upon axotomy leads to mTOR signaling and subsequent regeneration, but perhaps without high growth factor levels (IGF) reported in Duan *et al.,* 2015, the α-RGCs would instead be inhibited by axotomy-induced burst activities. Future studies should focus on these hypotheses in order to gain a deeper understanding of subtype-specific regeneration.

There are other studies suggesting that subtype-specific neuron regeneration may result from other mechanisms such as integrin expression (reviewed in Nieuwenhuis *et al.*, 2018). It is notable that integrins regulate neural activity in wound healing and they also regulate calcium activities through L-type VGCCs in neural development (Davis *et al.*, 2002; Gui *et al.*, 2006; Wu and Samba Reddy, 2012). Intriguingly, while α-RGCs are selectively regenerated upon PTEN deletion (Duan *et al.*, 2015), Sox11 expression kills α-RGCs while allowing other subtypes of RGC to regenerate (Norsworthy *et al.*, 2017). This is further evidence that not all neurons have equal regenerative capacity, different subtypes of neurons respond to pro-regenerative treatments differently. Could

neuron activity be related to this finding? It seems plausible, as Sox11 is a transcription factor that inhibits dendrite morphogenesis (Hoshiba *et al.*, 2016). Coincidentally, increased spontaneous neural activity leads to the opposite phenotype, premature dendrite branching (Bando *et al.*, 2016). This has led some to speculate that perhaps Sox11 supresses dendrite morphogenesis by inhibiting neural activity (Hoshiba *et al.*, 2016). Consistent with this idea, Sox11 expression has also been shown to down-regulate genes involved in synaptic transmission (Goldberg, Klassen, *et al.*, 2002; Norsworthy *et al.*, 2017). Here is one hypothetical explanation: it is possible that all RGCs have moderate to high activity levels, as these experiments were performed in light, which activates RGCs, but only α-RGCs express the correct set of growth factors to result in axon growth in the presence of neural activity. Perhaps all other RGCs express a different set of growth factors receptors whose axon growth is inhibited by neural activity. Then when Sox11 is expressed, perhaps neural activity is supressed and now α-RGCs axon growth is inhibited while other RGCs can now regenerate, oweing to their set of growth factors, which promote axon growth only with lower levels of neural activity. Future studies on subtype-specific regeneration should focus on neural activity levels to determine if activity plays a role in which pro-regenerative treatment will work best for that neuron subtype.

Mechanisms downstream of activity leading to axon regeneration

There are a growing number of studies that have identified neuron activity as a pro-regenerative signal (Ming *et al.*, 2001; Udina *et al.*, 2008; Lim *et al.*, 2016; S. Li *et al.*, 2016). However, not all studies agree that neuron activity is pro-regenerative. One study examining the effect of neuron activity on regeneration concluded that neuron activity is reduced upon priming (pre-cut in periphery) and inhibitory to axon growth (Enes *et al.*, 2010). There are several reasons why different neuron types might regenerate best with different levels of neuron activity. First, In a neural development study, neural activity strongly promotes axon extension in the presence of the growth factor NGF, but in the absence of NGF neural activity actually has an inhibitory effect on axon extension (Singh and Miller, 2005). It is possible that not all neurons are exposed to the same growth factors and perhaps our finding that neural activity mediates axon regeneration will not be true in neurons not exposed to the correct growth factors. If this is true, maybe a combinatory approach of providing neural activity together with growth factors will prove a winning therapeutic strategy. There were also several caveats to the study by Enes et al. 2010, they show that sensory evoked response activity was significantly reduced, but this is expected as they are cutting the dendrites (sense environment) and then measuring the response to pinch, brush, etc. If they have severed the receptive field they should expect to see reduced sensory responses. Enes et al. do not observe significantly decreased baseline neural activity upon priming. Other studies have shown increased baseline firing in the DRG after axotomy (Govrin and Lippmann, 1978;

Abdulla and Smith, 2000; Michaelis, Liu and Janig, 2000). The authors next show that electrical activity by chronic K^+ depolarization inhibits axon growth. It is unsurprising that axons couldn't grow during the 3 day K^+ culture with membrane potentials around -17mV, this is not a physiological level of activity. They next use 60V field electrical stimulation, much stronger than other studies (Hamid and Hayek, 2008; Udina *et al.*, 2008), but instead of measuring axon growth after a day or several, they measure real time growth, in just one hour. The work in my Thesis suggests that neuron activity promotes regeneration after transcriptional changes have occurred (starting 6-30 hours post axotomy). One hour of activation and axon measurement might not capture the dynamic processes that actually happen after axon injury. They also show that axon regeneration is inhibited when the cell is exposed to caffeine, which is also a very strong stimulation likely leading to non-physiological levels of Ca^{2+} and cytotoxicity based on their cellular morphology. Also, most of these experiments were done in 'bald' neurons after isolation, which means they lose all dendrites which leads to structural and functional changes (Enes *et al.*, 2010). They should do at least one regeneration experiment *in vivo*. The main drawback of the Enes et al. study is that they used non-physiological electrical stimulation to strongly stimulate non-physiological neurons (bald). Other studies have shown that neuron activation (via VGCC agonist) can be pro-regenerative at one dose, but inhibitory at higher doses (Unlu *et al.,* 2002; Nehrt *et al.*, 2007). Due to these limitations, it

is not surprising that Enes et al (2010) drew the opposite conclusions from our study.

L-type VGCCs translate synaptic activity into changes in gene expression (Olson *et al.*, 2005). Neuron activity regulates transcription factors like cAMP response element-binding protein (CREB) (Murphy, Worley and Baraban, 1991; Bading, Ginty and Greenberg, 1993). In our system, both Caα-1D and neural activity have the potential to induce transcriptional changes in C4da to promote axon regeneration upon axotomy. The strong influx of Ca^{2+} into the soma upon bursting suggests this could have a strong transcriptional response. Optogenetic stimulation to induce bursting in C3da also likely results in changes in transcription that promote axon regeneration. The different patterns of neural activity induced in C3da produce dramatically different levels of regeneration. These different patterns also result in different levels calcium signaling based on calcium imaging, calcium likely acts as a second messenger. This explains how the different patterns of activity in C3da might produce different calcium responses and therefore differentially affect gene expression and ultimately regeneration.

Upon axotomy, there is an immediate strong influx of calcium into the neuron that is necessary for regeneration (Ziv and Spira, 1995; MANDOLESI *et al.*, 2004; Ghosh-Roy *et al.*, 2010). We also observed this initial calcium wave at the time of axotomy in C3da and C4da (not shown). Increased Ca^{2+} raises the levels of Ca^{2+}-dependent enzymes such as adenyl cyclase (AC) and cAMP for

several hours, which is thought to be the rate limiting step in axon regeneration (Appenzeller and Palmer, 1972; Carlsen, 1982). In fact, cAMP injeciton is sufficient to reproduce the regenerative effects seen in priming studies (Neumann *et al.*, 2002). These calcium waves are critical for axon-soma communication, the injured axon must send a retrograde signal to the soma so the neuron knows it has been injured (reviewed in Rishal and Fainzilber, 2013). In our study we did not investigate this early Ca^{2+} response, only the calcium spiking activity we observed ~6-48 hours post axotomy. It would be worthwhile to investigate whether we also see increased AC and PKA in C4da after axotomy, and whether expression of AC/PKA was different in the non-regenerative C3da neuron. Similarly, we could look for differences in the level of Ca^{2+} signaling upon axotomy between our two neuron subtypes. Perhaps C3da does not have as robust of a Ca^{2+} response, as C3da does not express as much Caα-1D as C4da. Caα-1D homologue EGL-19 was shown to be necessary for this initial Ca^{2+} wave of activity in *C. elegans* (Ghosh-Roy *et al.*, 2010). It is also possible that the reduced regeneration phenotype we see in C4da neurons lacking Caα-1D is at least partly due to a reduced initial Ca^{2+} wave upon axotomy.

A transient increase in intracellular calcium can lead to remodeling of the axon cytoskeleton (Spira *et al.*, 2002; reviewed in Gomez and Zheng, 2006). In particular, Ca^{2+} regulates the movement of actin filaments, filament turnover, as well as protein synthesis and degradation, which can occur locally in growth cones (Campbell and Holt, 2001; Spira *et al.*, 2002; reviewed in Gomez and

Zheng, 2006). Ca^{2+} exerts these effects through calcium-binding proteins such as CaMKII, calcium dependent proteases, and PKA (Spira *et al.*, 2002; Fink *et al.*, 2003; Wayman *et al.*, 2004; Wen *et al.*, 2004). It is likely that upon axotomy, the bursting we observe is required for calcium-induced changes in growth cone dynamics through these calcium-binding proteins. Further investigation into growth cone dynamics in our system is essential gain a complete picture of the process of bursting-induced axon regeneration. In addition to whole-neuron calcium transients, local calcium signals have been observed in axon growth cones (Zheng *et al.*, 1994; Gomez *et al.*, 2001). Our data from calcium imaging reveals increased calcium activity localized to the axon distal tip upon axotomy. Whether this is an artifact of axon injury (we do observe axon swelling) or a process to regulate growth cone dynamics remains to be determined. Live imaging of the growth cone dynamics, together with calcium imaging would clarify this point. Notably, L-type VGCCs are required for the Ca^{2+} elevations induced by neurotrophic growth factor netrin-1 in growth cones (Hong *et al.*, 2000).

Bursting, but not tonic, activity pattern promotes regeneration

The work in my Thesis is the first study to demonstrate that the pattern of neural activity is important for robust regeneration. Although we delivered the same total number of AP with each pattern, we altered the pattern to make consolidated bursts resembling C4da after axotomy, a tonic pattern with frequent

singlet AP, and a semi-tonic pattern that was somewhere in between. Tonic

activation of C3da did not result in significant regeneration while burst activation

resulted in regeneration comparable to C4da. Semi-tonic activation resulted in

weaker regeneration. Although we cannot conclude that increased AP alone has

no effect on regeneration, as there is a slight trend towards higher regeneration

in both the tonic and semi-tonic patterns, but we can conclude that its effect is

not nearly as robust as what we observed after the burst activation. We can

safely draw the conclusion that neural burst activity promotes robust

regeneration. This difference in regeneration ability of the three activity patterns

can be explained by the differing downstream calcium signaling that we observed

upon C3da activation. Ca^{2+} acts as a second messenger to regulate

regeneration, the tonic activity protocol did not result in observable calcium

signaling while the burst activity protocol resulted in strong calcium signaling.

This is likely why burst, but not tonic, activity can promote regeneration.

Neuronal activity can lead to long-term changes via these second

messenger pathways: calcium, cAMP, cGNP, DAG and IP3 (Reviewed in West,

Griffith and Greenberg, 2002). This short list of possible messengers for so many

various cellular changes means that it is not likely the concentration of second

messenger but rather their spatial localization and dynamic properties (Dunn *et

al.*, 2006). Indeed, spontaneous oscillations in cAMP/PKA activity correlate with

neural activity in the developing mouse retina (Dunn *et al.*, 2006). This further

supports our hypothesis that the burst pattern of neural activity is physiologically distinct from tonic activation.

The enhanced regeneration we observe by promoting bursting instead of tonic neural activity also contributes to the 'coding debate' (reviewed in Eyherabide *et al.*, 2009; Zeldenrust, Wadman and Englitz, 2018), does neural bursting contain information in the number or firing rate of APs within a burst? Does the AP pattern carry information or is it all just binary information? Our data suggests that the bursting pattern of AP is indeed different information than tonic AP firing.

Why can PNS, not CNS axons regenerate with induced bursting?

To understand why our C4da induced bursting in the CNS did not promote regeneration, we need to first think about our experimental limitations. Simultaneous ChR2 stimulation and soma recording suggested that we were inducing strong bursts comparable to axotomized C4da, but we are limited by only recording in the soma. The CNS is millimeters away and whether the signal can propagate faithfully, especially through a damaged axon, is unknown. As discussed in Chapter II, future studies should use GCaMP imaging of the CNS to confirm bursting fully propagates distally. We could also try the drug 4-AP, which promotes faithful AP propagation in injured axons (Bei *et al.*, 2016).

Assuming the burst signal is reaching the CNS, there are still many well-studied inhibitory factors thought to prevent axon regeneration in the CNS: glia

scarring (Ramon y Cajal, 1928; Windle and Chambers, 1950; Pasterkamp *et al.*, 1999; Bundesen *et al.*, 2003), myelin associated inhibitors (Schnell and Schwab, 1990; McKerracher *et al.*, 1994; Huang *et al.*, 1999; Wang *et al.*, 2002), and lack of neurotrophic factors (Lindsay, 1988; Lewin *et al.*, 1997; Sterne *et al.*, 1997). While any of these factors certainly could prevent C4da CNS bursting-induced regeneration, recent evidence, including priming studies (a pre-cut to the PNS allows regeneration in the CNS), suggests that intrinsic promoters of regeneration can overcome these extrinsic barriers (Mcquarrie and Grafstein, 1973; Richardson and Issa, 1984; Neumann and Woolf, 1999). Even work in *Drosophila* has shown that neuron priming can result in C4da CNS regeneration, overcoming any extrinsic inhibitors (Song *et al.*, 2012). Therefore the first hypothesis, that our bursting was not strong enough in the CNS, is likely correct.

Limitations of our study

Currently, we cannot make any overarching statements about neuron bursting mediating regeneration in this Thesis simply because we only examined two neurons, C3da and C4da. Future studies should look for more correlations between neuron activity and regeneration in other cells types. We are also only looking at one of many possible mechanisms for promoting regeneration. Future studies should try to get a bigger picture of neuron activity together with growth factor availability, mTOR activity, etc. This multidisciplinary approach will likely be the winning strategy for promoting therapeutically significant regeneration.

Another reasonable criticism of our single-axon axotomy model is that *Drosophila* larvae are developing systems. Upon hatching they go through three larval stages: first instar, second instar, and third instar. We do our bursting and regeneration assays during this third instar larval period, and immediately after, the larvae pupate and later hatch into adult flies. Many gene programs are changing as the larvae increase drastically in size and prepare for pupation. It is reasonable to question how these changes might affect axon regeneration and neuron bursting in an adult system. Is neuron bursting and regeneration an artifact of pupation? Although this is unlikely, as we can still observe bursting and regeneration in the earlier developmental stage (second instar, not shown), it is still worth asking if we can see neuron bursting and regeneration after axotomy in the adult fly. This experiment would be challenging in C4da/C3da because the neurons in the adult fly are protected by thick, opaque cuticle. Future studies should focus on accessible sensory neurons, such as those found in the adult wing or leg, to investigate the relationship between neuron bursting after axotomy and regeneration (Soares, Parisi and Bonini, 2014).

Our conclusions are also limited by our uncertainly about the high selectivity of our so-called single-cell axotomy. Although fluorescent markers suggest that at least the glia and neighboring C4da axons remain intact, and brightfield microscopy reveals no epidermal or muscle damage (not shown), without electron microscopy (EM) with a C4da marker we cannot be sure that we

are in fact cutting only one single axon. EM images showing the selectivity of our axotomy would strengthen our claims of single-cell axotomy.

Our combination of calcium imaging and/or electrophysiology recording for analysis of bursting as a mediator of axon regeneration leaves some uncertainty about what is actually regulating the axon regeneration phenotype, calcium spikes or neuron AP bursting. In particular, our Ca-α1D mutant analysis relies on calcium imaging to look at a calcium mutant, it is unclear whether this mutant has a phenotype in AP bursting. Our conclusions could be strengthen by use of a more sensitive assay than calcium imaging, for example a genetically encoded voltage indicator (Jin *et al.*, 2012; St-Pierre *et al.*, 2014). This would allow us higher resolution of neural activities. In addition, we could use this tool to measure the resting membrane potential of axotomized C4da and C3da neurons to determine if they are more excitable than uncut control neurons.

Linking neuron bursting to known regenerative pathways

We now know that axotomy leads to bursting through L-type VGCCs, but how neuron bursting can then translate into regeneration remains unknown. One likely candidate is Protein Kinase A (PKA). Increased PKA has been shown to promote regeneration in many systems including *C. elegans*, mammalian DRG, and *Drosophila* (Cai *et al.*, 1999; Ghosh-Roy *et al.*, 2010; C. L. Li *et al.*, 2016). Neuron activity leads to increased PKA activity (Dunn *et al.*, 2006; Knight *et al.*, 2012). PKA promotes regeneration by directly activating DLK-1 (Ghosh-Roy *et*

al., 2010; C. L. Li *et al.*, 2016). It is possible that C4da neuron bursting also leads to increased PKA signaling, which in turn activates DLK-1 to promote regeneration. PKA activity is dependent on cyclic AMP (cAMP) levels. Interestingly, priming studies show that cAMP levels more than double in 24 hours after the peripheral cut; cAMP elevation alone is sufficient to reproduce the effects of peripheral priming cut (Neumann *et al.*, 2002; Qiu *et al.*, 2002). This is notable because high neural activity is correlated with increased cAMP. Perhaps priming studies are also increasing neural activity, which leads to more cAMP/PKA.

If PKA is not involved in C4da burst-induced regeneration, another likely candidate is CAMKII. Ca^{2+} oscillations drive CaMKII activity, the amplitude and duration of calcium spikes are decoded into distinct amounts of CaMKII activity (Koninck and Schulman, 1998). In addition, a neural development study revealed that patterned electrical stimulation, in the presence of growth factors, promotes axon extension by activating the CamKII/MEK pathway (Singh and Miller, 2005). This suggests that CaMKII has the potential to decode C4da neural burst activities into pro-regenerative signals.

Understanding how neural bursting fits together with other known regenerative pathways is crucial for having a complete picture of the regeneration process. This could also be valuable information clinically, as it is possible that one could bypass promoting neural bursting and instead activate PKA/CaMKII directly to achieve similar regeneration. Finding the link between

bursting and regeneration is also critical for understand subtype-specific regeneration. Perhaps neuron bursting leads to higher levels of PKA and neurons that have higher levels of PKA might be the subtypes that are more amendable to regeneration. Perhaps manipulating PKA levels could also turn a non-regenerative neuron, like C3da, into a regenerative neuron.

Finding new targets to modulate neuron regeneration is the goal therapeutically, especially because other mediators of regeneration, like the PTEN/mTOR pathway, is actually a tumor suppressor, manipulating this may have serious side effects (Li *et al.*, 1997). There are already therapeutic protocols being developed for optogenetics use to treat epilepsy (Paz *et al.*, 2013) and restore vision (Doroudchi *et al.,* 2011). It is likely that optogenetics will be a routine therapeutic in humans soon, so using neuron activation to promote regeneration should be viable. Current therapies after nerve injury can only try to save remaining axons from degenerating, pro-axon regeneration treatment is limited to physical therapy and occasionally experimental stem cell transplants (Case and Tessier-lavigne, 2005; Tsintou, Dalamagkas and Seifalian, 2015). Physical therapy has been shown to have some benefits, and this is likely due to increased neural activity.

Future Studies

Our data suggests that neuron bursting is necessary for regeneration in C4da and sufficient for regeneration in C3da. In our ChR2 experiments in C3da,

we delivered the burst light pattern from 6-48 hpa, based on the time course of bursting in axotomized C4da neurons. It would be informative to know the minimum light delivery time required for robust regeneration. For example, is there just a short critical period where the neuron needs to be bursting for regeneration to occur? Or is there a linear relationship, the longer the light delivery, the more robust the regeneration? This is important therapeutically and experimentally. For patients with nerve lesion, it is impractical to activate their neurons for days as a therapy for regeneration if this is not necessary. For scientists, future experiments promoting regeneration with activity would be simpler with the minimum required neuron-activating period. *Drosophila* C3/4da neurons are easy to activate with ChR2 in their transparent body, they can be freely moving and feeding. Mouse neurons are more challenging to activate with ChR2, as they often require optical cables being inserted into their brains. This can limit natural movement and feeding. Some neurons might also become habituated to 48 hours of ChR2 activation. C3/4da neurons still responded robustly after 48 hours of stimulation (not shown), but neurons in other systems might not have such robust firing. Limited light stimulation during a critical period would be ideal for future experiments and future therapeutics based on this work.

Another interesting question regarding neuron activation timing is, what happens if we 'pre-treat' the neurons with bursting before we perform axotomy? In priming studies it has been shown that a pre-cut to DRG neurons in the PNS enhances their regenerative capacity in the CNS (Mcquarrie and Grafstein, 1973;

Richardson and Issa, 1984; Neumann and Woolf, 1999). Could we observe C4da

CNS regeneration after pre-treating C4da neurons by optogenetics-induced

bursting before axotomy? Song et al. (2012) observed C4da CNS regeneration

after making a priming cut in the PNS. We did not observe C4da CNS

regeneration with optogenetic bursting, but perhaps if we began the optogenetic

treatment even before axotomy, as a pre-treatment, we could observe CNS

regeneration. It would also be informative to determine if bursting pre-treatment

could enhance the regeneration phenotype in non-regenerative C3da neurons.

Our study did not delve into growth cone dynamics, but certainly formation

of a functional growth cone is the important first step in regeneration (Tedeschi

and Bradke, 2017). In fact, electrical activity can steer the growth cone (Rajnicek,

Foubister and McCaig, 2006). L-type VGCCs promote bursting that regulates

growth cone (Tang, Dent and Kalil, 2003). Ca^{2+} spikes have a profound effect on

growth cone motility (reviewed in Gomez and Zheng, 2006). It is plausible that

the calcium spikes and neuron bursting we see after axotomy has some effect on

growth cone formation and guidance during axon regeneration. It is sensible for

future studies to test this hypothesis.

Part II: L-type VGCC Ca-α1D promotes neuron bursting and subsequent

regeneration after axotomy

We performed a candidate-based RNAi reverse-genetic screen to identify

ion channels that affect neuron bursting in C4da. Of the channels screened, we

saw a phenotype on bursting for just 2 channels: Ca-α1D and BK. RNAi against

Ca-α1D reduced bursting in axotomized C4da neurons, while RNAi against BK

resulted in *de novo* bursting in intact C4da neurons. After confirming the RNAi

results with several mutants we looked to see if these channels, when mutated,

had an effect on C4da regeneration. We predicted mutant BK might enhance

regeneration in C4da or C3da, or even in the CNS of C4da. However, BK

mutation had no effect on regeneration. Hypomorphic Ca-α1D mutants had

significantly reduced C4da regeneration, suggesting that Ca-α1D is necessary for

both C4da neural bursting activities and the regeneration that follows. We next

generated a Crispr-mediated endogenous knock-in line to examine Ca-α1D

expression level. Interestingly, the non-bursting, non-regenerative C3da neuron

showed low Ca-α1D expression whereas the bursting and regenerative C4da

neuron showed strong Ca-α1D expression. This correlation between Ca-α1D

level and bursting ability suggests that Ca-α1D expression is what allows some

neuron subtypes to burst but not other subtypes. Taken together, our data

suggests that Ca-α1D is the intrinsic molecular mechanism of subtype-specific

neuron regeneration.

L-type VGCCs in regeneration

L-type voltage gated calcium channels (VGCCs) have a <u>**L**ong-lasting</u>

<u>length of activation, hence their name. These channels are sensitive to a class of</u>

<u>drugs called dihydropyridines (DHPs) including nimodipine. Cav1-mediated</u>

calcium signals activate intracellular pathways controlling gene transcription in the brain (Murphy, Worley and Baraban, 1991; Bading, Ginty and Greenberg, 1993). Cav1.3 activates quickly and at a more negative membrane potential allowing for spontaneous activity in dopaminergic neurons of the substantia nigra (Olson *et al.*, 2005). Cav1.3 is expressed in soma, axon, and dendrites. Cav1.3 has been implicated in fear conditioning, depressive-like behavior, and sound transduction in the inner ear (Platzer *et al.*, 2000; Sinnegger-Brauns *et al.*, 2004; Mckinney and Murphy, 2006). Mouse models lacking Cav1.3 are in fact congenitally deaf (Platzer *et al.*, 2000). Recently, a role for Cav1.3 pacemaking activity in neurons susceptible to the effects of Parkinson's disease has been discovered (C Savio Chan *et al.*, 2007; Branch, Sharma and Beckstead, 2014). α-RGCs are known to express Cav1.3, but unfortunately RNA-seq to determine the expression profile of individual subtypes of RGCs has been largely unsuccessful, likely because RGCs are a rare cell type (<1% of cells in retina) (Macosko *et al.*, 2015; Poulin *et al.*, 2016; Shi *et al.*, 2017).

VGCCs have been implicated in regulating axon growth during development (Tang, Dent and Kalil, 2003; Sann *et al.*, 2008). In mammals, an L-type VGCC agonist has been shown to promote CNS regeneration (Unlu *et al.*, 2002; Nehrt *et al.*, 2007). In C. elegans, the L-type VGCC, called EGL-19, is required for regeneration, however, the authors hypothesize that EGL-19 plays an essential role in the immediate calcium transient that is observed upon axotomy (Chung *et al.*, 2016). This immediate calcium response is required for

regeneration (Ghosh-Roy *et al.*, 2010). It is possible that the Ca-α1D mutant in our system also has a reduced immediate calcium response upon axotomy. This regeneration-reducing effect could work in the same or a parallel pathway to neural bursting activities. In the same pathway, Ca-α1D could inhibit the immediate calcium response, which would directly inhibit neural bursting. In a parallel pathway, Ca-α1D might inhibit the immediate calcium response and neural bursting independently. These possibilities could be distinguished by manipulating either the immediate calcium response via the temporally controllable calcium sponge parvalbumin (Weavers *et al.*, 2016) or neural bursting activity via the optogenetic inhibitor halorhodopsin (Zhang *et al.*, 2007). The effect on regeneration of each treatment independently versus the cumulative effects of both treatments simultaneously could be compared. In the same pathway, cumulative effects would not be enhanced; in a parallel pathway, cumulative effects would be enhanced. Alternatively, temporal knock down of Ca-α1D starting after the immediate calcium response, but before neuron bursting, could distinguish these effects.

Limitations

In Chapter II we demonstrated that neural bursting activity mediates subtype-specific regeneration. In Chapter III we cannot make such bold statements about Ca-α1D. We showed that Ca-α1D is required for bursting and subsequent regeneration in C4da. We also showed that C3da has weak Ca-α1D

expression and we suggest that this could be the reason that C3da is unable to burst and regenerate, while C4da has strong Ca-α1D expression and can therefore burst and regenerate robustly. To strengthen our hypothesis, we need to test the role of Ca-α1D in bursting and regeneration as rigorously as we tested the role of neural activity in regeneration. Mainly, we should test whether overexpressing Ca-α1D in C3da can promote bursting and regeneration. With this information, we can say that Ca-α1D is both necessary and sufficient for regeneration, allowing us to make bolder claims such as: Ca-α1D mediates subtype-specific neural bursting and regeneration. Without this last piece of the puzzle we can only say our data suggests that Ca-α1D mediates subtype-specific bursting and regeneration.

Our superficial characterization of BK also limits the conclusions we can draw from this study. Contrary to what we observed, a recent study found that blocking BK channels reduces hyperexcitability and mechanical sensitization in axotomized axons (Chen, Cai and Pan, 2009). However, in another study it was shown that blocking BK channel does increase the excitability of intact neurons, but has the opposite effect in axotomized neurons (Cao *et al.*, 2012). This effect is mediated by the growth factor BDNF, axotomized neurons have high BDNF concentrations that blocked BK current (Cao *et al.*, 2012). In our study we only looked at the effect of BK reduction on intact neurons, future studies should look at the effect of BK reduction on axotomized neurons. If the effect is reduced, this

suggests that what we observe in *Drosophila* is in parallel with what has been observed in mammals.

Therapeutic implications

The work in Chapter III suggests that the L-type VGCC is an important molecular mediator of subtype-specific neuron regeneration. Ca-α1D is highly expressed in C4da where it promotes neural bursting activities and regeneration. Neurons with low Ca-α1D expression do not burst or regenerate. This means that one potential strategy for promoting regeneration in non-regenerative subtypes of neurons is to promote L-type VGCC activity/expression. This will conceivably result in increased neural activities and subsequent regeneration of that neuron. Luckily, there are many drugs that block VGCCs that have been used in patients for decades, especially for hypertension and hyperinsulinemia (Takahara, 2009; Arnoux *et al.*, 2010; Ritz *et al.*, 2010). This means that future studies using pharmacology to promote L-type VGCC activity, and thereby regeneration, will have an established platform with known targets, agonists/antagonists, and assays for toxicity and efficacy. These drugs are likely to be safe and effective.

Future Studies

We have shown that Ca-α1D knock out results in reduced C4da bursting and regeneration. There are several important remaining questions: Does overexpression of Ca-α1D in C4da cause neuron bursting, even without

axotomy, like the BK mutant? Does this overexpression lead to more robust

regeneration in C4da PNS or CNS? Many studies have shown that only specific

doses of VGCC activity and neural activity is required for regeneration, excess

may actually inhibit regeneration (Unlu *et al.,* 2002; Nehrt *et al.*, 2007; Enes *et al.*, 2010). Therefore it is possible that Ca-α1D overexpression in C4da may

actually inhibit regeneration.

Future studies should also examine the relationship between Ca-α1D and

C3da. We don't know if ChR2 burst-induced C3da neurons require Ca-α1D for

strong regeneration. Alternatively, induced bursts may bypass the need for Ca-

α1D activity in C3da. Does overexpression of Ca-α1D in C3da also promote

bursting and regeneration? Do C3da and C4da share the same downstream

molecular pathway for burst-induced regeneration? Or is Ca-α1D only required in

C4da to promote bursting, but not necessary in C3da? Knowing more information

about the differences between C3da and C4da will help us to better understand

subtype-specific regeneration.

Future studies should place emphasis on connecting this new knowledge

of VGCCs role in regeneration with known regeneration pathways. L-type

VGCCs have been tightly linked to BDNF expression (Tabuchi *et al.*, 2000;

Zheng *et al.*, 2011; Danesi *et al.*, 2018; Yu *et al.*, 2018). During axon

development, BDNF application results in VGCC-dependent calcium spikes

(Lang *et al.*, 2007). The role of nerve growth factors in axon regeneration has

been well characterized (reviewed in Terenghi, 1999). BDNF has been

demonstrated to promote axon regeneration (Lindsay, 1988; Xu *et al.*, 1995; Liu *et al.*, 1999). It is plausible that Ca-α1D regulates BDNF expression, which regulates axon regeneration. Furthermore, neural activity has been extensively shown to promote BDNF expression, in a calcium dependent manner (Tao *et al.*, 2002; Palomer *et al.*, 2016). Perhaps high L-type VGCC expression in C4da leads to increased neural bursting activity, which leads to increased BDNF expression, which is what ultimately leads to regeneration. If this hypothesis is true, we would expect high levels of BDNF in the regenerating C4da neuron, but low levels in the non-regenerating C3da neuron, which has low VGCC expression and low neural activity.

Alternatively, neural bursting activity through Ca-α1D could recruit growth factor receptors, such as TrkB, to the plasma membrane by stimulating exocytosis (Meyer-Franke *et al.*, 1998). PKA also appears to regulate VGCCs (Wang and Sieburth, 2013; Sang, Dick and Yue, 2016). PKA promotes regeneration (Cai *et al.*, 1999; Ghosh-Roy *et al.*, 2010; C. L. Li *et al.*, 2016) by directly activating DLK-1 (Ghosh-Roy *et al.*, 2010; C. L. Li *et al.*, 2016). There are many potential regeneration pathways to test for interaction.

Concluding remarks

Neuron regeneration is a complex process; there are many factors that inhibit regeneration, but very few factors that can promote regeneration reliably across different neuron subtypes. The identification of new pro-regenerative

factors that promote regeneration across subtypes is crucial for developing novel and effective therapeutics. My Thesis work reveals neural bursting activity as a mediator of subtype-specific neural regeneration. We have shown that neuron bursting activity is necessary for regeneration of a regenerative neuron subtype and sufficient for regeneration of a non-regenerative neuron subtype. We have also demonstrated that a particular neuron activity pattern, bursting, is better at promoting regeneration than a tonic neuron activity pattern. We identified Ca-α1D as necessary for C4da neuron bursting and regeneration. High Ca-α1D expression in the bursting and regenerative C4da neuron and low Ca-α1D expression in the non-bursting and non-regenerative C3da neuron suggest that Ca-α1D expression levels dictate subtype-specific neuron regeneration.

Our main contributions to the field include identification of neuron activity by an L-type VGCC as an intrinsic mechanism of subtype-specific regeneration, and the concept that not just neuron activity, but activity pattern, is important for optimal regeneration. Together, this study sheds light on the cellular and molecular intrinsic mechanism of subtype-specific neuron regeneration.

Appendix I

Additional physiological changes to the regenerating neuron: neuropathic

pain

ABSTRACT

Chronic pain is a major burden. The current opioid crisis highlights the need for safer drugs to relieve pain. There are 2 types of chronic pain: inflammatory and neuropathic. Neuropathic pain arises after nerve injury, the mechanisms are poorly understood. Nerve injury in regeneration models, including sciatic nerve lesion (SNL) show spontaneous bursting and mechanical hypersensitivity, key symptoms of neuropathic pain. The regenerative Class IV dendritic arborization neuron (C4da) from Chapters II & III also showed spontaneous bursting, which lead to regeneration. We wondered if there were any other physiological changes to this regenerating neuron. We found that C4da also becomes mechanically hypersensitive after axotomy. These changes have remarkable parallels to mammalian SNL in models of neuropathic pain.

INTRODUCTION

Regenerating neurons undergo massive transcriptional changes, both pro-regenerative pathways and the injury response are initiated. Do these changes have any physiological effects on the neuron's normal function as a nociceptor? In mammals, when sensory neurons are cut, they show a variety of phenotypes including hypersensitization and spontaneous bursting (X. J. Song *et al.*, 1999; Chuang *et al.*, 2018). The sciatic nerve lesion (SNL) model was in fact first created to study neuropathic pain, and then later adopted by the regeneration field (Kim and Chung, 1992).

100 Million Americans suffer from chronic pain, that's more than diabetes, heart disease, and cancer combined (Julius 2013). The economic impact is staggering. A recent report estimates that chronic pain costs the nation around $635 billion each year in medical treatments and lost productivity (Gaskin 2012). Unfortunately, these medical treatments are often ineffective and can have serious side effects. The identification of potent and specific therapeutic strategies to treat chronic pain would alleviate this financial and emotional burden. Mammalian models of chronic pain have identified molecules required for inflammatory and neuropathic pain (reviewed in Basbaum *et al.*, 2009; Julius, 2013). Variability and low resolution of these models have prevented deeper understanding of the cellular and molecular mechanisms of pain sensitization.

There are two types of chronic pain: inflammatory and neuropathic. Neuropathic pain is debilitating, and difficult to treat (Costigan, Scholz and Woolf, 2009). 7% of people are currently experiencing neuropathic pain (Bouhassira *et al.*, 2008), which is caused by nerve damage via mechanical trauma, metabolic diseases, neurotoxic chemicals, tumors and infection (reviewed in Costigan, Scholz and Woolf, 2009). Neuropathic pain can originate in the CNS (central sensitization, (Latremoliere and Woolf, 2009)) or in the PNS (peripheral sensitization, reviewed in (James N. Campbell and Meyer, 2006), this Chapter will focus on peripheral sensitization.

Neuropathic pain often manifests as spontaneous pain arising without an identifiable stimulus (Costigan, Scholz and Woolf, 2009). This is thought to be

due to ectopic generation of action potentials of the injured neuron (X. J. Song *et al.*, 1999). In addition to experiencing spontaneous pain, patients with neuropathic pain often complain of mechanical allodynia, or a reduced threshold for mechanical pain, and less commonly, thermal allodynia, or a reduced threshold for thermal pain (hot or cold) (Costigan, Scholz and Woolf, 2009). Mechanical allodynia can be so severe that even putting on clothes can cause excruciating pain (Costigan, Scholz and Woolf, 2009). Mouse models such as chronic compression of DRG have been able to recapitulate spontaneous bursting, mechanical allodynia, and thermal allodynia, allowing us some insight into the molecular underpinnings of allodynia (X. J. Song *et al.*, 1999).

These models have allowed identification of myriad molecules/processes thought to be associated with neuropathic pain, unfortunately, our limited insights into the molecular mechanisms of neuropathic pain hasn't resulted in effective and specific therapeutics (Basbaum *et al.*, 2009). The current opioid crisis is certainly evidence of that. To better understand the mechanism of neuropathic pain, we should critically examine the limitations of our current mouse models. Firstly, SNL and/or DRG crush sever tens of thousands of diverse sensory and motor neurons. Second, the heterogeneity of mammalian nociceptors at the cellular, biochemical, and molecular levels prevent precise identification, quantification, and manipulation of nociceptors at high resolution (Gold and Gebhart, 2010; C. L. Li *et al.*, 2016). Taken together, this means that researchers often do not know the identity of the cell they are recording, the nature of the

injury to that particular neuron (severed, crushed, or intact), or whether behavioral phenotypes are the result of injured sensory neurons or injured motor neurons being unable to perform that particular behavior (usually paw withdrawal).

Excitingly, our single-cell axotomy model in *Drosophila* larvae can overcome many of these barriers. C4da is relatively homogenous cellularly, biochemically, and molecularly and between different animals. C4da is easily accessible for imaging, 2-photon cutting, and recording under the transparent cuticle and is easy to genetically manipulate with precise spatial and temporal control. This represents the first single-cell model for neuropathic pain. We can finally learn what is happening to a single cell after axotomy.

C4da shows strong neural bursting after axotomy using both electrophysiology and calcium imaging (Chapter II). In addition to spontaneous pain, patients with neuropathic pain can also have sensitization to mechanical stimuli so intense that even putting clothes on can cause excruciating pain (Ochoa 1993). Very little is known about mechanical hypersensitivity and treatment options are limited. Mouse models show mechanical sensitization upon SNL (Chuang 2018). We found that after axotomy, C4da shows *de novo* mechanical sensitization. We hope to use this model in the future to uncover the molecular underpinnings of mechanical sensitization after axon injury and hopefully illuminate new therapeutic targets.

Our axotomy model displays both regeneration and neuropathic pain-like phenotypes simultaneously. This puts us in a unique position to draw parallels between the processes of regeneration and pain. Perhaps researchers from the two fields of regeneration and neuropathic pain should look to each other's work for inspiration, they might have a lot to learn from each other.

RESULTS

The regenerating C4da neuron shows mechanical allodynia

We recorded from axotomized C4da neurons and measured their response to saline perfusion, a gentle mechanical force. We noted that while control, uncut, neurons had no increase in firing rate upon perfusion stimulation, axotomized neurons had a strong response to perfusion (**Fig. A1.1A, B**). This saline perfusion response might mimic the flow of hemolymph within the body wall of *Drosophila*, which C4da dendrites are directly exposed to. We confirmed these results with GCaMP imaging by delivering a mechanical stimulation, either perpendicular touch with an electrode or mild stretching of the epidermis with an electrode, and found that exclusively axotomized neurons, not intact neurons, respond to this mechanical stimulation (**Fig. A1.1C, D**). To confirm we were not seeing a damage response, multiple stimulations were performed on the same cell, which was able to recover between stimulations and have multiple mechanical responses. This suggests that the calcium influx we see if not due to

cell death. We also tried cutting the dendrite instead of the axon, but this didn't
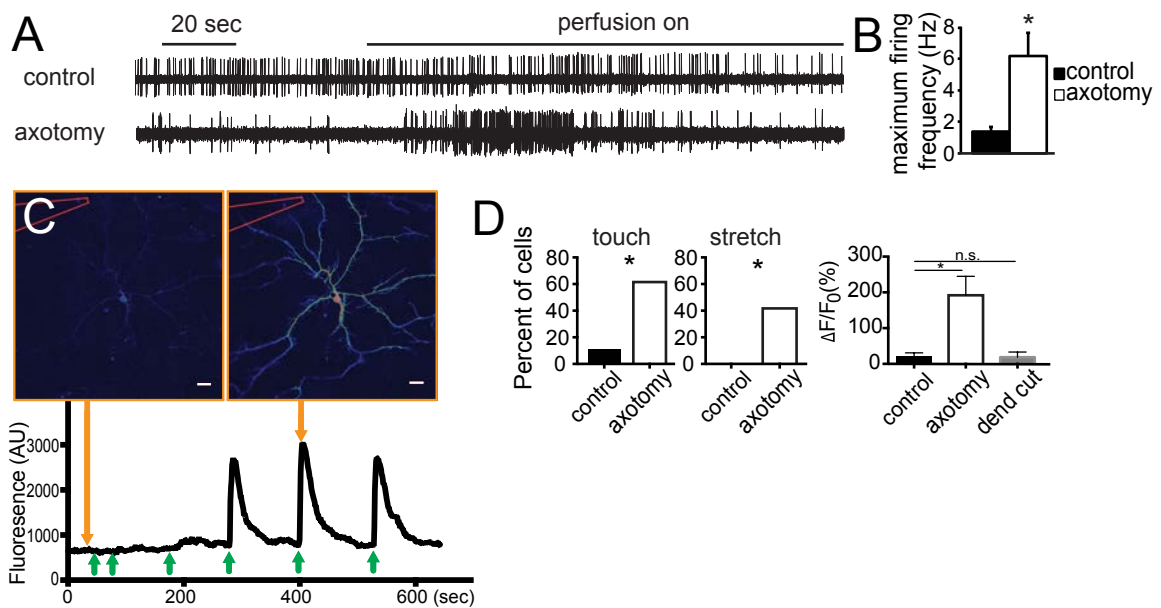
elicit any mechanical response (**Fig. A1.1D**).

Figure A1.1. C4da shows de novo mechanosensitization after axotomy.
A, Electrophysiology trace recordings from control and axotomized C4da
neurons. Onset of perfusion results in a strong, transient response from
axotomized, but not control neurons. **B,** Quantification of maximum firing
frequency (in Hertz) during perfusion response in axotomized and control
neurons. Student's t-test *$p<.05$, error bars represent SEM. **C,** Bottom,
calcium imaging trace during mechanical stimulation. Each stimulation is
represented by green arrow, stimulation intensity range from 10-60 μm cuticle
deformation with an interval of 10 μm. Top, insets of pseudocolored GCaMP
to distinguish fluorescence levels at times indicated by orange arrows. Touch
electrode outlined in red. **D,** Quantification of GCaMP responses after touch
and stretch electrode stimulation in axotomized and control neurons. Fishers
exact test *$p<.05$, error bars represent SEM. Right, axon cutting but not
dendrite cutting results in mechanosensitization. One-way ANOVA followed
by Bonferroni correction *$p<.05$, error bars represent SEM.

To determine the molecular mechanism of this mechanical sensitization, we looked at known mechanically activated ion channels. There is a short list of known mechanosensitive ion channels in *Drosophila*: Piezo (a transmembrane protein, (Coste *et al.*, 2011; Kim *et al.*, 2012)), Ppk (a DEG/ENaC channel, (Zhong, Hwang and Tracey, 2010)), and NompC (a TRP channel, (Walker, Willingham and Zuker, 2000)). We examined the mechanical sensitization response after axotomy in larvae mutant for Piezo, Ppk, or NompC. We observed no decrease in the mechanical response in any of the mutants, suggesting that this *de novo* mechanosensitization occurs through a yet unidentified channel or perhaps a combination of channels (pilot studies). Identification of this channel and conservation studies in mammals will determine if this novel mechosensitive ion channel will be a useful therapeutic target for patients with mechanical hypersensitivity.

DISCUSSION

Upon axotomy, the nociceptor C4da displays burst firing. This is reminiscent of mouse models for neuropathic pain (X. J. Song *et al.*, 1999). In the mouse, sciatic nerve lesion (SNL) involves severing the sciatic nerve (massive axotomy), which leads to spontaneous bursting and mechanical sensitization. We observe parallel effects in our single-cell C4da axotomy model. We believe that our model for single axon cutting is a simpler and more genetically powerful model to investigate these physiological changes to the regenerating neuron.

Identification of mechanosensitive ion channel

Only a handful of mechanosensitive ion channels have been discovered, mainly belonging to these three conserved superfamilies: TRP channels, PIEZO channels, and DEG/ENaC channels (ppk) (Terada *et al.*, 2016). In *Drosophila* piezo and ppk are the known mechanosensitive ion channels (Zhong, Hwang and Tracey, 2010; Kim *et al.*, 2012). Pilot studies suggest that neither is required for *de novo* mechanosensation of C4da after axotomy. This suggests that a novel mechanosensitive ion channel is mediating this phenotype.

A new model for screening for new molecules involved in neuropathic pain

2-photon mediated axotomy represents a powerful new single-cell model for fast screening of molecules involved in neuropathic pain. We have already identified the highly conserved ion channels BK and Ca-α1D as mediators of ectopic bursting. These channels have also been implicated in neuropathic pain (Chen, Cai and Pan, 2009; Perret and Luo, 2009; Park and Luo, 2010). We are in a unique position, with our single-cell model for ectopic bursting and genetic/optogenetic tools to modify and observe these ion channels, we can search for the network of genes leading to spontaneous pain, and hopefully provide novel therapeutic targets.

Perhaps some of our other findings about regeneration will also give us new insights into neuropathic pain. Is ectopic bursting, and therefore

spontaneous pain, just the result of a neuron trying to regenerate? If so, can we identify a 'regeneration-complete' signal that can stop neural bursting for patients experiencing spontaneous neuropathic pain?

Linking regeneration and neuropathic pain

It is clear that the two fields of regeneration and neuropathic pain have much in common, but their relationship is poorly understood and warrants further investigation, the delivery of axon growth factors to enhance axon regeneration has been explored as a potential therapy for neuropathic pain (Landowski *et al.*, 2016). There are just a handful of studies starting to connect the dots between regeneration and neuropathic pain (Xie, Strong and Zhang, 2017; Chuang *et al.*, 2018). There is mounting evidence of the extensive overlap of ion channels, growth factors, neurotransmitters and cytoskeletal components in neuron regeneration and neuropathic pain (Navarro, Vivo and Valero-Cabre, 2007; Chuang *et al.*, 2018).

In Chapter III we found that reducing the BK channel led to increased neural bursting in intact neurons. In fact, mammalian models have identified that calcium-gated BK channels are important for the regulation of neural excitability and play a role in neuropathic pain (Chen, Cai and Pan, 2009; Cao *et al.*, 2012). An interesting new hypothesis based off research in *C. elegans* is that electrical activity regulated by mechanosensory channels could promote axon regeneration (Chen *et al.*, 2011). This hypothesis neatly ties together all of our findings.

Limitations of our study

The main drawback of our single-cell model for neuropathic pain is the relatively inverted nature of our C4da neuron compared to mouse DRG neurons. In the bipolar mouse neuron, the soma resides in the DRG and upon sciatic nerve lesion, all axon distal to the cut site degenerates leaving the soma and the other axon tract to the CNS intact. In the multipolar C4da neuron, the soma resides far in the periphery, on the end of the single axon. Upon axotomy, all axon distal to the cut site degenerates, including the entire axon tract to the CNS. This leaves C4da as an independent and disconnected soma and dendrites. (**Fig 2.1B**). This means that we cannot easily observe behavioral phenotypes after axotomy. Our model has strong potential to uncover changes to the nociceptor upon axotomy, but this model does not have a behavioral correlate, as mouse studies do (X. J. Song *et al.*, 1999) because we sever the connection to the CNS with axotomy. We are developing alternative behavioral paradigms for neuropathic pain in *Drosophila*. We know that reduction of the BK channel promotes bursting in an intact neuron (discussed in Chapter III) and can exploit that to develop a behavioral assay for genetic sensitization.

C4da allows larva to sense noxious mechanical stimulation (Kim *et al.*, 2012). There are behavioral paradigms for measuring mechanical avoidance in *Drosophila* larvae, this involves poking a free moving larva on the epidermis and quantifying the rolling avoidance response (Kim *et al.*, 2012). Pilot studies in our

lab have not demonstrated significant behavioral sensitization upon axotomy. This may be due to two reasons, first, the minimal number of activated C4da neurons required for a behavioral response is unknown. It may be that we must axotomize at least several C4da axons before we can see a behavioral response. Secondly, upon axotomy, the connection between the C4da soma and CNS has been severed. It is possible that other neurons, like C3da, are co-activated during this response and augment the behavior, especially since C4da and C3da synapse into the same neuron in the CNS (Ohyama *et al.*, 2015). If this is true, we might be able to observe behavioral sensitization of the mechano-nociceptive response. If C4da is working completely autonomously, it is unlikely that we will observe this behavioral sensitization in our paradigm.

Without a behavioral paradigm, this model still provides valuable information about what is happening to the nociceptor itself with single-cell resolution. This model is not yet useful in the investigation of central sensitization.

MATERIALS AND METHODS

Axotomy

Axotomy was performed 80-85h AEL (after egg laying) unless otherwise stated. We followed the protocol in *Song et. al 2012* with several modifications. Briefly, a larva was anesthetized with Sevofluorane for 3 minutes and mounted dorsal side up (for PNS) or ventral side up (for CNS). The bleaching function of a Zeiss 2-

photon laser damaged a small circle on the axon with an ROI of ~1.5μm. We found 910nm worked well for this. PNS axons were cut three quarters of the way to the bipolar dendrite, while CNS axons were cut as in *Song et al 2012*. Following axotomy, larva recovered on a damp Kim Wipe (BRAND) and then were transferred to recovery vials containing regular brown food or white grape juice agar plates (for following optogenetic stimulation).

Mechanical stimulation

For electrophysiology, a saline perfusion system was switched on at indicated time point perfusing about 3 mL per minute. For calcium imaging, a wide diameter pipette was fire-polished in a microforge until the end sealed forming a smooth ball. The pipette touch the epidermis in an area apparently clear of dendrites and moved laterally (stretch) or vertically (touch).

Electrophysiology

Extracellular recording of C4da neuronal activity was performed as described previously (Xiang *et al.*, 2010). Axotomy was performed ~80h AEL. ~104 h AEL third instar larvae were dissected to make fillet preparations. Fillets were prepared in external saline solution composed of (in mM): NaCl 120, KCl 3, $MgCl_2$ 4, $CaCl_2$ 1.5, $NaHCO_3$ 10, trehalose 10, glucose 10, TES 5, sucrose 10, HEPES 10. The Osmolality was 305 mOsm kg^{-1} and the pH was 7.25. GFP-positive (C4da) neurons were located under a Zeiss D1 microscope with a

40X/1.0 NA water immersion objective lens. Gentle negative pressure was applied to the C4da neuron to trap the soma in a recording pipette (5 µm tip opening; 1.5–2.0 MΩ resistance) filled with external saline solution. Recordings were performed with a 700A amplifier (Molecular Devices, Sunnyvale, CA), and the data were acquired with Digidata 1440A (Molecular Devices) and Clampex 10.6 software (Molecular Devices). Extracellular recordings of action potentials were obtained in voltage clamp mode with a holding potential of 0 mV, a 2 kHz low-pass filter and a sampling frequency of 20 kHz.

Calcium Imaging

GCaMP calcium imaging of C4da neuronal activity was performed as described previously (Xiang *et al.*, 2010). For *in vitro* calcium imaging, axotomy was performed at 96h AEL and 120h AEL 3rd instar larvae were pinned ventral side up on silicone elastomer plates and dissected in the same external saline solution as electrophysiology. The internal organs were removed with fine forceps and the body wall was stretched with insect pins after opening body wall. Time-lapse imaging was performed under water objective lens (W Plan-Apochromat 20x/1.0 DIC CG=0.17 M27 75mm) by Zeiss LSM 700 confocal microscope. Frame rate is 0.97Hz. All soma ROIs were corrected for horizontal drifting with ImageJ slice alignment. Uncut C4da neurons from the same 3rd instar larvae were used as negative controls.

ACKNOWLEDGEMENTS

Kendra Takle Ruppell[a], Fei Wang[a], Yang Xiang[a, b]

[a]Department of Neurobiology, University of Massachusetts Medical School, 364

Plantation Street-LRB725, Worcester, USA 01605

[b]Corresponding author, University of Massachusetts Medical School, 364

Plantation Street-LRB725, Worcester, USA 01605. Yang.Xiang@umassmed.edu

Contributions Summary: F.W., K.T.R., and Y.X. designed the experiments.

K. T. R. performed experiments shown in Figure 4.2 A-B

F. W. performed experiments shown in Figure 4.2 C-D

K.T.R wrote the manuscript.

Appendix 2

Dye-Sensitized Core/Active Shell Upconversion Nanoparticles for

Optogenetics and Bioimaging Applications

Reprinted with permission from "Wu X*, Zhang Y*, Takle K*, Bisel O, Li Z, Lee H,

Lois C, Xiang Y, Han G. Dye-Sensitized Core/Active Shell Upconversion

Nanoparticles for Optogenetics and Bioimaging Applications. (2015) *ACS nano*.

Copyrighted 2016 American Chemical Society.

*co-first authors

Abstract

Near-infrared (NIR) dye-sensitized upconversion nanoparticles (UCNPs) can broaden the absorption range and boost upconversion efficiency of UCNPs. Here, we achieved significantly enhanced upconversion luminescence in dye-sensitized core/active shell UCNPs via the doping of ytterbium ions (Yb3+) in the UCNP shell, which bridged the energy transfer from the dye to the UCNP core. As a result, we synergized the two most practical upconversion booster effectors (dye-sensitizing and core/shell enhancement) to amplify upconversion efficiency. We demonstrated two biomedical applications using these UCNPs. By using dye-sensitized core/ active shell UCNP embedded poly(methyl methacrylate) polymer implantable systems, we successfully shifted the optogenetic neuron excitation window to a biocompatible and deep tissue penetrable 800 nm wavelength. Furthermore, UCNPs were water-solubilized with Pluronic F127 with high upconversion efficiency and can be imaged in a mouse model.

Introduction

Optogenetic techniques have been developed to control the activities and functions of neurons and to probe the interconnection of neural activities.(1, 2) When neural cells are excited by a specific wavelength of light, ion channels that are expressed with microbial opsins after viral transduction or transgenesis can activate or silence neuronal activity.(3) The high spatiotemporal resolution of optogenetic tools has enabled researchers to identify causal relationships

between brain activity and behavior. These studies may lead to new therapies for neuropsychiatric diseases. Currently, optogenetic tools rely on visible light that has a shallow depth of tissue penetration, such as ~470 nm for channelrhodopsin-2(3) and ~530 nm for halorhodopsin.(2) In order to deliver visible light into organs and tissues,(4, 5) optogenetic protocols typically require the permanent insertion of fiber-optic probes. However, this approach has limitations for chronic stimulation in animals because of potential tissue infections and constraint of the animal with fiber-optic tethers. To address this issue, micro light-emitting diodes (μ-LEDs) have been implanted inside the mouse brain; however, this approach is largely limited by the working distance, replacement, and renewability needs of the energy power source.(6, 7) These problems with optogenetics can be addressed by shifting the excitation wavelength to a region with a greater tissue penetration depth and less tissue scattering and blood absorption. For instance, a red-shifted variant of channelrhodopsin (ReaChR) was recently developed that can be excited from 470 to 630 nm.(8) Despite this advance, shifting the optogenetic operation window to the near-infrared (NIR) range (~700–1000 nm) is desirable to allow a deeper light penetration than red light.(9, 10)

With recent advances in nanotechnology, lanthanide-doped upconverting nanoparticles (UCNPs) have been developed that can be excited by NIR light and have emissions in the visible spectrum that can overlap with opsin's activation wavelengths.(11-13) UCNPs are currently used for *in vivo* deep tissue

imaging,(14-16) drug delivery,(17, 18) photodynamic therapy,(10, 19, 20)immunotherapy,(21) photoactivation,(22-24) and solar cell development.(25) NIR light at ~800 nm can penetrate transcranially to a depth of at least 4 cm through the human skull, meninges, scalp, and brain.(26) We thus envision the development of UCNPs in an optogenetic application to enhance the penetration of light for activation of neurons.

Despite the considerable potential of UCNPs for diverse applications, there is a need to increase the intensity of upconverting luminescence, as the quantum efficiency of these probes is still suboptimal.(27-29) The following are arguably the two most practical and effective ways to improve UC efficiency. First, utilization of shell growth can synthetically block the surface quenchers to the UCNP core layer.(27, 30, 31) Second, use of an organic NIR dye can alleviate inherently weak and narrow near-infrared absorption of the lanthanide ions (*e.g.*, Yb^{3+} or Nd^{3+}).(16, 32-35) Here, we combine these two strategies to overcome the low quantum efficiency of UCNPs and report the development of dye-sensitized core/active shell upconversion nanoparticles with significantly enhanced upconversion luminescence and a broadened absorption range. Specifically, we doped ytterbium ions into the UCNP shells. As a result, the energy of NIR excitation light peaked at the 800 nm that was absorbed by IR-806 dyes was able to be effectively transferred to the UCNP core *via* doped ytterbium ions in the shells. Further, we demonstrate the proof-of-concept that neurons can be activated by such dye-sensitized core/active shell UCNP embedded

poly(methyl methacrylate) (PMMA) matrix when excited at 800 nm. Moreover, these UCNPs were water-solubilized with Pluronic F127 and can be further imaged in a mouse model.

Results

We initially synthesized dye-sensitized core/shell UCNPs using β-NaYF$_4$ shell layers. More specifically, NaYF$_4$:20%Yb, 2%Er core (~20 nm) was used for the epitaxial growth of β-NaYF$_4$shells with varied thickness (*i.e.*, 2.5, 5, 7.5, 10, and 12.5 nm, respectively) (Figure S1) using a previously reported method.(36) Afterward, we explored the optimal ratio of IR-806 dyes *versus*UCNP cores using a modified method from the literature,(35) and in our study the optimal ratio was determined to be ~60:1 (6 μmol/L:0.1 μmol/L) (Figure S8). We then examined the upconversion emission for the core only and the core/shell UCNPs with IR-806 dye sensitizing under 800 nm continuous wave (CW) laser excitation. As can be seen in Figure 1, the results show that as the thickness of the NaYF$_4$ shell increased, such dye-sensitized core/shell UCNPs decreased in regard to luminescence intensity, reaching nearly its lowest point at a shell thickness of 7.5 nm. This result clearly suggests that a thicker β-NaYF$_4$ shell has an adverse effect on dye-sensitized upconversion emission and that the energy transfer from the IR dye to these UCNPs was blocked due to the increased shell thickness of β-NaYF$_4$. Thus, dye sensitization enhancement

could not be extended into core/shell UCNPs with commonly used inert

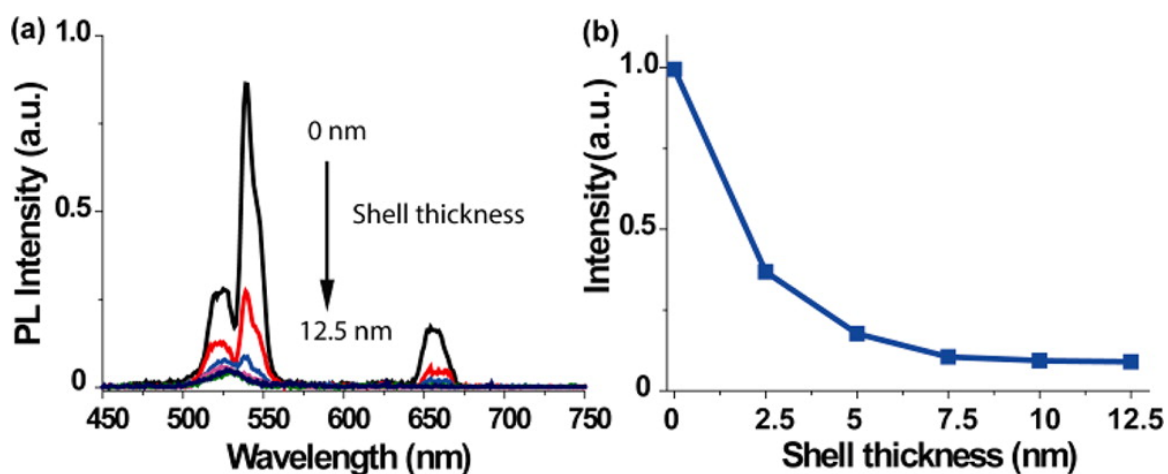hexagonal-phased β-NaYF$_4$ shells.

Figure A2.1. (a) Emission spectra of IR-806-dye-senstized UCNPs exhibiting

various β-NaYF$_4$ shell thickness (*i.e.*, 0, 2.5, 5, 7.5, 10, and 12.5 nm,

respectively) upon 800 nm CW laser excitation. (b) The integrated emission peak

area (from 500 to 700 nm) of those dye-sensitized UCNPs decreases as the shell

thickness increases. Note: In order to guide the eye, the data points are

connected by lines.

Next, we examined the doping of Yb^{3+} ions in the shell. Yb^{3+} ions can relay

energy from dyes to the emitters in a core-only UCNP.(35) In addition, in

core/active shell UCNP system, Yb^{3+} in the shell can absorb and transfer NIR

light (*e.g.*, 980 nm) energy into a UCNP's inner core.(37, 38)Here, we envisioned

that by doping Yb^{3+} ions in the shell the excitation energy absorbed by the dyes

can be transferred to the shell and then transferred from the shell Yb^{3+} into the core. In this regard, we chose to dope Yb^{3+} into the shell of core/shell UCNPs that had a 7.5 nm thick shell. In doing so, we found that such IR-806 dye-sensitized core/Yb^{3+} active shell nanoparticles (10% Yb^{3+} in the shell layer, *i.e.*, β-NaYF$_4$:20%Yb^{3+}, 2%Er@β-NaYF$_4$:10% Yb^{3+} UCNP) (Figures S3, S13, and S14) exhibited an enhanced upconversion emission under 800 nm excitation. When comparing the integrated upconversion emission area (from 450 to 700 nm), it showed 8 times enhancement in comparison to dye-sensitized core UCNPs (β-NaYF$_4$:20%Yb^{3+}, 2%Er^{3+}) and 70 times greater than the same sized dye-sensitized core/NaYF$_4$ shell UCNP (β-NaYF$_4$:20%Yb^{3+}, 2%Er^{3+}@β-NaYF$_4$) (Figure 2b). Note that IR dyes per UCNP were ~60:1 in the above experiments.

In this study, we also varied the Yb^{3+} content (10% Yb^{3+}, 30% Yb^{3+}, and 50% Yb^{3+}) in the shell layer (Figures S3 and S4) and found not only that 10% Yb^{3+} is the optimal doping concentration but that the further increase of Yb^{3+} concentration causes the upconversion intensity to decrease (Figure S11). This decrease is presumably caused by Yb^{3+} cross-relaxation quenching.(37) A controlled experiment of ~20 nm core only β-NaYF$_4$:30%Yb, 2%Er (Figures S5 and S6) was also carried out (*i.e.*, with the same total combined Yb^{3+} concentration as the core/Yb^{3+}-doped shell nanoparticles). The resulting upconversion emission intensity of IR-806-sensitized NaYF$_4$:30%Yb^{3+}, 2%Er^{3+} under 800 nm excitation was also much lower than that of the core/Yb^{3+} shell nanoparticles (Figure S9).

Further, the absolute quantum yield (QY) of our dye-sensitized core/Yb^{3+} shell UCNPs (IR-806-β-NaYF$_4$:20%Yb^{3+}, 2% Er^{3+}@β-NaYF$_4$:10%Yb) in DMF was measured to be ~5% at 2 W/cm^2 of 800 nm. Compared to the current highest value (0.18% at 31 W/cm^2)(39) reported for existing 800 nm excitable UCNPs, our result yields a higher QY at a lower power density.
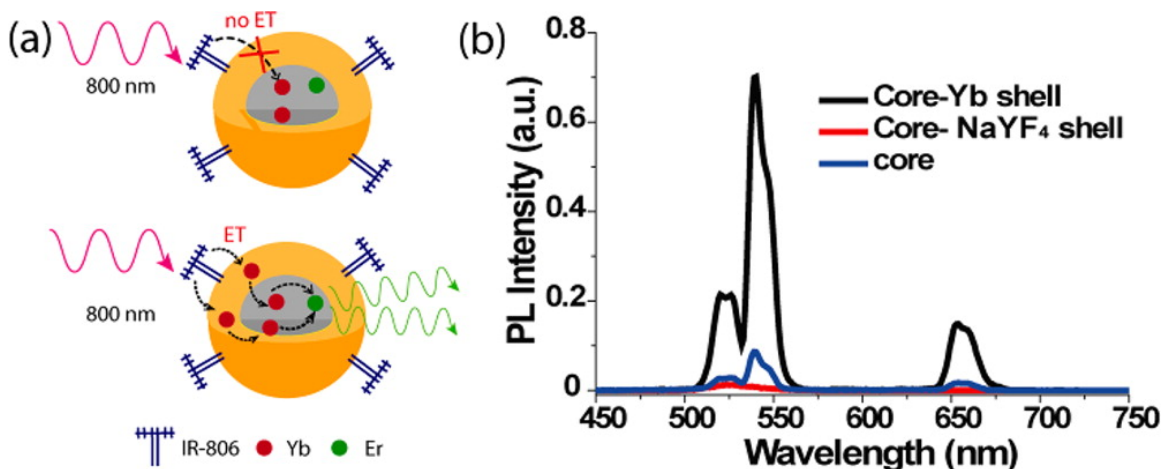
Figure A2.2 (a) Schematic showing the proposed energy transfer mechanism for core/shell UCNPs without (top) and with (bottom) Yb^{3+} doping. (b) Emission spectra of IR-806-sensitized core only (β-NaYF$_4$:20%Yb^{3+}, 2%Er^{3+}), core/NaYF$_4$shell (β-NaYF$_4$:20%Yb^{3+}, 2%Er^{3+}@β-NaYF$_4$), core/Yb^{3+} shell (β-NaYF$_4$:20%Yb^{3+}, 2%Er^{3+}@β-NaYF$_4$:10%Yb^{3+}). Note: The shell exhibited a controlled thickness of ~7.5 nm for core/NaYF$_4$ shell and core/Yb^{3+} shell UCNPs. The measurements were performed under 800 nm continuous wave laser excitation (2 W/cm^2), with a UCNP concentration of 0.1 µmol/L (ET: energy transfer).

Moreover, we found that the dye-sensitized core/Yb^{3+}-doped active shell UCNPs have a broadened absorption range. Utilizing this method, the integrated spectral response of the dye-sensitized core/Yb^{3+} shell UCNPs in the wavelength range 720–1000 nm is enhanced ~20-fold when compared to the same UCNPs without dye sensitizing (Figure 3). When compared at a single wavelength of 800 nm, the IR-806-sensitized core/Yb^{3+}-doped active shell shows ~1000 times upconversion luminescence enhancement. Further, when comparing an IR-806-sensitized core/Yb^{3+} active shell UCNP excited at 800 nm to a core-Yb^{3+} active shell UCNP without dye modification that is excited at its optimal wavelength of 980 nm, the IR-806 sensitizion also shows a 7 times enhancement (Figures 3 and S12). This result shows that the upconversion luminescence of UCNPs can be effectively enhanced by using organic dye molecules as the sensitizer in a core/active shell structure.
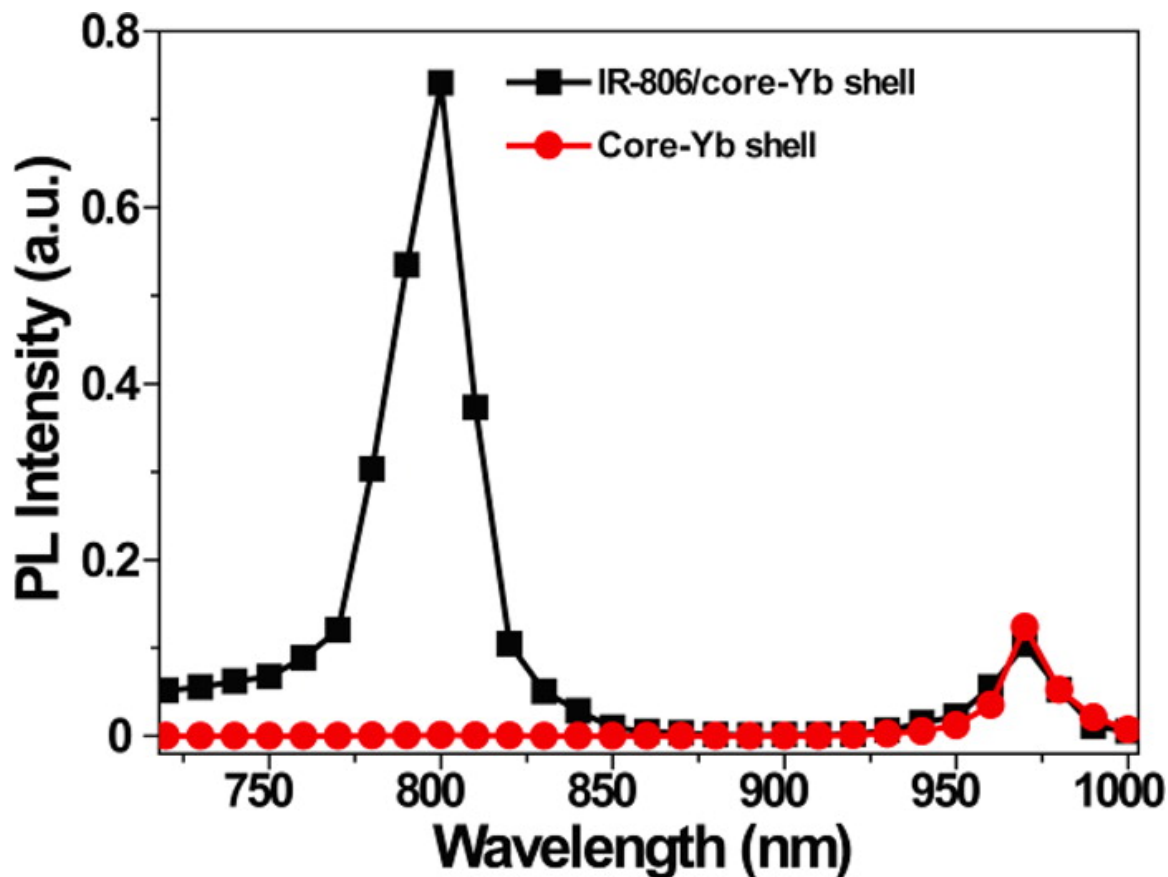
Figure A2.3 Excitation spectrum of β-NaYF$_4$:20%Yb^{3+}, 2%Er^{3+}@β-NaYF$_4$:10%Yb^{3+}(core/Yb^{3+} active shell) nanoparticle with (black squares) and without (red circles) IR-806 dye sensitization.

Since we are now able to combine the two best strategies to significantly improve upconversion efficiency, we envision that these dye-sensitized core/Yb^{3+} active shell UCNPs can address the limitation of poor tissue penetration depth of current optogenetic tools. As an initial proof-of-principle, we set out to develop an implantable device to test whether our UCNP systems can function as a relay for NIR light in regard to the activation of optogenetic

constructs in neuronal cells. We encapsulated our dye-sensitized core/Yb^{3+} active shell UCNPs into PMMA polymers so as to fabricate a thin film. We found that this film is resistant to water quenching in PBS buffer (Figure S17). This film was then placed directly beneath a glass coverslip containing cultured hippocampal neurons. Red light activatable channelrhodopsin revealed consistent depolarization and the act of potential firing in response to the light whose wavelength overlaps with the emission of dye-sensitized core/Yb^{3+} shell UCNPs(8) (Figure S15). Notably, in our study, when 800 nm NIR light was delivered in order to stimulate neurons, we observed robust neuronal activation in a light intensity-dependent manner (Figure 4). Neuronal depolarization depends on the intensity of the NIR (Figure 4c), and the threshold intensities for significant depolarization and the act of potential firing are 0.117 and 1.5 W/mm^2, respectively (Figure 4c and d). These power densities are about two to three magnitudes lower than what is currently used in two-photon technology for neuron cell activation (*e.g.*, 1×10^5 W/cm^2 (40) or 4.5×10^4 W/cm^2 (41)). Importantly, the UCNP system allows for precise temporal control of neuronal activation, as neuronal action potential was able to follow patterns of light pulses (*e.g.*, 100 ms, 500 ms, 2 s) in a time-locked fashion (Figure 4b). Next, to control for possible thermal and other potential side effects that are associated with NIR light delivery, we tested cultured hippocampal neurons in the following ways: without the UCNPs, without the ReaChR transfection, or with core/Yb^{3+} active shell UCNPs in absence of core Er^{3+}ion doping (~35 nm β-NaYF$_4$:20%Yb^{3+} @β-

$NaYF_4$, $10\%Yb^{3+}$) (Figure S7) where NIR absorption does not generate the emission of visible light under 800 nm excitation (Figure S10). In all three sets of control experiments, we found a great deal of reduced neuronal depolarization and the act of potential firing compared to the conditions that included opsin and our dye-sensitized core/Yb^{3+}active shell UCNPs (Figure 4c). It is noteworthy that we noticed that NIR light at high intensities (*i.e.*, 4.29 W/mm^2) does, in rare cases, activate the neuron (Figure 4d). Our results clearly demonstrate that NIR light at 800 nm is able to activate optogenetic constructs in order to manipulate neuronal activities. Moreover, optogenetic applications rely on pulsed light delivery compared to long exposure times with other application realms using upconversion nanoparticles (for example, photouncage(23)). We have observed that quite a short duration laser exposure (*i.e.*, 100 ms) can trigger neuron cell action potential firing.

(a) 4s
50 mV
1 s

(b) 500ms   100ms   2s
50 mV
1 s

(c)

depolarization (mV)

■ Dye/UCNP+ReaChR
■ Dye +ReaChR
■ Dye/UCNP(no ReaCHR)
■ Dye/UCNP(No Er)+ReaChR

n.s.   n.s.   *   ***   ****   ****   ****
            **   ****   ****   ****   ****
            **   ****   ****   ****   ****

(d)

% cells firing

0.0006   0.0588   0.117   1.5   2.34   3.315   4.29
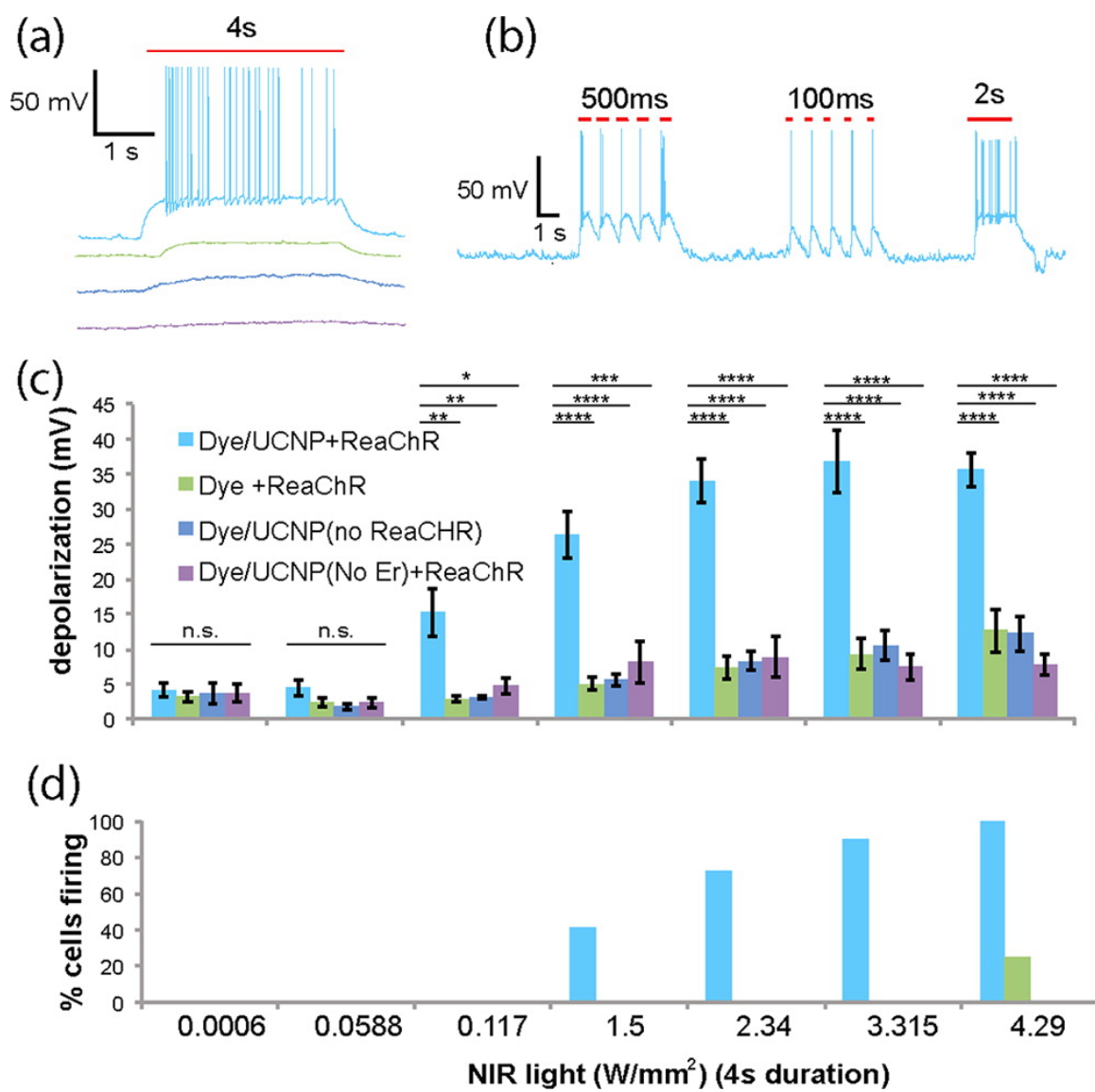
NIR light (W/mm²) (4s duration)

Figure A2.4. Near infrared light activation of ReaChR in cultured hippocampal neurons. Examples of the act of potential firing in response to (a) prolonged (4 s) and (b) pulsed (100 ms, 500 ms, 2 s) delivery of 800 nm NIR light (2.34 W/mm^2). (c) Neuronal depolarization and (d) firing triggered by 800 nm NIR light at different intensities for a duration of 4 s. Note that there can be depolarization and neuronal activation even in some control cases. **, $p < 0.01$, ****, $p < 0.0001$. One-way ANOVA with Bonferroni correction. The four color squares in (c) are annotations for (a)–(d).

Furthermore, we also water-solubilized our dye-sensitized core/active shell UCNPs (IR806-β-NaYF$_4$:20%Yb^{3+}, 2%Er^{3+}@β-NaYF$_4$, 10%Yb^{3+}) for bioimaging applications. Hydrophobic dye-sensitized core/Yb^{3+} active shell UCNPs were rendered water-soluble *via* wrapping them in the amphiphilic triblock copolymer Pluronic F127.(42, 43) The resultant triblock copolymer micelle possessed a hydrophobic core to encapsulate the hydrophobic oleic acid ligand coated UCNPs through van der Waal's force. It also has a hydrophilic shell, offering it aqueous stability (Figure 5). The as-synthesized micelles were able to disperse in aqueous solution with an average hydrodynamic size of ~110 nm in water. In PBS, the resulting micelle encapsulation has an average particle size that is similar to that in pure water (Figure S19). After micelle encapsulation, the luminescence of these UCNPs can be visualized by the naked eye (Figure 5b inset). Its upconversion luminescence remained above 30% under 2 W/cm^2 of 800 nm laser (Figure 5b). It is noteworthy that we noticed that there was a certain luminescence decrease over 10 min (Figure S16). The *in vivo* animal imaging study of such micelle-encapsulated dye-sensitized UCNPs was evaluated *via* the use of a Maestro EX small-animal optical imaging system. Following subcutaneous administration of micelle-encapsulated dye-sensitized core/Yb^{3+} shell UCNPs, we observed clear UCNP characteristic luminescent signals *in vivo* under 800 nm excitation (Figure S20). This suggests the feasibility of biophotonic application for dye-sensitized core/Yb^{3+} active shell UCNPs.
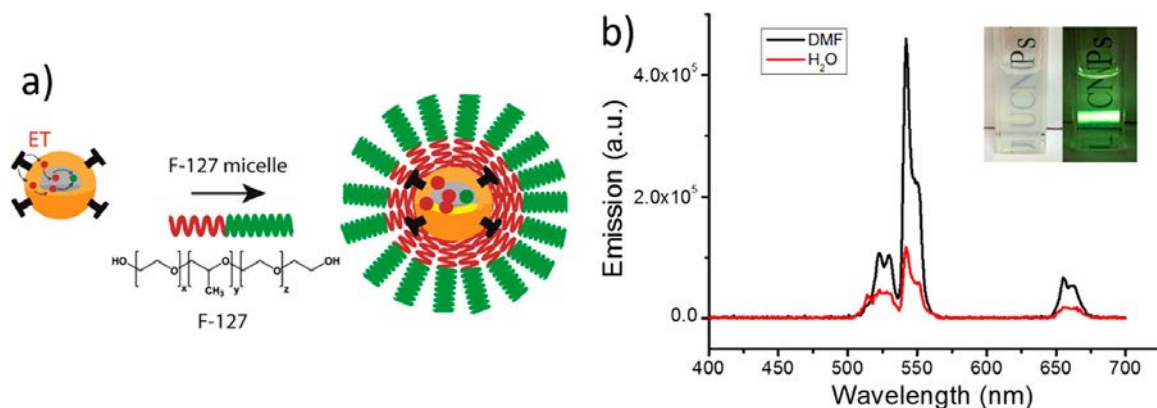
Figure A2.5 (a) Schematic of the phase transfer procedure using Pluronic F-127 as encapsulation material. (b) Emission spectra of dye-sensitized core/Yb^{3+} shell UCNPs (1 mg/mL) before micelle encapsulation in DMF (black curve) and after encapsulation in PBS (red curve), acquired upon 800 nm CW laser excitation (2 W/cm^2). The inset displays photographs of micelle-encapsulated dye-sensitized core/Yb^{3+} shell UCNPs dispersed in PBS with and without 800 nm CW laser excitation obtained by an Apple iphone 5S camera.

Discussion

In conclusion, we synergized two state-of-the-art approaches for the enhancement of upconversion efficiency and were able to demonstrate dye-sensitized core/Yb^{3+} active shell UCNPs with broadened absorption and elevated upconversion efficiency. We doped Yb^{3+} ions in the shell in order to bridge the energy transfer from the NIR dye to UCNP core, the latter of which is otherwise blocked by the commonly used core/$NaYF_4$ shell UCNPs. These dye-sensitized UCNPs were further applied for optogenetic analysis in the NIR tissue optical window for potential use in controlling neuronal activity. We further water-solubilized these UCNPs and demonstrated their use for bioimaging applications. We offer an interesting strategy to improve the upconversion efficiency of UCNPs, which will pave the way for new biological and medical applications.

Materials and Methods

General Chemicals

IR-780 iodide (99%), 4-mercaptobenzoic acid (99%), Y_2O_3 (99.9%), Yb_2O_3 (99.9%), Er_2O_3 (99.9%), CF_3COONa (99.9%), CF_3COOH, 1-octadecene (90%), oleic acid (90%), oleylamine (90%), *N,N*-dimethylformamide (DMF, anhydrous, 99.8%), and dichloromethane (DCM, AR grade) were all purchased from Sigma-Aldrich and used without further purification. The lanthanide (Ln) trifluoroacetates, $Ln(CF_3COO)_3$, were prepared as described in the literature.(10)

Instrumentation

^{1}H NMR spectra were recorded on a Varian AMX400 (400 MHz) using d_6-DMSO as solvent at room temperature. Transmission electron microscopy (TEM) was performed on a Philips CM10 transmission electron microscope operating at an accelerating voltage of 100 kV. Images were recorded on a Gatan slow-scan CCD camera. The powder X-ray diffraction (XRD) patterns were recorded by a Vantec-500 area detector using Co Kα radiation (1.79 Å). The 2θ angle of the XRD spectra was recorded at a scanning rate of 5 deg/min and then was converted to Cu Kα radiation values by Bragg's law. The size distribution of the samples was determined by dynamic light scattering (DLS) equipped with a Zetasizer Nano-ZS (He–Ne laser wavelength at 633 nm) and an autotitrator (Malvern Instruments, Malvern, UK). The upconversion photoluminescence emission spectrum was measured using a fluorospectrophotometer (Fluorolog-3, HORIBA, USA). The samples were excited by either a 980 or 800 nm continuous wave laser under the power density of 2 W/cm^2 (Hi-Tech Optoelectronics Co., Ltd., China). BALB/c mice (female, 4–8 weeks, from Jackson Laboratory) were used for the imaging experiment. Hair on the back of the mice was shaved, and the mice were anesthetized using iv-injected ketamine/xylazine during imaging (Maestro EX system). Micelle-encapsulated dye-sensitized UCNPs (200 μL, 10 mg/mL) were injected subcutaneously 10 min before imaging (800 nm CW laser excitation, 1 W/cm^2, 1 s exposure time). The animal procedures were approved by the University of Massachusetts Medical School Institutional Animal Care and

Use Committee. The NIR photoluminescence emission spectrum of IR-806 dye was measured with excitation at 750 nm and emission measured from 775 to 1200 nm using a Horiba Nanolog spectrofluorometer with a 5509 PMT detector and 450 W xenon lamp. For the upconversion excitation spectrum measurements, the Ti:sapphire laser was switched to continuous-wave mode, and the absence of mode-locking was confirmed by monitoring the laser output using a 400 MHz oscilloscope and fast photodiode. The detection utilized a bandpass filter (FF01-524/24-25, Semrock, Rochester, NY, USA) and a PMH100-6 photomultiplier tube module from Becker-Hickl. A pulse generator provided a 5 MHz sync signal to the TCSPC electronics, and the photons over the time-to-amplitude converter range were integrated to provide the total signal for each excitation wavelength. In order to use a constant excitation intensity (2 mW) at each wavelength, a 1 mm thick quartz plate was used to pick off part of the excitation beam and direct it to a calibrated power meter (corrected for the excitation wavelengths, Newport 1830-C with 818 series detector).

Synthetic Procedures

The synthesis of IR-806

The IR-806 was synthesized the same as the method described in the literature.

Synthesis of β-NaYF$_4$:20%Yb, 2%Er Core UCNPs, β-NaYF$_4$:20%Yb Core UCNPs, and β-NaYF$_4$:30%Yb, 2%Er UCNPs

Synthesis of β-NaYF$_4$:Ln core UCNPs: The β-NaYF$_4$:Ln core UCNPs were prepared by a two-step thermolysis method. In the first step, CF$_3$COONa (0.5 mmol) and proper Ln(CF$_3$COO)$_3$((Y+Yb+Er) 0.5 mmol in total; for β-NaYF$_4$:20%Yb, 2%Er, Y:Yb:Er = 78%:20%:2%; for β-NaYF$_4$:20%Yb, Y:Yb = 80%:20%; for β-NaYF$_4$:30%Yb, 2%Er, Y:Yb:Er = 68%:30%:2%) precursors were mixed with oleic acid (5 mmol), oleyamine (5 mmol), and 1-octadecene (10 mmol) in a two-neck reaction flask. The slurry mixture was heated to 110 °C to form a transparent solution followed by 10 min of degassing. Then the flask was heated to 300 °C at a rate of 15 °C/min under dry argon flow, and it was maintained at 300 °C for 30 min. The α-NaYF$_4$:Ln intermediate UCNPs were gathered from the cooled reaction solution by centrifugal washing with excessive ethanol (7500g, 30 min). In the second step, the α-NaYF$_4$:Ln intermediate UCNPs were redispersed into oleic acid (10 mmol) and 1-octadecene (10 mmol) together with CF$_3$COONa (0.5 mmol) in a new two-neck flask. After degassing at 110 °C for 10 min, this flask was heated to 325 °C at a rate of 15 °C/min under dry argon flow, and it remained at 325 °C for 30 min. Then, β-NaYF$_4$:Ln UCNPs were centrifugally separated from the cooled reaction media and preserved in hexane (10 mL) as stock solution.

Synthesis of Core/NaYF$_4$ Shell and Core/Yb^{3+}-Doped Shell UCNPs

In this thermolysis reaction, as-synthesized 20 nm β-NaYF$_4$:20%Yb, 2%Er UCNPs or β-NaYF$_4$:20%Yb (for the synthesis of ~35 nm β-NaYF$_4$:20%Yb/β-

NaYF$_4$:10%Yb control core/shell) served as cores for the epitaxial growth of undoped β-NaYF$_4$ shells and Yb^{3+}-doped shells. Typically, a stock solution of β-NaYF$_4$:20%Yb, 2%Er UCNPs (5 mL, *ca*. 1 μmol/L core UCNPs) was transferred into a two-neck flask, and hexane was sequentially removed by heating. To prepare core/NaYF$_4$ shell β-NaYF$_4$:20%Yb, 2%Er/β-NaYF$_4$ UCNPs with increased shell thickness, increasing amounts of CF$_3$COONa (0.1, 0.25, 0.5, 0.75, and 1 mmol) and Y(CF$_3$COO)$_3$(0.1, 0.25, 0.5, 0.75, and 1 mmol) were used, respectively. To prepare ~35 nm core/Yb^{3+} shell UCNPs, CF$_3$COONa (0.5 mmol) and Ln(Y+Yb) (CF$_3$COO)$_3$ (0.5 mmol) were used, The mole percentages of Y(CF$_3$COO)$_3$ of 90%, 70%, and 50% and Yb(CF$_3$COO)$_3$ of 10%, 30%, and 50% were used. In these reactions, the above-mentioned precursors were introduced as UCNP shell precursors with oleic acid (10 mmol) and 1-octadecene (10 mmol). After 10 min of degassing at 110 °C, the flask was heated to 325 °C at a rate of 15 °C/min under dry argon flow and was kept at 325 °C for 30 min. The products were precipitated by adding 20 mL of ethanol to the cooled reaction flask. After centrifugal washing with hexane/ethanol (7500*g*, 30 min), the core/shell UCNPs were redispersed in 10 mL of hexane.

Dye-Sensitized Upconversion Nanoparticle Preparation

IR-806 dye-sensitized UCNPs were prepared based on a modified literature method. More specifically, they were prepared by mixing different amounts of IR-806 into UCNPs in DCM/hexane (v/v 1:10). The final concentrations of UCNPs

are 0.1 μmol/L; the final concentrations of IR-806 are 0, 2, 4, 6, 25, 50, and 100 μmol/L. All the solutions mentioned above stood for 1 h at room temperature before measurements. The dye-conjugated core/shell UCNPs can be isolated by centrifugation (12000g, 30 min) and can be redissolved in DMF.

Fabrication of UCNP-Encapsulated PMMA Film

IR-806 and 35 nm β-NaYF$_4$:20%Yb, 2% Er/β-NaYF$_4$:10%Yb core/Yb active shell UCNPs (0.06 mmol:1 μmol) were first mixed in DCM/hexane (1 mL, 1:10, v/v). After 1 h of continuous stirring, the dye-conjugated core/shell UCNPs were isolated by centrifugation. The dye-coated nanoparticles were redissolved in a small amount of DMF. Meanwhile, 200 mg of PMMA was dissolved in 1 mL of DMF at 100 °C. This was then cooled to room temperature. Then a dye-conjugated UCNP DMF solution was blended with the above prepared PMMA. The resulting mixture was pasted onto a cover glass and remained overnight at room temperature to obtain a transparent PMMA thin film that includes dye-sensitized core/Yb^{3+} active shell UCNPs. Control samples were prepared using the same amount of reagents with IR dye only or with dye-modified ~35 nm (20 nm core and 7.5 nm shell) β-NaYF$_4$:20%Yb/β-NaYF$_4$, 10%Yb UCNPs (*i.e.*, in the absence of Er^{3+} emitters).

Micelle Encapsulation

A 2 mg amount of dye-coated core/Yb^{3+} shell UCNPs in 0.2 mL of hexane/DCM (10:1, v/v) was slowly added into 2 mL of a Pluronic F-127 aqueous solution (0.5%, w/v). Under vigorous stirring conditions, the organic solvent was allowed to slowly evaporate at room temperature for 4 h. Micelle-encapsulated dye-sensitized UCNPs were collected *via* centrifugation at 12000*g* at a temperature below 4 °C for 30 min.

Electrophysiology

Whole-cell patch clamp recordings of the neurons virally infected with red activatable channelrhodopsin and red fluorescent protein (RFP) were performed 2–3 weeks after plating on an upright microscope with a 40× (NA 1.0) water immersion lens. The 800 nm CW laser was delivered at increasing intensities through the objective. Neurons growing on glass coverslips were removed from the culture dish and placed in external saline solution composed of (in mM) NaCl 125, KCl 2.5, NaH_2PO_4 1.25, $MgCl_2$ 1, $CaCl_2$ 2, $NaHCO_3$ 26, glucose 20. The osmolality was 312 mOsm kg^{-1}, and the pH was 7.3. RFP-positive neurons were located under a Zeiss D1 microscope with a 40×/1.0 NA water immersion objective lens. Neurons were recorded with a recording pipet (5 µm tip opening) filled with internal saline solution composed of (in mM) potassium gluconate 120, KCl 10, HEPES 10, MgATP 4, NaGTP 0.3, Na phosphocreatine·H_2O 5, EGTA 0.2, pH 7.3, OSM 290 mM. Recordings were performed with a 700B amplifier (Molecular Devices), and the data were acquired with Digidata 1440A (Molecular

Devices) and Clampex 10.6 software (Molecular Devices). Electrophysiological recordings of action potentials were obtained in current clamp mode with current injection to sustain −65 mV at rest. A 2 kHz low-pass filter and a sampling frequency of 20 kHz were used. Only excitable cells with a membrane resistance of >200 MΩ and with action potential firing upon green light exposure (except for nontransfected controls) were analyzed. After each recording sweep, we injected a hyperpolarizing current to measure passive membrane properties. Any cell with >10% change during the recording was discarded.

Neuronal Culture

All experiments were approved by the local Animal Welfare Committee. Embryonic day 17 hippocampi from Sprague-Drawley rats were dissected in Hank's balanced salt solution (Invitrogen) containing $MgCl_2$ and Hepes (Sigma) and digested with papain (Worthington). Papain was inactivated by ovomucoid (Worthington), and the tissue was dissociated in culture medium [neurobasal medium containing B27 supplement, penicillin, streptomycin, and glutamine (Invitrogen)]. Cells were infected with a self-inactivating lentiviral vector in which the RSV promoter drives expression of ReacHR fused to the red fluorescent protein mcherry. The lentiviral vector was prepared, concentrated, and titrated. Dissociated neurons were incubated for 1 h at 37 °C in suspension with the lentiviral vector at a multiplicity of infection of 1:1 (1 viral particle per 1 neuron) and plated at a density of 150 000 cells per milliliter of medium on coverslips

coated with poly-D-lysine (Sigma) and laminin (Invitrogen). Culture medium was exchanged after 24 h and subsequently changed twice a week. Neurons were recorded after 14 days *in vitro*.

Absolute Quantum Yield Measurement

This testing was done at the Molecular Foundry, a User Facility of the U.S. Department of Energy. A cylindrical quartz cuvette was loaded with 500 µL of a freshly prepared solution of dye-conjugated nanoparticles (0.01 µmol/L). The cuvette was placed in a calibrated integrating sphere coupled with fiber-optics to a Horiba Jobin Yvon Fluorolog-3 spectrometer. Samples were excited with an 800 nm laser (2 W/cm^2, Hi-Tech Optoelectronics), and emission spectra (450–720 nm) and spectra of scattered excitation light (797–804 nm) of the samples and the solvent blank were recorded. All spectra were corrected for the wavelength-dependent sensitivity of the apparatus. The absolute quantum yield of each sample was determined according to the equation QY = ($I_{em,sample}$ − $I_{em,blank}$)/($I_{ex,blank}$ − $I_{ex,sample}$). Here, I_x is the integrated intensity of the emission (em) or scattering (ex) spectrum for the sample or blank (*x*).

Appendix II Bibliography

(1) Fenno, L.; Yizhar, O.; Deisseroth, K. The Development and Application of Optogenetics. Annu. Rev. Neurosci. 2011, 34, 389−412.

(2) Zhang, F.; Wang, L. P.; Brauner, M.; Liewald, J. F.; Kay, K.; Watzke, N.; Wood, P. G.; Bamberg, E.; Nagel, G.; Gottschalk, A.; Deisseroth, K. Multimodal Fast Optical Interrogation of Neural Circuitry. Nature 2007, 446, 633−U4.

(3) Boyden, E. S.; Zhang, F.; Bamberg, E.; Nagel, G.; Deisseroth, K. Millisecond-Timescale, Genetically Targeted Optical Control of Neural Activity. Nat. Neurosci. 2005, 8, 1263−1268.

(4) Grill, W. M.; Norman, S. E.; Bellamkonda, R. V. Implanted Neural Interfaces: Biochallenges and Engineered Solutions. Annu. Rev. Biomed. Eng. 2009, 11, 1−24.

(5) Huang, H.; Delikanli, S.; Zeng, H.; Ferkey, D. M.; Pralle, A. Remote Control of Ion Channels and Neurons Through MagneticField Heating of Nanoparticles. Nat. Nanotechnol. 2010, 5, 602−606.

(6) McCall, J. G.; Kim, T. I.; Shin, G.; Huang, X.; Jung, Y. H.; AlHasani, R.; Omenetto, F. G.; Bruchas, M. R.; Rogers, J. A. Fabrication and Application of Flexible, Multimodal Light-Emitting Devices for Wireless Optogenetics. Nat. Protoc. 2013, 8, 2413−2428.

(7) Kim, T. I.; McCall, J. G.; Jung, Y. H.; Huang, X.; Siuda, E. R.; Li, Y. H.; Song, J. Z.; Song, Y. M.; Pao, H. A.; Kim, R. H.; Lu, C.; Lee, S. D.; Song, I.S.; Shin, G.; Al-Hasani, R.; Kim, S.; Tan, M. P.; Huang, Y.; Omenetto, F. G.; Rodger, J. A.; et

al. Injectable, Cellular-Scale Optoelectronics with Applications for Wireless Optogenetics. Science 2013, 340, 211−216.

(8) Lin, J. Y.; Knutsen, P. M.; Muller, A.; Kleinfeld, D.; Tsien, R. Y. ReaChR: A Red-Shifted Variant of Channelrhodopsin Enables Deep Transcranial Optogenetic Excitation. Nat. Neurosci. 2013, 16, 1499− 1508.

(9) Kam, N. W. S.; O'Connell, M.; Wisdom, J. A.; Dai, H. J. Carbon Nanotubes as Multifunctional Biological Transporters and NearInfrared Agents for Selective Cancer Cell Destruction. Proc. Natl. Acad. Sci. U. S. A. 2005, 102, 11600−11605.

(10) Punjabi, A.; Wu, X.; Tokatli-Apollon, A.; El-Rifai, M.; Lee, H.; Zhang, Y. W.; Wang, C.; Liu, Z.; Chan, E. M.; Duan, C. Y.; Han, G. Amplifying the Red-Emission of Upconverting Nanoparticles for Biocompatible Clinically Used Prodrug-Induced Photodynamic Therapy. ACS Nano 2014, 8, 10621−10630.

(11) Haase, M.; Schafer, H. Upconverting Nanoparticles. Angew. Chem., Int. Ed. 2011, 50, 5808−5829.

(12) Zhou, J.; Liu, Z.; Li, F. Y. Upconversion Nanophosphors for Small-Animal Imaging. Chem. Soc. Rev. 2012, 41, 1323−1349.

(13) Wang, F.; Liu, X. G. Recent Advances in the Chemistry of Lanthanide-Doped Upconversion Nanocrystals. Chem. Soc. Rev. 2009, 38, 976−989.

(14) Liu, Q.; Sun, Y.; Yang, T. S.; Feng, W.; Li, C. G.; Li, F. Y. Sub-10 nm Hexagonal Lanthanide-Doped NaLuF4 Upconversion Nanocrystals for Sensitive Bioimaging In Vivo. J. Am. Chem. Soc. 2011, 133, 17122−17125.

(15) Chen, G. Y.; Shen, J.; Ohulchanskyy, T. Y.; Patel, N. J.; Kutikov, A.; Li, Z. P.; Song, J.; Pandey, R. K.; Agren, H.; Prasad, P. N.; Han, G. Alpha-NaYbF4:Tm3+)/CaF2 Core/Shell Nanoparticles with Efficient Near-Infrared to Near-Infrared Upconversion for High-Contrast Deep Tissue Bioimaging. ACS Nano 2012, 6, 8280−8287.

(16) Wu, X.; Chen, G.; Shen, J.; Li, Z.; Zhang, Y.; Han, G. Upconversion Nanoparticles: A Versatile Solution to Multiscale Biological Imaging. Bioconjugate Chem. 2015, 26, 166−175.

(17) Yang, D. M.; Ma, P. A.; Hou, Z. Y.; Cheng, Z. Y.; Li, C. X.; Lin, J. Current Advances in Lanthanide Ion (Ln3+)-Based Upconversion Nanomaterials for Drug Delivery. Chem. Soc. Rev. 2015, 44, 1416− 1448.

(18) Shen, J.; Zhao, L.; Han, G. Lanthanide-Doped Upconverting Luminescent Nanoparticle Platforms for Optical Imaging-Guided Drug Delivery and Therapy. Adv. Drug Delivery Rev. 2013, 65, 744− 755.

(19) Idris, N. M.; Jayakumar, M. K. G.; Bansal, A.; Zhang, Y Upconversion Nanoparticles AsVersatile Light Nanotransducers for Photoactivation Applications. Chem. Soc. Rev. 2015, 44, 1449−1478.

(20) Chen, Q.; Wang, C.; Cheng, L.; He, W. W.; Cheng, Z.; Liu, Z. Protein Modified Upconversion Nanoparticles for Imaging-Guided Combined Photothermal and Photodynamic Therapy. Biomaterials 2014, 35, 2915−2923.

(21) Xiang, J.; Xu, L. G.; Gong, H.; Zhu, W. W.; Wang, C.; Xu, J.; Feng, L. Z.; Cheng, L.; Peng, R.; Liu, Z. Antigen-Loaded Upconversion Nanoparticles for Dendritic Cell Stimulation, Tracking, and Vaccination in Dendritic Cell-Based Immunotherapy. ACS Nano 2015, 9, 6401−6411.

(22) Jayakumar, M. K. G.; Idris, N. M.; Zhang, Y. Remote Activation of Biomolecules in Deep Tissues Using Near-Infrared-to-UV Upconversion Nanotransducers. Proc. Natl. Acad. Sci. U. S. A. 2012, 109, 8483−8488.

(23) Yang, Y. M.; Shao, Q.; Deng, R. R.; Wang, C.; Teng, X.; Cheng, K.; Cheng, Z.; Huang, L.; Liu, Z.; Liu, X. G.; Xing, B. G. In Vitro and In Vivo Uncaging and Bioluminescence Imaging by Using Photocaged Upconversion Nanoparticles. Angew. Chem., Int. Ed. 2012, 51, 3125− 3129.

(24) Shen, J.; Chen, G.; Ohulchanskyy, T. Y.; Kesseli, S. J.; Buchholz, S.; Li, Z.; Prasad, P. N.; Han, G. Tunable Near Infrared to Ultraviolet Upconversion Luminescence Enhancement in (Alpha-NaYF4:Yb,Tm)/CaF2 Core/Shell Nanoparticles for In Situ Real-Time Recorded Biocompatible Photoactivation. Small 2013, 9, 3213−3217.

(25) Wang, H. Q.; Batentschuk, M.; Osvet, A.; Pinna, L.; Brabec, C. J. Rare-Earth Ion Doped Up-Conversion Materials for Photovoltaic Applications. Adv. Mater. 2011, 23, 2675−2680.

(26) Tedford, C. E.; DeLapp, S.; Jacques, S.; Anders, J. Quantitative Analysis of Transcranial and Intraparenchymal Light Penetration in Human Cadaver Brain Tissue. Lasers Surg. Med. 2015 , 47, 312 −322.

(27) Han, S. Y.; Deng, R. R.; Xie, X. J.; Liu, X. G. Enhancing Luminescence in Lanthanide-Doped Upconversion Nanoparticles. Angew. Chem., Int. Ed. 2014 , 53, 11702 −11715.

(28) Chen, G. Y.; Han, G. Theranostic Upconversion Nanoparticles (I). Theranostics 2013 , 3, 289 −291.

(29) Chan, E. M.; Levy, E. S.; Cohen, B. E. Rationally Designed Energy Transfer in Upconverting Nanoparticles. Adv. Mater. 2015 , 27, 5753 −5761.

(30) Chen, X.; Peng, D.; Ju, Q.; Wang, F. Photon Upconversion in Core-Shell Nanoparticles. Chem. Soc. Rev. 2015 , 44, 1318 −1330.

(31) Wang, F.; Wang, J.; Liu, X. Direct Evidence of a Surface Quenching Effect on Size-Dependent Luminescence of Upconversion Nanoparticles. Angew. Chem., Int. Ed. 2010 , 49, 7456 −7460.

(32) Shen, J.; Chen, G. Y.; Vu, A. M.; Fan, W.; Bilsel, O. S.; Chang, C. C.; Han, G. Engineering the Upconversion Nanoparticle Excitation Wavelength: Cascade Sensitization of Tri-doped Upconversion Colloidal Nanoparticles at 800 nm. Adv. Opt. Mater. 2013 , 1 (9), 644 −650.

(33) Wang, Y. F.; Liu, G. Y.; Sun, L. D.; Xiao, J. W.; Zhou, J. C.; Yan, C. H. Nd3+-Sensitized Upconversion Nanophosphors: Efficient In Vivo Bioimaging Probes with Minimized Heating Effect. ACS Nano 2013 , 7, 7200 −7206.

(34) Xie, X.; Liu, X. Photonics: Upconversion Goes Broadband. Nat. Mater. 2012 , 11, 842 −843.

(35) Zou, W. Q.; Visser, C.; Maduro, J. A.; Pshenichnikov, M. S.; Hummelen, J. C. Broadband Dye-Sensitized Upconversion of NearInfrared Light. Nat. Photonics 2012, 6, 560−564.

(36) Mai, H. X.; Zhang, Y. W.; Si, R.; Yan, Z. G.; Sun, L. D.; You, L. P.; Yan, C. H. High-Quality Sodium Rare-Earth Fluoride Nanocrystals: Controlled Synthesis and Optical Properties. J. Am. Chem. Soc. 2006 , 128, 6426 −6436.

(37) Vetrone, F.; Naccache, R.; Mahalingam, V.; Morgan, C. G.; Capobianco, J. A. The Active-Core/Active-Shell Approach: A Strategy to Enhance the Upconversion Luminescence in Lanthanide-Doped Nanoparticles. Adv. Funct. Mater. 2009 , 19, 2924 −2929.

(38) Yang, D. M.; Li, C. X.; Li, G. G.; Shang, M. M.; Kang, X. J.; Lin, J. Colloidal Synthesis and Remarkable Enhancement of the Upconversion Luminescence of BaGdF 5:Yb3+/Er3+ Nanoparticles by Active-Shell Modification. J. Mater. Chem. 2011 , 21, 5923 −5927.

(39) Liu, B.; Chen, Y.; Li, C.; He, F.; Hou, Z.; Huang, S.; Zhu, H.; Chen, X.; Lin, J. Poly(Acrylic Acid) Modification of Nd3+-Sensitized Upconversion Nanophosphors for Highly Efficient UCL Imaging and pH-Responsive Drug Delivery. Adv. Funct. Mater. 2015 , 25, 4717 − 4729.

(40) Mohanty, S. K.; Reinscheid, R. K.; Liu, X.; Okamura, N.; Krasieva, T. B.; Berns, M. W. In-Depth Activation of Channelrhodopsin 2-Sensitized Excitable Cells with High Spatial Resolution Using Two-Photon Excitation with a Near-Infrared Laser Microbeam. Biophys. J. 2008 , 95, 3916 −3926.

(41) Papagiakoumou, E.; Anselmi, F.; Begue, A.; de Sars, V.; Gluckstad, J.; Isacoff, E. Y.; Emiliani, V. Scanless Two-Photon Excitation of Channelrhodopsin-2. Nat. Methods 2010 , 7, 848 −854.

(42) Basak, R.; Bandyopadhyay, R. Encapsulation of Hydrophobic Drugs in Pluronic F127 Micelles: Effects of Drug Hydrophobicity, Solution Temperature, and pH. Langmuir 2013 , 29, 4350 −4356.

(43) Liu, L.; Yong, K. T.; Roy, I.; Law, W. C.; Ye, L.; Liu, J.; Kumar, R.; Zhang, X.; Prasad, P. N. Bioconjugated Pluronic TriblockCopolymer Micelle-Encapsulated Quantum Dots for Targeted Imaging of Cancer: in vitro and in vivo Studies. Theranostics 2012 , 2 , 705 −713.

Bibliography

Abdulla, F. A. and Smith, P. A. (2000) 'Axotomy- and Autotomy-Induced Changes in the Excitability of Rat Dorsal Root Ganglion Neurons', *Journal of Physiology*, pp. 630–643.

Anderson, M. A. *et al.* (2016) 'Astrocyte scar formation aids CNS axon regeneration', *Nature*, 532(7598), pp. 195–200. doi: 10.1038/nature17623.Astrocyte.

Apfel, S. C. (2002) 'Is the therapeutic application of neurotrophic factors dead?', *Annals of Neurology*, 51(1), pp. 8–11. doi: 10.1002/ana.10099.

Appenzeller, O. and Palmer, G. (1972) 'The cyclic AMP (adenosine 3′,5′-phosphate) content of sciatic nerve: changes after nerve crush', *Brain Research*, 42(2), pp. 521–524. doi: https://doi.org/10.1016/0006-8993(72)90553-7.

Arnoux, J.-B. *et al.* (2010) 'Congenital hyperinsulinism', *Early Human Development*. Elsevier Ltd, 86(5), pp. 287–294. doi: 10.1016/j.earlhumdev.2010.05.003.

Babcock, D. T., Landry, C. and Galko, M. J. (2009) 'Cytokine signaling mediates UV-induced nociceptive sensitization in Drosophila larvae', *Current Biology*, 19(10), pp. 799–806. doi: 10.1016/j.cub.2009.03.062.Cytokine.

Bading, H., Ginty, D. D. and Greenberg, M. E. (1993) 'Regulation of gene expression in hippocampal neurons by distinct calcium signaling pathways', *Science*, 260(5105), p. 181 LP-186. doi: 10.1126/science.8097060.

Bando, Y. *et al.* (2016) 'Control of Spontaneous Ca 2 + Transients Is Critical for Neuronal Maturation in the Developing Neocortex', *Cerebral Cortex*, 26(1), pp. 106–117. doi: 10.1093/cercor/bhu180.

Basbaum, A. I. *et al.* (2009) 'Review Cellular and Molecular Mechanisms of Pain', *Cell*, 139, pp. 267–284. doi: 10.1016/j.cell.2009.09.028.

Bei, F. *et al.* (2016) 'Restoration of Visual Function by Enhancing Conduction in Regenerated Axons', *Cell*. Elsevier, 164(1–2), pp. 219–232. doi: 10.1016/j.cell.2015.11.036.

Belardetti, F. and Zamponi, G. W. (2012) 'Calcium channels as therapeutic targets', *WIREs Membr Transp Signal*, 1, pp. 433–451. doi: 10.1002/wmts.38.

Bouhassira, D. *et al.* (2008) 'Prevalence of chronic pain with neuropathic characteristics in the general population', *Pain*, 136(3), pp. 380–387. doi: 10.1016/j.pain.2007.08.013.

Branch, S. Y., Sharma, R. and Beckstead, M. J. (2014) 'Aging Decreases L-Type Calcium Channel Currents and Pacemaker Firing Fidelity in Substantia Nigra Dopamine Neurons', *Journal of Neuroscience*, 34(28), pp. 9310–9318. doi: 10.1523/JNEUROSCI.4228-13.2014.

Bundesen, L. Q. *et al.* (2003) 'Ephrin-B2 and EphB2 Regulation of Astrocyte-Meningeal Fibroblast Interactions in Response to Spinal Cord Lesions in Adult Rats', *The Journal of Neuroscience*, 23(21), pp. 7789–7800.

Cai, D. *et al.* (1999) 'Prior exposure to neurotrophins blocks inhibition of axonal regeneration by MAG and myelin via a cAMP-dependent mechanism', *Neuron*,

22(1), pp. 89–101. doi: 10.1016/S0896-6273(00)80681-9.

Calin-Jageman, I. and Lee, A. (2008) 'Cav1 L-type Ca2+channel signaling complexes in neurons', *Journal of Neurochemistry*, 105(3), pp. 573–583. doi: 10.1111/j.1471-4159.2008.05286.x.

Campbell, D. S. and Holt, C. E. (2001) 'Chemotropic Responses of Retinal Growth Cones Mediated by Rapid Local Protein Synthesis and Degradation', *Neuron*. Elsevier, 32(6), pp. 1013–1026. doi: 10.1016/S0896-6273(01)00551-7.

Canty, A. J. *et al.* (2013) 'In-vivo single neuron axotomy triggers axon regeneration to restore synaptic density in specific cortical circuits', *Nature Communications*. Nature Publishing Group, 4(May), pp. 1–10. doi: 10.1038/ncomms3038.

Cao, X. *et al.* (2012) 'Nerve injury increases brain‑derived neurotrophic factor levels to suppress BK channel activity in primary sensory neurons', *Journal of neurochemistry*, 121(6), pp. 944–953. doi: 10.1111/j.1471-4159.2012.07736.x.Nerve.

Carlsen, R. C. (1982) 'Axonal transport of adenylate cyclase activity in normal and axotomized frog sciatic nerve', *Brain Research*, 232(2), pp. 413–424. doi: https://doi.org/10.1016/0006-8993(82)90284-0.

Case, L. C. and Tessier-lavigne, M. (2005) 'Regeneration of the adult central nervous system', *Current Biology*, 15, pp. 749–753.

Chan, C. S. *et al.* (2007) '" Rejuvenation " protects neurons in mouse models of Parkinson ' s disease', *Nature*, 447, pp. 1081–1089. doi: 10.1038/nature05865.

Chan, C. S. *et al.* (2007) '"Rejuvenation" protects neurons in mouse models of Parkinson's disease', *Nature*, 447(7148), pp. 1081–1086. doi: 10.1038/nature05865.

Chen, L. *et al.* (2011) 'Axon regeneration pathways identified by systematic genetic screening in C. elegans', *Neuron*, 71(6), pp. 1043–1057. doi: 10.1016/j.neuron.2011.07.009.Axon.

Chen, S.-R., Cai, Y.-Q. and Pan, H.-L. (2009) 'Plasticity and Emerging Role of BKCa Channels in Nociceptive Control in Neuropathic Pain', *J Neurochem*, 110(1), pp. 352–362. doi: 10.1088/1367-2630/15/1/015008.Fluid.

Chen, S. *et al.* (2018) 'Altered Synaptic Vesicle Release and Ca2+ Influx at Single Presynaptic Terminals of Cortical Neurons in a Knock-in Mouse Model of Huntington's Disease', *Frontiers in Moecular Neuroscience*, 11, pp. 1–17. doi: 10.3389/fnmol.2018.00478.

Cheng, H., Liao, K. and Liao, S. (2004) 'Spinal Cord Repair With Acidic Fibroblast Growth Factor as a Treatment for a Patient With Chronic Paraplegia', *Spine*, 29(14), pp. 284–288.

Chuang, Y. *et al.* (2018) 'Involvement of advillin in somatosensory neuron subtype-specific axon regeneration and neuropathic pain', *PNAS*, 111(36), pp. 8557–8566. doi: 10.1073/pnas.1716470115.

Chung, S. H. *et al.* (2016) 'Novel DLK-independent neuronal regeneration in Caenorhabditis elegans shares links with activity-dependent ectopic outgrowth', *PNAS*, pp. 2852–2860. doi: 10.1073/pnas.1600564113.

Cooper, D. C. and White, F. J. (2000) 'L-type calcium channels modulate glutamate-driven bursting activity in the nucleus accumbens in vivo', *Brain Research*, 880(1–2), pp. 212–218. doi: 10.1016/S0006-8993(00)02868-7.

Coste, B. *et al.* (2011) 'Piezo1 and Piezo2 are essential components of distinct mechanically-activated cation channels', *Science*, 330(6000), pp. 55–60. doi: 10.1126/science.1193270.Piezo1.

Costigan, M., Scholz, J. and Woolf, C. J. (2009) 'Neuropathic pain', *Annu Rev Neurosci*, (32), pp. 1–32. doi: 10.1146/annurev.neuro.051508.135531.Neuropathic.

Danesi, C. *et al.* (2018) 'Increased Calcium Influx through L-type Calcium Channels in Human and Mouse Neural Progenitors Lacking Fragile X Mental Retardation Protein', *Stem Cell Reports*, 11, pp. 1449–1461. doi: 10.1016/j.stemcr.2018.11.003.

David, S. and Aguayo, A. J. (1981) 'Axonal Elongation into Peripheral Nervous System "Bridges''' after Central Nervous System Injury in Adult Rats''', *Science*, 214(4523), pp. 931–933.

Davie, J. T., Clark, B. A. and Häusser, M. (2008) 'The Origin of the Complex Spike in Cerebellar Purkinje Cells', *Journal of neurophysiology*, 28(30), pp. 7599–7609. doi: 10.1523/JNEUROSCI.0559-08.2008.The.

Davis, M. J. *et al.* (2002) 'Regulation of Ion Channels by Integrins', *Cell Biochemistry and Biophysics*, 36.

Day, M. *et al.* (2006) 'Selective elimination of glutamatergic synapses on striatopallidal neurons in Parkinson disease models', *Nature Neuroscience*, 9(2), pp. 251–259. doi: 10.1038/nn1632.

Duan, X. *et al.* (2015) 'Subtype-Specific regeneration of retinal ganglion cells following axotomy: Effects of osteopontin and mtor signaling', *Neuron*. Elsevier Inc., 85(6), pp. 1244–1256. doi: 10.1016/j.neuron.2015.02.017.

Dunn, T. *et al.* (2006) 'Imaging of cAMP levels and PKA activity reveals that retinal waves drive oscillations in second messenger cascades', *Journal of Neuroscience*, 26(49), pp. 12807–12815. doi: 10.1021/nn300902w.Release.

Eberl, D. F. *et al.* (1998) 'Genetic and Developmental Characterization of Dmca1D, a Calcium Channel ?1 Subunit Gene in Drosophila melanogaster', *Genetics*, 148, pp. 1159–1169.

Enes, J. *et al.* (2010) 'Article Electrical Activity Suppresses Axon Growth through Ca v 1 . 2 Channels in Adult Primary Sensory Neurons', *Current Biology*, 20, pp. 1154–1164. doi: 10.1016/j.cub.2010.05.055.

Eyherabide, H. G. *et al.* (2009) 'Bursts generate a non-reducible spike-pattern code', *Frontiers in Neuroscience*, 3(1), pp. 8–14. doi: 10.3389/neuro.01.002.2009.

Fink, C. C. *et al.* (2003) 'Selective Regulation of Neurite Extension and Synapse Formation by the ɴʟ but not the ␣ Isoform of CaMKII', *Neuron*, 39, pp. 283–297.

Ghosh-Roy, A. *et al.* (2010) 'Calcium and Cyclic AMP Promote Axonal Regeneration in Caenorhabditis elegans and Require DLK-1 Kinase', *Journal of Neuroscience*, 30(9), pp. 3175–3183.

Gold, M. S. and Gebhart, G. F. (2010) 'Nociceptor sensitization in pain pathogenesis', *Nature Medicine*, 16(11), pp. 1248–1257. doi: 10.1038/nm.2235.Nociceptor.

Goldberg, J. L., Klassen, M. P., *et al.* (2002) 'Amacrine-Signaled Loss of Intrinsic Axon Growth Ability by Retinal Ganglion Cells', *Science*, 296, pp. 1860–1865.

Goldberg, J. L., Espinosa, J. S., *et al.* (2002) 'Retinal Ganglion Cells Do Not Extend Axons by Default', *Neuron*, 33(5), pp. 689–702. doi: 10.1016/S0896-6273(02)00602-5.

Gomez, T. M. *et al.* (2001) 'Filopodial Calcium Transients Promote Substrate-Dependent Growth Cone Turning', *Science*, 291(5510), p. 1983 LP-1987. doi: 10.1126/science.1056490.

Gomez, T. M. and Zheng, J. Q. (2006) 'The molecular basis for calcium-dependent axon pathfinding', *Nature Reviews Neuroscience*, 7, pp. 115–125. doi: 10.1038/nrn1844.

Grueber, W. B. *et al.* (2003) 'Dendrites of Distinct Classes of Drosophila Sensory Neurons Show Different Capacities for Homotypic Repulsion', *Current Biology*, 13, pp. 618–626. doi: 10.1016/S.

Gui, P. *et al.* (2006) 'Integrin Receptor Activation Triggers Converging Regulation of Cav1 . 2 Calcium Channels by c-Src and Protein Kinase A Pathways', *The Journal of Biological Chemistry*, 281(20), pp. 14015–14025. doi: 10.1074/jbc.M600433200.

Hamid, S. and Hayek, R. (2008) 'Role of electrical stimulation for rehabilitation and regeneration after spinal cord injury : an overview', *Eur Spine J*, 17, pp. 1256–1269. doi: 10.1007/s00586-008-0729-3.

Hammarlund, M. *et al.* (2009) 'Axon Regeneration Requires a Conserved MAP Kinase Pathway', *Science*, 323(February). doi: 10.1126/science.1112699.

He, Z. and Jin, Y. (2016) 'Intrinsic Control of Axon Regeneration', *Neuron*. Elsevier Inc., 90(3), pp. 437–451. doi: 10.1016/j.neuron.2016.04.022.

Hong, K. *et al.* (2000) 'Calcium signalling in the guidance of nerve growth by netrin-1', *Nature*, 403(6765), pp. 93–98. doi: 10.1038/47507.

Hoshiba, X. Y. *et al.* (2016) 'Sox11 Balances Dendritic Morphogenesis with Neuronal Migration in the Developing Cerebral Cortex', *The Journal of Neuroscience*, 36(21), pp. 5775–5784. doi: 10.1523/JNEUROSCI.3250-15.2016.

Hu, G. *et al.* (2016) 'Single-cell RNA-seq reveals distinct injury responses in different types of DRG sensory neurons', *Scientific Reports.* Nature Publishing Group, pp. 1–11. doi: 10.1038/srep31851.

Huang, D. W. *et al.* (1999) 'A therapeutic vaccine approach to stimulate axon regeneration in the adult mammalian spinal cord', *Neuron*, 24(3), pp. 639–647. doi: 10.1016/S0896-6273(00)81118-6.

Hughes, C. and Thomas, J. (2007) 'A Sensory Feedback Circuit Coordinates Muscle Activity in Drosophila', *Mol Cell Neurosci*, 35(2), pp. 383–396. doi: 10.1016/j.surg.2006.10.010.Use.

James N. Campbell and Meyer, R. A. (2006) 'Mechanisms of neuropathic pain', *Neuron*, 52(1), pp. 77–92. doi: 10.1016/j.euroneuro.2011.05.005.

Jin, L. *et al.* (2012) 'Single Action Potentials and Subthreshold Electrical Events Imaged in Neurons with a Fluorescent Protein Voltage Probe', *Neuron*, 75(5), pp. 779–785. doi: https://doi.org/10.1016/j.neuron.2012.06.040.

Julius, D. (2013) 'TRP Channels and Pain', *The Annual Review of Cell and Developmental Biology*, 29, pp. 355–384. doi: 10.1146/annurev-cellbio-101011-155833.

Kadoya, K. *et al.* (2009) 'Combined Intrinsic and Extrinsic Neuronal Mechanisms Facilitate Bridging Axonal Regeneration One Year After Spinal Cord Injury', *Neuron*, 64(2), pp. 165–172. doi: 10.1016/j.neuron.2009.09.016.Combined.

Kim, S. E. *et al.* (2012) 'The role of Drosophila Piezo in mechanical nociception', *Nature*, 483(7388), pp. 209–212. doi: 10.1038/nature10801.The.

Kim, S. H. and Chung, J. M. (1992) 'An experimental model for peripheral neuropathy produced by segmental spinal nerve ligation in the rat', *Pain*, 50(2), pp. 355–363. doi: 10.1016/0304-3959(94)90090-6.

Knight, Z. A. *et al.* (2012) 'Molecular Profiling of Activated Neurons by Phosphorylated Ribosome Capture', *Cell*, 151(5). doi: 10.1016/j.cell.2012.10.039.Molecular.

Koninck, P. De and Schulman, H. (1998) 'Sensitivity of CaM kinase II to the frequency of Ca2+ oscillations.', *Science*, 279, pp. 227–30. doi: 10.1126/science.279.5348.227.

Krahe, R. and Gabbiani, F. (2004) 'Burst firing in sensory systems', *Nature Reviews Neuroscience*, 5, pp. 13–24. doi: 10.1038/nrn1296.

Krieger, B. *et al.* (2017) 'Four alpha ganglion cell types in mouse retina: Function , structure , and molecular signatures', *PLOS One*, pp. 1–21.

Kunimoto, M. (1995) 'A Neuron-specific Isoform of Brain Ankyrin , 440-kD Ankyrin-B , Is Targeted to the Axons of Rat Cerebellar Neurons', *The Journal of Cell Biology*, 131(6), pp. 1821–1829.

Kurimoto, T. *et al.* (2010) 'Long-distance axon regeneration in the mature optic nerve: Contributions of Oncomodulin, cAMP, and pten gene deletion', *Journal of Neuroscience*, 30(46), pp. 15654–15663. doi: 10.1523/JNEUROSCI.4340-10.2010.Long-distance.

Landowski, L. M. *et al.* (2016) 'Axonopathy in peripheral neuropathies : Mechanisms and therapeutic approaches for regeneration', *Journal of Chemical Neuroanatomy*. Elsevier B.V., 76, pp. 19–27. doi: 10.1016/j.jchemneu.2016.04.006.

Lang, S. B. *et al.* (2007) 'Endogenous Brain-Derived Neurotrophic Factor Triggers Fast Calcium Transients at Synapses in Developing Dendrites', *The Journal of Neuroscience*, 27(5), pp. 1097–1105. doi: 10.1523/JNEUROSCI.3590-06.2007.

Latremoliere, A. and Woolf, C. (2009) 'Central Sensitization: a generator of pain hypersensitivity by Central Neural Plasticity', *J Pain*, 10(9), pp. 895–926. doi: 10.1016/j.jpain.2009.06.012.Central.

Levi, A. D. O. *et al.* (2002) 'Peripheral nerve grafts promoting central nervous system regeneration after spinal cord injury in the primate', *Journal of*

Neurosurgery: Spine. Journal of Neurosurgery Publishing Group, 96(2), pp. 197–205. doi: 10.3171/spi.2002.96.2.0197.

Lewin, S. L. *et al.* (1997) 'Simultaneous Treatment With BDNF and CNTF After Peripheral Nerve Transection and Repair Enhances Rate of Functional Recovery Compared With BDNF Treatment Alone', *The Laryngoscope*, 107, pp. 992–999.

Li, C. L. *et al.* (2016) 'Somatosensory neuron types identified by high-coverage single-cell RNA-sequencing and functional heterogeneity', *Cell Research*, 26(1), pp. 83–102. doi: 10.1038/cr.2015.149.

Li, J. *et al.* (1997) 'PTEN, a Putative Protein Tyrosine Phosphatase Gene Mutated in Human Brain, Breast, and Prostate Cancer', *Science*, 275(5308), pp. 1943–1947. doi: 10.1126/science.275.5308.1943.

Li, S. *et al.* (2016) 'Promoting axon regeneration in the adult CNS by modulation of the melanopsin / GPCR signaling', *PNAS*, 113(7), pp. 1937–1942. doi: 10.1073/pnas.1523645113.

Liao, Y. *et al.* (2010) 'Neuronal Ca 2 + -Activated K + Channels Limit Brain Infarction and Promote Survival', *PLOS One*, 5(12), pp. 1–8. doi: 10.1371/journal.pone.0015601.

Lim, J. H. A. *et al.* (2016) 'Neural activity promotes long-distance, target-specific regeneration of adult retinal axons', *Nature Neuroscience*, 19(8), pp. 1073–1084. doi: 10.1038/nn.4340.

Lindsay, R. (1988) 'Nerve growth factors (NGF, BDNF) enhance axonal regeneration but are not required for survival of adult sensory neurons', *The Journal of Neuroscience*, 8(7), pp. 2394–2405.

Liu, K. *et al.* (2011) 'Neuronal Intrinsic Mechanisms of Axon Regeneration', *Annual Review of Neuroscience*, 34(1), pp. 131–152. doi: 10.1146/annurev-neuro-061010-113723.

Liu, Y. *et al.* (1999) 'Transplants of Fibroblasts Genetically Modified to Express BDNF Promote Regeneration of Adult Rat Rubrospinal Axons and Recovery of Forelimb Function', *The Journal of Neuroscience*, 19(11), pp. 4370–4387.

MacDonald, J. M. *et al.* (2006) 'The Drosophila Cell Corpse Engulfment Receptor Draper Mediates Glial Clearance of Severed Axons', *Neuron*, 50(6), pp. 869–881. doi: 10.1016/j.neuron.2006.04.028.

Macosko, E. Z. *et al.* (2015) 'Highly Parallel Genome-wide Expression Profiling of Individual Cells Using Nanoliter Droplets Resource Highly Parallel Genome-wide Expression Profiling of Individual Cells Using Nanoliter Droplets', *Cell*. Elsevier, 161(5), pp. 1202–1214. doi: 10.1016/j.cell.2015.05.002.

Maklad, A., Sharma, A. and Azimi, I. (2019) 'Calcium Signaling in Brain Cancers : Roles and Therapeutic Targeting', *Cancers*, 11(145). doi: 10.3390/cancers11020145.

MANDOLESI, G. *et al.* (2004) 'Acute physiological response of mammalian central neurons to axotomy: ionic regulation and electrical activity', *The FASEB Journal*. Federation of American Societies for Experimental Biology, 18(15), pp. 1934–1936. doi: 10.1096/fj.04-1805fje.

McConnell, P. and Berry, M. (1982) 'Regeneration of axons in the mouse retina

after injury.', *Bibliotheca anatomica*, (23), pp. 26–37. Available at: http://www.ncbi.nlm.nih.gov/pubmed/7138488.

McKerracher, L. *et al.* (1994) 'Identification of myelin-associated glycoprotein as a major myelin-derived inhibitor of neurite growth', *Neuron*, 13(4), pp. 805–811. doi: 10.1016/0896-6273(94)90247-X.

Mckinney, B. C. and Murphy, G. G. (2006) 'The L-Type voltage-gated calcium channel Ca v 1 . 3 mediates consolidation , but not extinction , of contextually conditioned fear in mice', *Learning and Memory*, (734), pp. 584–589. doi: 10.1101/lm.279006.584.

Mcquarrie, I. G. and Grafstein, B. (1973) 'Axon Outgrowth Enhanced by a Previous Nerve Injury', *Archives of Neurology*, 29(1), pp. 53–55. doi: 10.1001/archneur.1973.00490250071008.

Meyer-Franke, A. *et al.* (1998) 'Depolarization and cAMP elevation rapidly recruit TrkB to the plasma membrane of CNS neurons', *Neuron*, 21(4), pp. 681–693. doi: 10.1016/S0896-6273(00)80586-3.

Michaelis, M., Liu, X. and Janig, W. (2000) 'Axotomized and Intact Muscle Afferents But No Skin Afferents Develop Ongoing Discharges of Dorsal Root Ganglion Origin after Peripheral Nerve Lesion', *The Journal of Neuroscience*, 20(7), pp. 2742–2748.

Ming, G. *et al.* (2001) 'Electrical Activity Modulates Growth Cone Guidance by Diffusible Factors', *Neuron*, 29, pp. 441–452.

Moore, D. L. *et al.* (2009) 'KLF Family Members Regulate Intrinsic Axon Regeneration Ability', *Science*, 326(5950), pp. 298–301. doi: 10.1126/science.1175737.KLF.

Murphy, T. H., Worley, P. F. and Baraban, M. (1991) 'L-type VoltageSensitive Calcium Channels Mediate Synaptic Activation of Immediate Early', *Neuron*, 7, pp. 625–635.

Navarro, X., Vivo, M. and Valero-Cabre, A. (2007) 'Neural plasticity after peripheral nerve injury and regeneration �´', *Progress in Neurobiology*, 82, pp. 163–201. doi: 10.1016/j.pneurobio.2007.06.005.

Nehrt, A. *et al.* (2007) 'THE CRITICAL ROLE OF VOLTAGE-DEPENDENT CALCIUM CHANNEL IN AXONAL REPAIR FOLLOWING MECHANICAL TRAUMA', *Neuroscience*, 146(4), pp. 1504–1512. doi: 10.1016/j.neuroscience.2007.02.015.THE.

Neumann, S. *et al.* (2002) 'Regeneration of sensory axons within the injured spinal cord induced by intraganglionic cAMP elevation', *Neuron*, 34(6), pp. 885–893. doi: 10.1016/S0896-6273(02)00702-X.

Neumann, S. and Woolf, C. J. (1999) 'Regeneration of dorsal column fibers into and beyond the lesion site following adult spinal cord injury', *Neuron*, 23(1), pp. 83–91. doi: 10.1016/S0896-6273(00)80755-2.

Nieuwenhuis, B. *et al.* (2018) 'Integrins promote axonal regeneration after injury of the nervous system', *Biological Reviews*, 93, pp. 1339–1362. doi: 10.1111/brv.12398.

Norsworthy, M. *et al.* (2017) 'Sox11 Expression Promotes Regeneration of Some

Retinal Ganglion Cell Types but Kills Others', *Neuron*, 94(6), pp. 1112–1120. doi: 10.1016/j.neuron.2017.05.035.Sox11.

O'Donovan, K. J. (2016) 'Intrinsic Axonal Growth and the Drive for Regeneration', *Frontiers in Neuroscience*, 10, pp. 1–11. doi: 10.3389/fnins.2016.00486.

Ohyama, T. *et al.* (2015) 'A multilevel multimodal circuit enhances action selection in Drosophila', *Nature*, 520. doi: 10.1038/nature14297.

Olson, P. A. *et al.* (2005) 'G-Protein-Coupled Receptor Modulation of Striatal Ca V 1 . 3 L-Type Ca 2 2 Channels Is Dependent on a Shank-Binding Domain', *The Journal of Neuroscience*, 25(5), pp. 1050–1062. doi: 10.1523/JNEUROSCI.3327-04.2005.

Palomer, E. *et al.* (2016) 'Neuronal activity controls Bdnf expression via Polycomb de-repression and CREB/CBP/JMJD3 activation in mature neurons', *Nature Communications*, pp. 1–12. doi: 10.1038/ncomms11081.

Park, J. F. and Luo, Z. D. (2010) 'Calcium channel functions in pain processing', *Channels*, 4(6), pp. 510–517. doi: 10.4161/chan.4.6.12869.

Park, K. K. *et al.* (2008) 'Promoting Axon Regeneration in the Adult CNS by Modulation of the PTEN/mTOR Pathway', *Neurobiology*, 322(5903), pp. 963–966. doi: 10.1126/science.1161566.Promoting.

Pasterkamp, R. J. *et al.* (1999) 'Expression of the gene encoding the chemorepellent semaphorin III is induced in the fibroblast component of neural scar tissue formed following injuries of adult but not neonatal CNS', *Molecular and Cellular Neuroscience*, 13(2), pp. 143–166. doi: 10.1006/mcne.1999.0738.

Paz, J. T. *et al.* (2013) 'Closed-loop optogenetic control of thalamus as a tool for interrupting seizures after cortical injury', *Nature Neuroscience*, 16(1). doi: 10.1038/nn.3269.

Perret, D. and Luo, Z. D. (2009) 'Targeting Voltage-Gated Calcium Channels for Neuropathic Pain Management', *Neurotherapeutics*, 6(4), pp. 679–692. doi: 10.1016/j.nurt.2009.07.006.

Platzer, J. *et al.* (2000) 'Congenital Deafness and Sinoatrial Node Dysfunction in Mice Lacking Class D L-Type Ca2+ Channels', *Cell*, 102, pp. 89–97.

Poulin, J. *et al.* (2016) 'review Disentangling neural cell diversity using single-cell transcriptomics', *Nature Neuroscience*, 19(7), pp. 1131–1141. doi: 10.1038/nn.4366.

Qiu, J. *et al.* (2002) 'Spinal axon regeneration induced by elevation of cyclic AMP', *Neuron*, 34(6), pp. 895–903. doi: 10.1016/S0896-6273(02)00730-4.

Rajnicek, A. M., Foubister, L. E. and McCaig, C. D. (2006) 'Growth cone steering by a physiological electric field requires dynamic microtubules, microfilaments and Rac-mediated filopodial asymmetry', *Journal of Cell Science*, 119(9), pp. 1736–1745. doi: 10.1242/jcs.02897.

Richardson, P. M. and Issa, V. M. K. (1984) 'Peripheral injury enhances central regeneration of primary sensory neurones', *Nature*, 309(5971), pp. 791–793. doi: 10.1038/309791a0.

Rishal, I. and Fainzilber, M. (2013) 'Axon–soma communication in neuronal injury', *Nature Reviews Neuroscience*. Nature Publishing Group, a division of

Macmillan Publishers Limited. All Rights Reserved., 15, p. 32. Available at: https://doi.org/10.1038/nrn3609.

Ritz, B. *et al.* (2010) 'L-Type Calcium Channel blockers and Parkinson's Disease in Denmark', *Ann Neurol*, 67(5), pp. 600–606. doi: 10.1002/ana.21937.L-Type.

Ronaghi, M. *et al.* (2010) 'Challenges of Stem Cell Therapy for Spinal Cord Injury: Human Embryonic Stem Cells, Endogenous Neural Stem Cells, or Induced Pluripotent Stem Cells?', *STEM CELLS*, 28(1), pp. 93–99. doi: 10.1002/stem.253.

Sang, L., Dick, I. E. and Yue, D. T. (2016) 'Protein kinase A modulation of CaV1.4 calcium channels', *Nature Communications*, pp. 1–11. doi: 10.1038/nprot.2016.089.

Sann, S. B. *et al.* (2008) 'Neurite Outgrowth and In Vivo Sensory Innervation Mediated by a CaV2.2 – Laminin Beta2 Stop Signal', *The Journal of Neuroscience*, 28(10), pp. 2366–2374. doi: 10.1523/JNEUROSCI.3828-07.2008.

Schnell, L. and Schwab, M. E. (1990) 'Axonal regeneration in the rat spinal cord produced by an antibody against myelin-associated neurite growth inhibitors', *Nature*, 343, pp. 269–272. doi: 10.1016/0021-9797(80)90501-9.

Sheehan, D. *et al.* (1996) 'A somatodendritic distribution of Rab11 in rabbit brain neurons', *NeuroReport*, 7, pp. 1297–1300.

Shi, L. *et al.* (2017) 'The Contribution of L-Type Ca v 1 . 3 Channels to Retinal Light Responses', *Frontiers in Moecular Neuroscience*, 10(December), pp. 1–17. doi: 10.3389/fnmol.2017.00394.

Simms, B. A. and Zamponi, G. W. (2014) 'Review Neuronal Voltage-Gated Calcium Channels: Structure, Function, and Dysfunction', *Neuron*. Elsevier, 82, pp. 24–45. doi: 10.1016/j.neuron.2014.03.016.

Singh, K. K. and Miller, F. D. (2005) 'Activity regulates positive and negative neurotrophin-derived signals to determine axon competition', *Neuron*, 45(6), pp. 837–845. doi: 10.1016/j.neuron.2005.01.049.

Sinnegger-Brauns, M. J. *et al.* (2004) 'Isoform-specific regulation of mood behavior and pancreatic β cell and cardiovascular function by L-type Ca 2 + channels', *The Journal of Clinical Investigation*, 113(10). doi: 10.1172/JCI200420208.1430.

Skinner, F. K. *et al.* (1999) 'Bursting in Inhibitory Interneuronal Networks : A Role for Gap-Junctional Bursting in Inhibitory Interneuronal Networks : A Role for Gap-Junctional Coupling', *Journal of neurophysiology*. doi: 10.1152/jn.1999.81.3.1274.

Smith, P. D. *et al.* (2009) 'SOCS3 deletion promotes optic nerve regeneration in vivo', *Neuron*, 64(5), pp. 617–623. doi: 10.1016/j.neuron.2009.11.021.SOCS3.

So, K.-F. and Yip, H. K. (1998) 'Regenerative capacity of retinal ganglion cells in mammals', *Vision Research*, 38(10), pp. 1525–1535. doi: 10.1016/S0042-6989(97)00226-5.

Soares, L., Parisi, M. and Bonini, N. M. (2014) 'Axon injury and regeneration in the adult drosophila', *Scientific Reports*, 4. doi: 10.1038/srep06199.

Song, X.-J. *et al.* (1999) 'Mechanical and thermal hyperalgesia and ectopic

neuronal discharge after chronic compression of dorsal root ganglia', *Journal of Neurophysiology*, 82(6), pp. 3347–3358. doi: 10.1152/jn.1999.82.6.3347.

Song, X. J. *et al.* (1999) 'Mechanical and thermal hyperalgesia and ectopic neuronal discharge after chronic compression of dorsal root ganglia.', *Journal of neurophysiology*, 82(6), pp. 3347–3358. doi: 10.1152/jn.1999.82.6.3347.

Song, Y. *et al.* (2012) 'Regeneration of Drosophila sensory neuron axons and dendrites is regulated by the Akt pathway involving Pten and microRNA bantam', *Genes and Development*, 26(14), pp. 1612–1625. doi: 10.1101/gad.193243.112.

Song, Y. *et al.* (2015) 'Regulation of axon regeneration by the RNA repair and splicing pathway', *Nature Neuroscience*, 18(6), pp. 817–825. doi: 10.1038/nn.4019.

Spira, M. E. *et al.* (2002) 'Calcium , Protease Activation , and Cytoskeleton Remodeling Underlie Growth Cone Formation and Neuronal Regeneration', *Cellular and Molecular Neurobiology*, 21(6), pp. 591–604.

Spitzer, N. C. (2006) 'Electrical activity in early neuronal development', *Nature*, 444(7120), pp. 707–712. doi: 10.1038/nature05300.

St-Pierre, F. *et al.* (2014) 'High-fidelity optical reporting of neuronal electrical activity with an ultrafast fluorescent voltage sensor', *Nature neuroscience*. 2014/04/22, 17(6), pp. 884–889. doi: 10.1038/nn.3709.

Steinmetz, M. P. *et al.* (2005) 'Chronic Enhancement of the Intrinsic Growth Capacity of Sensory Neurons Combined with the Degradation of Inhibitory Proteoglycans Allows Functional Regeneration of Sensory Axons through the Dorsal Root Entry Zone in the Mammalian Spinal Cord', *The Journal of Neuroscience*, 25(35), pp. 8066–8076. doi: 10.1523/JNEUROSCI.2111-05.2005.

Sterne, G. D. *et al.* (1997) 'Neurotrophin-3 delivered locally via fibronectin mats enhances peripheral nerve regeneration', *European Journal of Neuroscience*, 9(7), pp. 1388–1396. doi: 10.1111/j.1460-9568.1997.tb01493.x.

Stone, M. C. *et al.* (2010) 'Global Up-Regulation of Microtubule Dynamics and Polarity Reversal during Regeneration of an Axon from a Dendrite', *Molecular biology of the cell*, 21, pp. 767–777. doi: 10.1091/mbc.E09.

Sun, F. *et al.* (2011) 'Sustained axon regeneration induced by co-deletion of PTEN and SOCS3', *Nature*. Nature Publishing Group, 480, pp. 372–375. doi: 10.1038/nature10594.

Tabuchi, A. *et al.* (2000) 'Differential Activation of Brain-derived Neurotrophic Factor Gene Promoters I and III by Ca2+ Signals Evoked via L-type Voltage-dependent and N-Methyl-D-aspartate Receptor Ca2+ Channels', *The Journal of Biological Chemistry*, 275(23), pp. 17269–17275. doi: 10.1074/jbc.M909538199.

Takahara, A. (2009) 'Cilnidipine : A New Generation Ca 2 + Channel Blocker with Inhibitory Action on Sympathetic Neurotransmitter Release', *Cardiovascular Therapeutics*, 27, pp. 124–139. doi: 10.1111/j.1755-5922.2009.00079.x.

Tang, F., Dent, E. W. and Kalil, K. (2003) 'Spontaneous Calcium Transients in Developing Cortical Neurons Regulate Axon Outgrowth', *The Journal of Neuroscience*, 23(3), pp. 927–936.

Tao, X. *et al.* (2002) 'A Calcium-Responsive Transcription Factor, CaRF, that

Regulates Neuronal Activity-Dependent Expression of BDNF', *Neuron*, 33, pp. 383–395.

Tedeschi, A. and Bradke, F. (2017) 'Spatial and temporal arrangement of neuronal intrinsic and extrinsic mechanisms controlling axon regeneration', *Current Opinion in Neurobiology*. Elsevier Ltd, 42, pp. 118–127. doi: 10.1016/j.conb.2016.12.005.

Terada, S. I. *et al.* (2016) 'Neuronal processing of noxious thermal stimuli mediated by dendritic ca2+influx in Drosophila somatosensory neurons', *eLife*, 5(e12959), pp. 1–26. doi: 10.7554/eLife.12959.

Terenghi, G. (1999) 'Peripheral nerve regeneration and neurotrophic factors', *J Anatomy*, 194, pp. 1–14.

Tracey, W. D. *et al.* (2003) 'painless, a Drosophila gene essential for nociception', *Cell*, 113(2), pp. 261–273. doi: 10.1016/S0092-8674(03)00272-1.

Tsintou, M., Dalamagkas, K. and Seifalian, A. M. (2015) 'Advances in regenerative therapies for spinal cord injury : a biomaterials approach', *Neural Regeneratino Research*, 10(5), pp. 726–742. doi: 10.4103/1673-5374.156966.

Udina, E. *et al.* (2008) 'Electrical stimulation of intact peripheral sensory axons in rats promotes outgrowth of their central projections', *Experimental Neurology*. Elsevier Inc., 210, pp. 238–247. doi: 10.1016/j.expneurol.2007.11.007.

Vetri, F. *et al.* (2014) 'BKCa channels as physiological regulators: a focused review', *Journal of Receptor, Ligand and Channel Research*. Dove Press, 7, p. 3. doi: 10.2147/JRLCR.S36065.

Vivas, O. *et al.* (2017) 'Proximal clustering between BK and Cav1.3 channels promotes functional coupling and BK channel activation at low voltage', *eLife*, 6, pp. 1–18. doi: 10.7554/eLife.28029.

Walker, R. G., Willingham, A. T. and Zuker, C. S. (2000) 'A Drosophila Mechanosensory Transduction Channel', *Science*, 287(5461), pp. 2229–2234. Available at: http://science.sciencemag.org/content/287/5461/2229.abstract.

Wang, H. and Sieburth, D. (2013) 'PKA Controls Calcium Influx into Motor Neurons during a Rhythmic Behavior', *PLOS Genetics*, 9(9). doi: 10.1371/journal.pgen.1003831.

Wang, K. C. *et al.* (2002) 'Oligodendrocyte-myelin glycoprotein is a Nogo receptor ligand that inhibits neurite outgrowth', *Nature*, 417(6892), pp. 941–944. doi: 10.1038/nature00867.

Wang, Z. *et al.* (2001) 'SLO-1 Potassium Channels Control Quantal Content of Neurotransmitter Release at the C. elegans Neuromuscular Junction', *Neuron*, 32, pp. 867–881.

Wayman, G. A. *et al.* (2004) 'Regulation of Axonal Extension and Growth Cone Motility by Calmodulin-Dependent Protein Kinase I', *The Journal of Neuroscience*, 24(15), p. 3786 LP-3794. doi: 10.1523/JNEUROSCI.3294-03.2004.

Weavers, H. *et al.* (2016) 'Corpse Engulfment Generates a Molecular Memory that Primes the Macrophage Inflammatory Response', *Cell*. The Author(s), 165(7), pp. 1658–1671. doi: 10.1016/j.cell.2016.04.049.

Wen, Z. *et al.* (2004) 'A CaMKII/Calcineurin Switch Controls the Direction of Ca^{2+}-Dependent Growth Cone Guidance', *Neuron*. Elsevier, 43(6), pp. 835–846. doi: 10.1016/j.neuron.2004.08.037.

West, A. E., Griffith, E. C. and Greenberg, M. E. (2002) 'Regulation of transcription factors by neuronal activity', *Nature Reviews Neuroscience*, 3(12), pp. 921–931. doi: 10.1038/nrn987.

Wilson, J. M. *et al.* (2000) 'EEA1 , a Tethering Protein of the Early Sorting Endosome , Shows a Polarized Distribution in Hippocampal Neurons , Epithelial Cells , and Fibroblasts', *Molecular biology of the cell*, 11, pp. 2657–2671.

Wu, X. and Samba Reddy, D. (2012) 'Integrins as Receptor Targets for Neurological Disorders', *Pharmacol Ther.*, 134(1), pp. 68–81. doi: 10.1016/j.pharmthera.2011.12.008.Integrins.

Xiang, Y. *et al.* (2010) 'NIH Public Access', *Light-avoidance-mediating photoreceptors tile the Drosophila larval body wall*, 468(7326), pp. 921–926. doi: 10.1038/nature09576.Light-avoidance-mediating.

Xie, W., Strong, J. A. and Zhang, J.-M. (2017) 'Active Nerve Regeneration with Failed Target Reinnervation Drives Persistent Neuropathic Pain', *Eneuro*, 4(1), p. ENEURO.0008-17.2017. doi: 10.1523/ENEURO.0008-17.2017.

Xu, X. M. *et al.* (1995) 'A Combination of BDNF and NT-3 Promotes Supraspinal Axonal Regeneration into Schwann Cell Grafts in Adult Rat Thoracic Spinal Cord', *Experimental Neurology*, 134, pp. 261–272.

Yan, D. *et al.* (2009) 'The DLK-1 Kinase Promotes mRNA Stability and Local Translation in C. elegans Synapses and Axon Regeneration', *Cell*. Elsevier Ltd, 138(5), pp. 1005–1018. doi: 10.1016/j.cell.2009.06.023.

Yan, Z. *et al.* (2013) 'Drosophila NOMPC is a mechanotransduction channel subunit for gentle-touch sensation', *Nature*, 6(8), pp. 221–225. doi: 10.1021/nn300902w.Release.

Yu, H. *et al.* (2018) 'The Requirement of L-Type Voltage-Dependent Calcium Channel (L-VDCC) in the Rapid-Acting Antidepressant-Like Effects of Scopolamine in Mice', *International Journal of Neuropsychopharmacology*, 21(2), pp. 175–186. doi: 10.1093/ijnp/pyx080.

Zeldenrust, F., Wadman, W. J. and Englitz, B. (2018) 'Neural Coding With Bursts — Current State and Future Perspectives', *Frontiers in Computational Neuroscience*, 12, pp. 1–14. doi: 10.3389/fncom.2018.00048.

Zhang, F. *et al.* (2007) 'Multimodal fast optical interrogation of neural circuitry', *Nature*, 446. doi: 10.1038/nature05744.

Zheng, F. *et al.* (2011) 'Regulation of Brain-Derived Neurotrophic Factor Exon IV Transcription through Calcium Responsive Elements in Cortical Neurons', *PLOS One*, 6(12). doi: 10.1371/journal.pone.0028441.

Zheng, J. Q. *et al.* (1994) 'Turning of nerve growth cones induced by neurotransmitters', *Nature*, 368(6467), pp. 140–144. doi: 10.1038/368140a0.

Zhong, L., Hwang, R. Y. and Tracey, W. D. (2010) 'Pickpocket is a DEG/ENaC protein required for mechanical nociception in Drosophila larvae', *Current Biology*, 20(5), pp. 429–434. doi: 10.1016/j.cub.2009.12.057.Pickpocket.

Ziv, N. E. and Spira, M. E. (1995) 'Axotomy induces a transient and localized elevation of the free intracellular calcium concentration to the millimolar range', *Journal of Neurophysiology*, 74(6), pp. 2625–2637. doi: 10.1152/jn.1995.74.6.2625.